Abundance and Distribution of WCSI Hector's dolphin:

Supplemental Material

D.I. MacKenzie,
D.M. Clement

April 2016

TABLE OF CONTENTS

EXECUTIVE SUMMARY

MacKenzie, D.I.; Clement, D.M. (2016). Abundance and distribution of WCSI Hector's dolphin.

New Zealand Aquatic Environment and Biodiversity Report No. 168 Supplemental Material 112 p.

The Ministry for Primary Industries and the Department of Conservation are currently reviewing the Hector's dolphin Threat Management Plan. For this review, up-to-date abundance and distribution estimates of Hector's dolphin are required. A survey programme was specifically designed for sampling the WCSI population using two separate aerial surveys over summer 2014/2015 and winter 2015. The WCSI surveys constitute the last abundance estimate of the three regional South Island Hector's dolphin sub-populations; following on from the east and north coast (ECSI) aerial surveys in 2013 (MacKenzie & Clement 2014) and south coast (SCSI) aerial surveys in 2010 (Clement et al. 2011). This report summarises the results from the recently completed WCSI surveys.

The WCSI survey area (about 26 333 km^2 between Farewell Spit and Milford Sound) was stratified into six coastal sections, which were further divided into offshore substrata of 0–4 nmi (inner), 4–12 nmi (middle) and 12–20 nmi (outer). This design was expected to encompass the offshore limits of Hector's dolphin distribution along the South Island's west coast. Double observer, line-transect methodology was used with transect lines orientated in the offshore direction and spaced parallel at equal intervals (according to strata-specific effort allocation) using systematic-random line placement.

WCSI abundance was estimated using an extension of mark-recapture distance sampling (MRDS) techniques that accounts for differing field of views between observer positions in the plane; similar to the approach developed for the ECSI survey (MacKenzie & Clement 2016). These methods also allow for a lack of independence between the observer detections. Availability bias is a fundamentally important component for obtaining a reliable estimate of total abundance; therefore, as in the ECSI survey, we utilise two availability methods; helicopter observations of dive cycles and circle-back redetection.

These aerial surveys constitute the only abundance study to date with substantial effort in offshore regions (more than 4 nmi from the coast) for Hector's dolphin along the entire west coastal waters of the South Island. Summer sightings results consisted of 250 dolphin groups (115 of which were seen by two observers) sighted within 0.3 km either side of the plane along 4001 km of transect lines. In winter, 272 dolphin groups (115 of which were seen by two observers) were sighted within 0.3 km either side of the plane along 4307 km of transect lines. Hector's dolphins were observed as far offshore as 12 km (6.5 nmi) and 17.7 km (9.5 nmi) in summer and winter, and in waters as deep as 160 m and 200 m, respectively. However, the majority of animals in both seasons occurred close to shore (less than 3 nmi) and within relatively shallow depths (less than 40 m).

Regional variation in dive cycle data was similar in both survey periods with slightly lower surface availability off the Okarito Lagoon region. Availability estimated from the circle-back data exhibited less regional variation than dive-profiles, although both the effects of region and offshore (0–4 nmi or 4–20 nmi) factors were incorporated into model average estimates of circle-back availability.

The WCSI Hector's dolphin summer abundance was estimated to be 5490 (CV: 26%; 95% CI: 3319–9079) and 5802 (CV: 21%, 95% CI: 3879–8679) in winter. These estimates were obtained by averaging the four sets of results for each season; from two different data sets using different truncation distances and two methods of estimating availability (dive cycle and circle-backs). These estimates are very similar to the previous 2000/2001 WCSI estimate of 5388 Hector's dolphins (CV: 21%; 95% CI: 3613–8034), even after accounting for differences in offshore survey areas.

Following a reanalysis of the ECSI and SCSI survey data, our estimate for the total Hector's population around the South Island (excluding sounds and harbours) is 14 849 (CV: 11%, 95% CI 11 923–18 492). This estimate is approximately double the previous estimate from surveys conducted in the late 1990s – early 2000s (7300; 95% CI 5303–9966), with the difference primarily due to a much larger estimated population along ECSI, distributed much further offshore than previously thought. Densities are similar along ECSI and WCSI. This new estimate has implications regarding the conservation, potential fisheries-related impact and our general understanding of the species.

SECTION A: SCSI Methods

The aerial survey and data collection protocols for the South Coast South Island (SCSI) Hector's dolphin surveys have been previously described by Clement et al. (2011), and the general analysis approach used here is the same as that described for West Coast South Island (WCSI) abundance estimates. Below a brief review of the survey design is given, along with details of the detection function analysis that are specific to this data set.

The SCSI survey area was 6186 km^2, extending from Puysegur Point in the west to Nugget Point in the east, and offshore to the lesser of the 100 m depth contour or halfway between the mainland and Stewart Island (Figure A.1). Transect lines were spaced 3.7 km (2 nmi) apart and oriented at 45° to the coast. Some stratification was used solely for the purpose of maintaining the configuration of the survey lines relative to the coastline. Aerial surveys were conducted during March and August 2010 using a high-wing, single-engine Gippsland Airvan, at a height of 152 m (500ft) and speed of 185 km/h (100 knots). Total survey effort was 1660 km in March and 1667 km in August. Four observers were located in the cabin of the aircraft, with front and rear observers on each side. Rear observers had a slightly bubbled window with a maximum observable downward angle of 75°, while front observers had a flat window. Both observers searched for dolphin groups using the same protocols as that described previously for the East Coast South Island (ECSI) and WCSI surveys.

Due to the low number of sightings during the actual survey, additional surveys were conducted for estimation of the detection function in both survey periods. Sightings made during these auxiliary surveys were only used to estimate the detection functions, and were not used to estimate abundance otherwise. The detection function estimation methods that were used for the WCSI sighting data were applied to the SCSI sighting data. A left truncation distance of 0.04 km and right truncation distance of 0.30 km were used for detections from either the front or rear observer position. Due to the low number of sightings (including auxiliary sightings) a common detection function was estimated for the March and August survey periods. The same set of detection function models used in the WCSI analysis were fit to the SCSI data, and compared using AIC.

Availability of dolphin groups to detection during the aerial line-transect surveys was estimated from dive-cycle data collected using a Robinson R44 helicopter. Helicopter surveys were conducted in Te Waewae Bay for both survey periods. Financial constraints and the lack of an available, suitable, helicopter meant that dive-cycle surveys were not conducted in the eastern portion of the study area. Dolphin availability was estimated from the dive-cycle data using the same methods as that used for the WCSI and ECSI surveys (MacKenzie & Clement, 2014). This approach allows for the time that a dolphin group may be in an observer's field of vision during the line-transect surveys (6 seconds), which differs from the instantaneous approach used by Clement et al. (2011) and others (e.g., Slooten et al. 2004, DuFresne & Mattlin 2009, DuFresne et al. 2010, Slooten et al. 2006). The raw dive-cycle data was re-evaluated to ensure consistency of processing with the ECSI and WCSI data. Availability was estimated separately for the two survey periods.

Hector's dolphin abundance was estimated from each of the top-ranked detection function models, in combination with the estimated availability and fraction of the survey area covered by the aerial transects. Model-averaging was used to combine the resulting estimates into a final abundance estimate for the March and August periods.
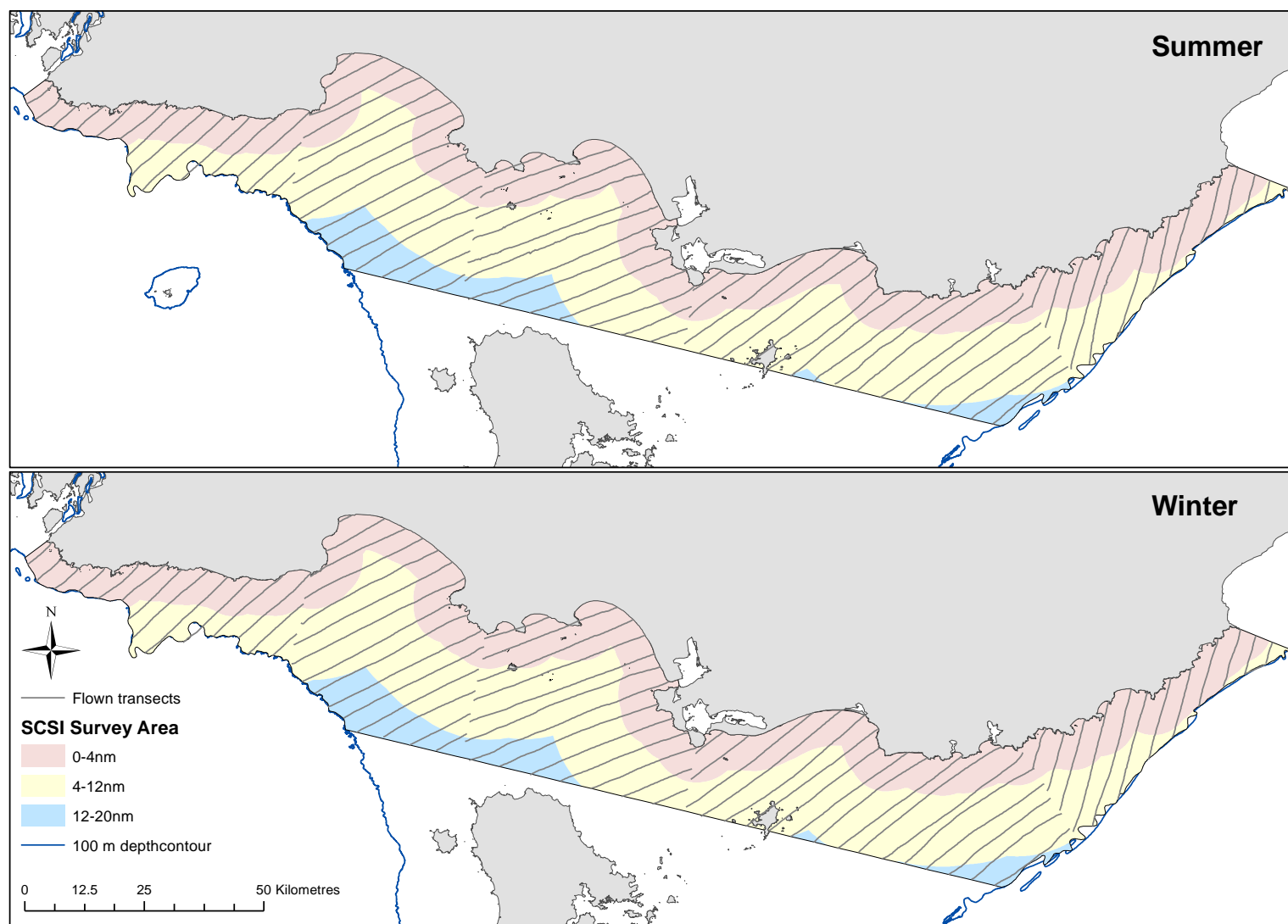
Figure A.1: SCSI summer survey transects flown between 4 and 21 March 2010 (top figure) and winter survey transects flown between 22 and 28 August 2010 (bottom figure). NOTE – the SCSI was not stratified into offshore strata (i.e. 0–4 nmi, etc.). These zones are shown on the figures only for comparison with later ECSI and WCSI surveys.

SECTION B: Model Averaging

Model averaging is a technique to combine estimates and standard errors from a range of models and is often used when a number of different models all have substantial support from the data which leads to model selection uncertainty (Burnham and Anderson 2002, Anderson 2008).

Given a set of model weights, w, which sum to 1 and indicate the level of support for each of the M models being considered, a model averaged estimate of the quantity θ can be calculated as:

$$\hat{\theta}_A = \sum_{m=1}^{M} w_m \hat{\theta}_m$$

Extending the variance equation from Anderson (2008) in the obvious manner, the covariance for two model averaged quantities $\hat{\theta}_A$ and $\hat{\delta}_A$ can be calculated as

$$Cov\left(\hat{\theta}_A, \hat{\delta}_A\right) = \sum_{m=1}^{M} w_m \left\{ Cov\left(\hat{\theta}_m, \hat{\delta}_m \middle| g_m\right) + \left(\hat{\theta}_m - \hat{\theta}_A\right)\left(\hat{\delta}_m - \hat{\delta}_A\right) \right\},$$

where $Cov\left(\hat{\theta}_m, \hat{\delta}_m \middle| g_m\right)$ is the covariance for the two quantities under model g_m.

The standard error for a single quantity is then

$$SE\left(\hat{\theta}_A\right) = \sqrt{Cov\left(\hat{\theta}_A, \hat{\theta}_A\right)}.$$

References

Anderson, D.R. Model based inference in the life sciences. 2008. Springer. New York, USA.

Burnham, K.P., and D.R Anderson. 2002. Model selection and multimodel inference. 2nd Ed., Springer-Verlag, New York, USA.

SECTION C: Summary of WCSI summer and winter sighting data

Table C.1: Summary of full summer sighting data by strata. Given in the number of unique groups sighted, number of groups sighted from the front position, number of groups sighted from the rear position and number of groups sighted from both positions (duplicates). Also presented are the total number of individuals and average number of individuals per group. Naïve is the estimated number of dolphins assuming a strip transect survey with perfect detection and availability.

Coastal Section	Offshore Stratum (nmi)	Unique Groups	Front	Rear	Duplicates	Total Individuals	Average Group Size	Naïve
Whanganui Inlet	0–4	0	0	0	0	0	0.00	0
	4–12	0	0	0	0	0	0.00	0
	12–20	0	0	0	0	0	0.00	0
Hector	0–4	82	57	75	50	190	2.32	598
	4–12	5	3	5	3	21	4.20	259
	12–20	0	0	0	0	0	0.00	0
Greymouth	0–4	47	25	38	16	85	1.81	533
	4–12	1	0	1	0	1	1.00	19
	12–20	0	0	0	0	0	0.00	0
Okarito Lagoon	0–4	95	60	74	39	181	1.91	563
	4–12	10	8	7	5	21	2.10	255
	12–20	0	0	0	0	0	0.00	0
Jackson Bay	0–4	9	4	7	2	13	1.44	80
	4–12	0	0	0	0	0	0.00	0
	12–20	0	0	0	0	0	0.00	0
Milford Sound	0–4	1	1	0	0	1	1.00	12
	4–12	0	0	0	0	0	0.00	0
	12–20	0	0	0	0	0	0.00	0
Total		**250**	**158**	**207**	**115**	**513**	**2.05**	**2319**

Table C.2: Summary of reduced summer sighting data by strata. Given in the number of unique groups sighted, number of groups sighted from the front position, number of groups sighted from the rear position and number of groups sighted from both positions (duplicates). Also presented are the total number of individuals and average number of individuals per group. Naïve is the estimated number of dolphins assuming a strip transect survey with perfect detection and availability.

Coastal Section	Offshore Stratum (nmi)	Unique Groups	Front	Rear	Duplicates	Total Individuals	Average Group Size	Naïve
Whanganui Inlet	0–4	0	0	0	0	0	0.00	0
	4–12	0	0	0	0	0	0.00	0
	12–20	0	0	0	0	0	0.00	0
Hector	0–4	60	57	53	50	150	2.50	618
	4–12	3	3	3	3	11	3.67	178
	12–20	0	0	0	0	0	0.00	0
Greymouth	0–4	30	25	21	16	59	1.97	485
	4–12	1	0	1	0	1	1.00	24
	12–20	0	0	0	0	0	0.00	0
Okarito Lagoon	0–4	71	60	50	39	129	1.82	526
	4–12	8	8	5	5	16	2.00	255
	12–20	0	0	0	0	0	0.00	0
Jackson Bay	0–4	4	4	2	2	6	1.50	48
	4–12	0	0	0	0	0	0.00	0
	12–20	0	0	0	0	0	0.00	0
Milford Sound	0–4	1	1	0	0	1	1.00	16
	4–12	0	0	0	0	0	0.00	0
	12–20	0	0	0	0	0	0.00	0
Total		**178**	**158**	**135**	**115**	**373**	**2.10**	**2150**

Table C.3: Summary of full winter sighting data by strata. Given in the number of unique groups sighted, number of groups sighted from the front position, number of groups sighted from the rear position and number of groups sighted from both positions (duplicates). Also presented are the total number of individuals and average number of individuals per group. Naïve is the estimated number of dolphins assuming a strip transect survey with perfect detection and availability.

Coastal Section	Offshore Stratum (nmi)	Unique Groups	Front	Rear	Duplicates	Total Individuals	Average Group Size	Naïve
Whanganui Inlet	0–4	3	3	2	2	3	1.00	55
	4–12	0	0	0	0	0	0.00	0
	12–20	0	0	0	0	0	0.00	0
Hector	0–4	53	20	49	16	84	1.58	264
	4–12	10	4	9	3	14	1.40	86
	12–20	0	0	0	0	0	0.00	0
Greymouth	0–4	95	56	77	38	211	2.22	658
	4–12	5	5	5	5	10	2.00	184
	12–20	0	0	0	0	0	0.00	0
Okarito Lagoon	0–4	73	48	63	38	138	1.89	430
	4–12	14	8	11	5	22	1.57	134
	12–20	0	0	0	0	0	0.00	0
Jackson Bay	0–4	19	11	16	8	37	1.95	228
	4–12	0	0	0	0	0	0.00	0
	12–20	0	0	0	0	0	0.00	0
Milford Sound	0–4	0	0	0	0	0	0.00	0
	4–12	0	0	0	0	0	0.00	0
	12–20	0	0	0	0	0	0.00	0
Total		**272**	**155**	**232**	**115**	**519**	**1.91**	**2039**

Table C.4: Summary of reduced winter sighting data by strata. Given in the number of unique groups sighted, number of groups sighted from the front position, number of groups sighted from the rear position and number of groups sighted from both positions (duplicates). Also presented are the total number of individuals and average number of individuals per group. Naïve is the estimated number of dolphins assuming a strip transect survey with perfect detection and availability.

Coastal Section	Offshore Stratum (nmi)	Unique Groups	Front	Rear	Duplicates	Total Individuals	Average Group Size	Naïve
Whanganui Inlet	0–4	3	3	2	2	3	1.00	72
	4–12	0	0	0	0	0	0.00	0
	12–20	0	0	0	0	0	0.00	0
Hector	0–4	28	20	24	16	46	1.64	189
	4–12	5	4	4	3	6	1.20	48
	12–20	0	0	0	0	0	0.00	0
Greymouth	0–4	64	56	46	38	138	2.16	563
	4–12	5	5	5	5	10	2.00	241
	12–20	0	0	0	0	0	0.00	0
Okarito Lagoon	0–4	56	48	46	38	110	1.96	449
	4–12	10	8	7	5	15	1.50	120
	12–20	0	0	0	0	0	0.00	0
Jackson Bay	0–4	13	11	10	8	27	2.08	218
	4–12	0	0	0	0	0	0.00	0
	12–20	0	0	0	0	0	0.00	0
Milford Sound	0–4	0	0	0	0	0	0.00	0
	4–12	0	0	0	0	0	0.00	0
	12–20	0	0	0	0	0	0.00	0
Total		**184**	**155**	**144**	**115**	**355**	**1.93**	**1901**

SECTION D: Histograms of verified distance data for WCSI sightings

Figure D.1: Histogram of the verified distance data prior to any truncation of summer sightings from A) the front observer position, B) the rear observer position, and C) from either observer position in the summer survey. Grey bars indicate sightings made by both observers (duplicates).

Figure D.2: Histogram of the distance data for summer sightings in the summer survey from A) the front observer position following left truncation at 0.071 km and right truncation at 0.300 km, B) from the rear observer position following setting two sightings with angles >90 degrees to 90 degrees and right truncation at 0.300 km, and C) either observer position following left truncation at 0.071 km for the front position, setting two sightings with angles >90 degrees to 90 degrees for the rear position, and right truncation at 0.300 km for both positions. Grey bars indicate the number of sightings made by both observers (duplicates)
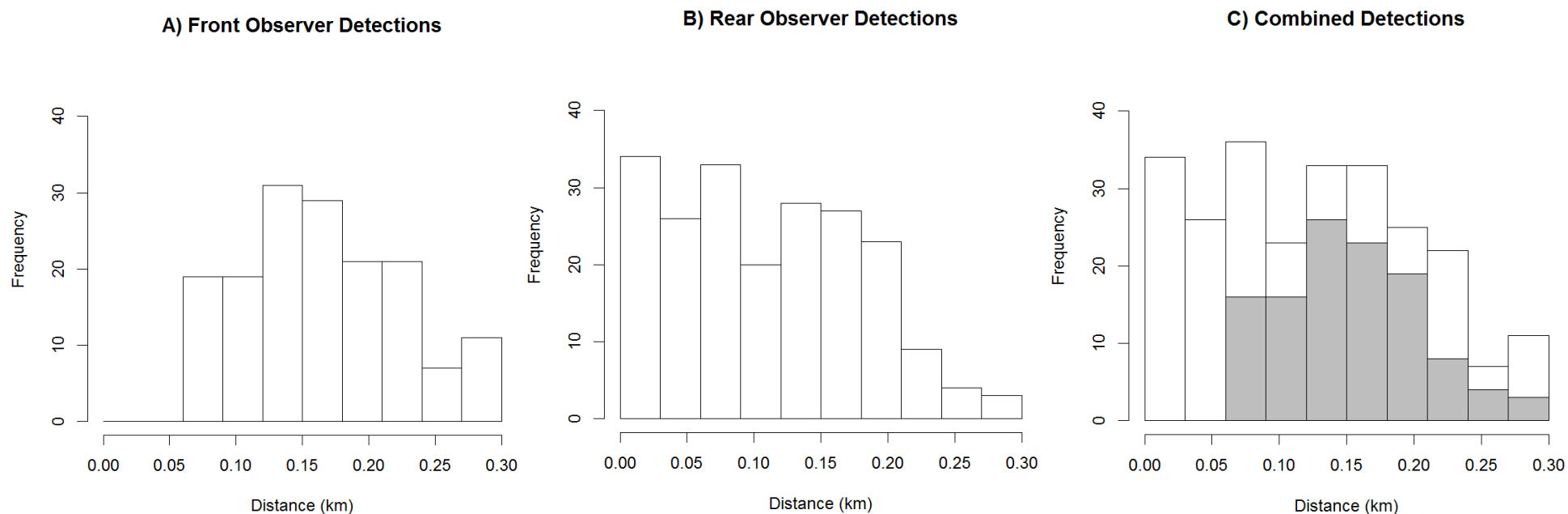
Figure D.3: Histogram of the distance data for summer sightings in the summer survey from A) the front observer position following left truncation at 0.071 km, right truncation at 0.300 km, B) the rear observer position following left truncation at 0.071 km and right truncation at 0.300 km, and C) either observer position following left truncation at 0.071 km and right truncation at 0.300 km for both positions. Distances have been rescaled such that the original distance of 0.071 km becomes 0 km. Grey bars indicate the number of sightings made by both observers (duplicates).
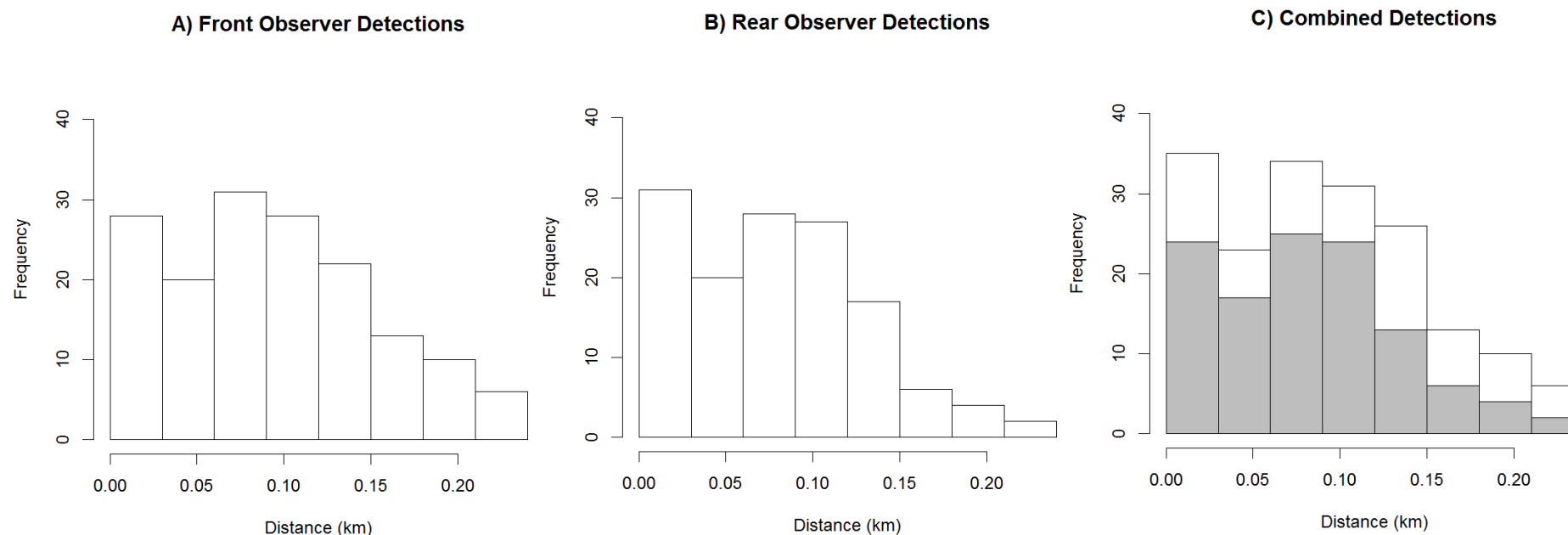
Figure D.4: Histogram of the verified distance data prior to any truncation of winter sightings from A) the front observer position, B) the rear observer position, and C) from either observer position in the winter survey. Grey bars indicate sightings made by both observers (duplicates).
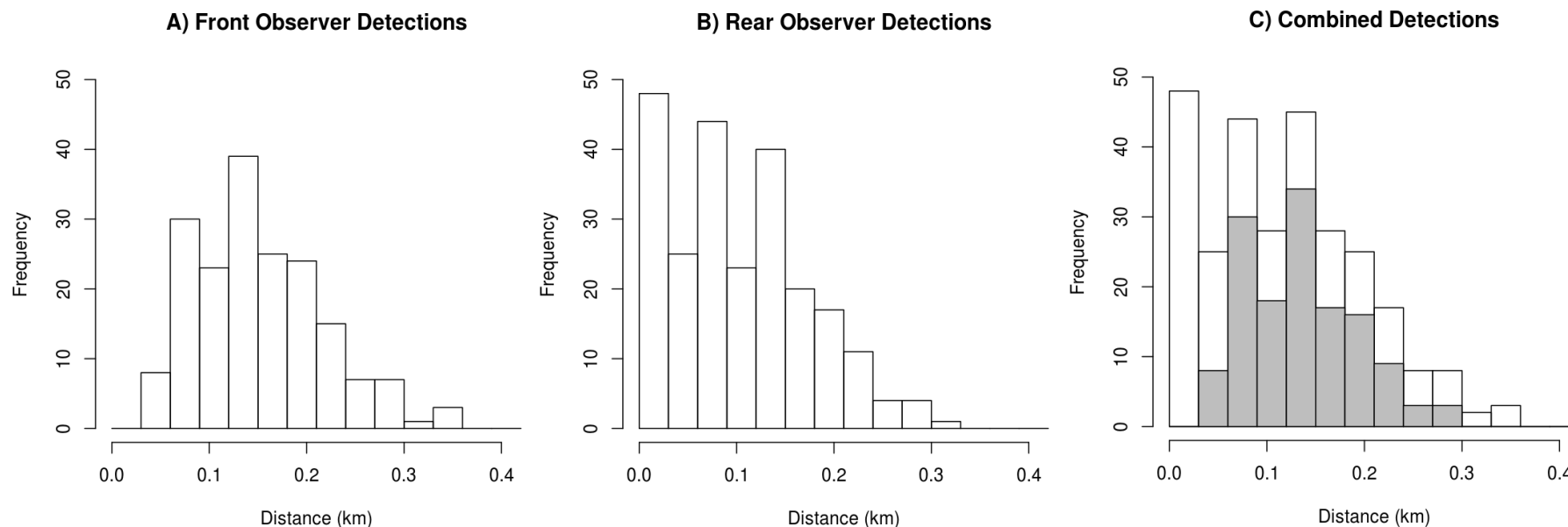
Figure D.5: Histogram of the distance data for sightings in the winter survey from A) the front observer position following left truncation at 0.071 km and right truncation at 0.300 km, B) from the rear observer position following setting two sightings with angles >90 degrees to 90 degrees and right truncation at 0.300 km, and C) either observer position following left truncation at 0.071 km for the front position, setting two sightings with angles >90 degrees to 90 degrees for the rear position, and right truncation at 0.300 km for both positions. Grey bars indicate the number of sightings made by both observers (duplicates).

A) Front Observer Detections

B) Rear Observer Detections

C) Combined Detections

S14 ● Abundance and Distribution of WCSI Hector's dolphin (Suppl.)
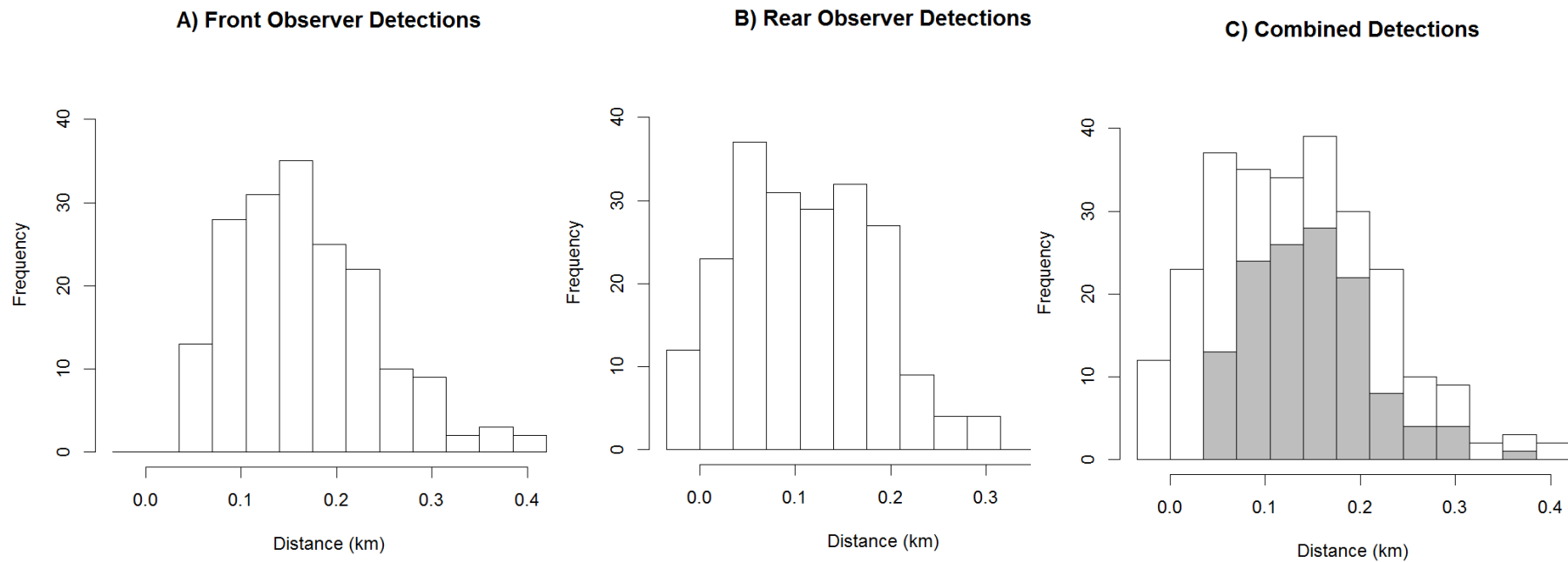
Ministry for Primary Industries
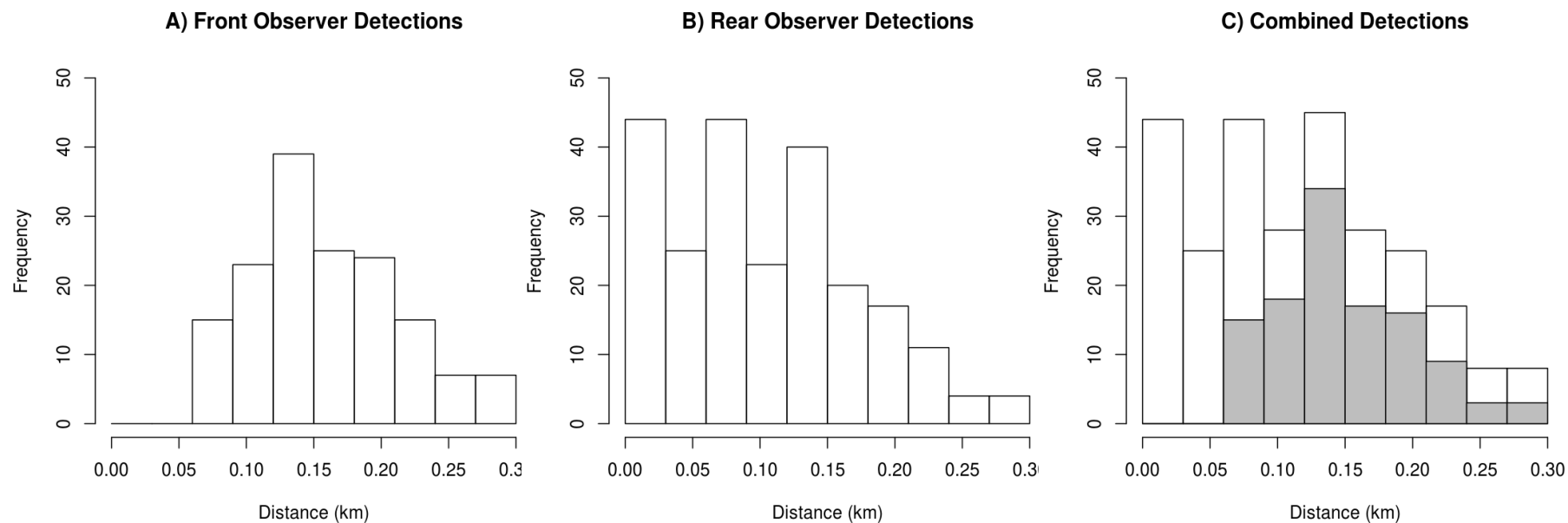
Figure D.6: Histogram of the distance data for sightings in the winter survey from A) the front observer position following left truncation at 0.071 km, right truncation at 0.300 km, B) the rear observer position following left truncation at 0.071 km and right truncation at 0.300 km, and C) either observer position following left truncation at 0.071 km and right truncation at 0.300 km for both positions. Distances have been rescaled such that the original distance of 0.071 km becomes 0 km. Grey bars indicate the number of sightings made by both observers (duplicates).

A) Front Observer Detections

B) Rear Observer Detections

C) Combined Detections
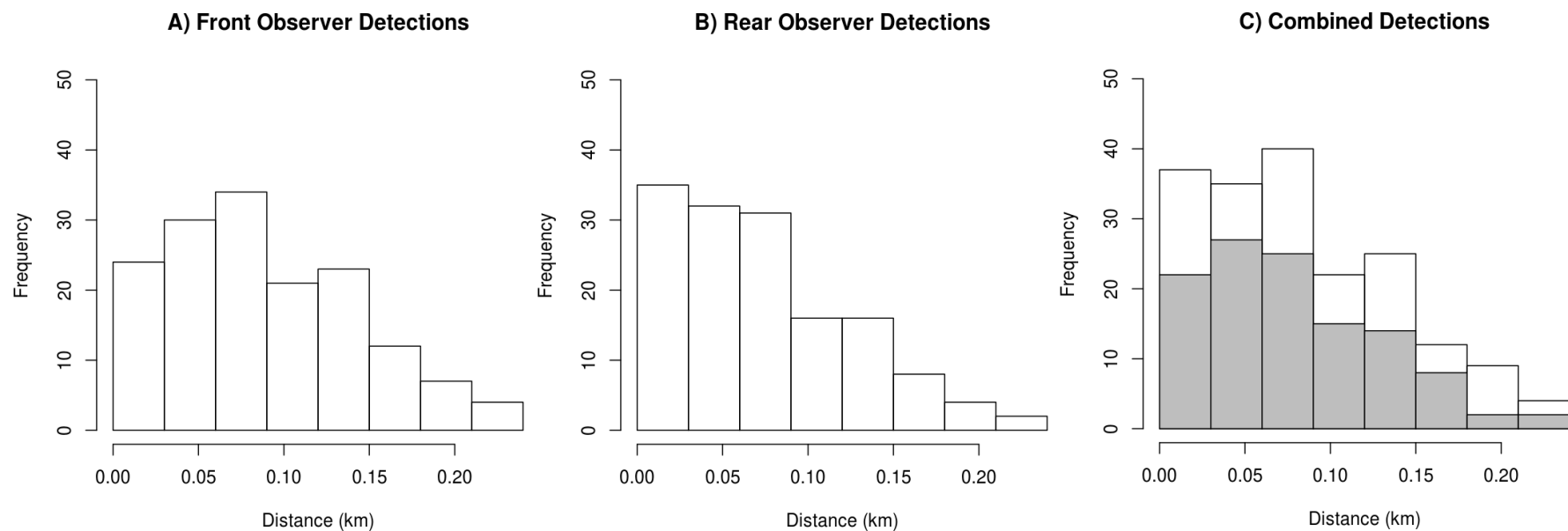
SECTION E: Diagnostic plots for detection function models fit to full WCSI summer sighting data; top seven models from Table 5

Figure E.1: Fitted detection functions and histograms of empirical detection probabilities from the top ranked model in Table 5. Left is $p_\bullet(d_i, s_i)$, centre is $p_F(d_i, s_i)$, and right is $p_R(d_i, s_i)$.

Figure E.2: Fitted detection functions and histograms of empirical detection probabilities from the second ranked model in Table 5. Left is $p_\bullet(d_i, s_i)$, centre is $p_F(d_i, s_i)$, and right is $p_R(d_i, s_i)$.

Figure E.3: Fitted detection functions and histograms of empirical detection probabilities from the third ranked model in Table 5. Left is $p_\bullet(d_i, s_i)$, centre is $p_F(d_i, s_i)$, and right is $p_R(d_i, s_i)$.

Figure E.4: Fitted detection functions and histograms of empirical detection probabilities from the fourth ranked model in Table 5. Left is $p_{\bullet}(d_i, s_i)$, **centre is** $p_F(d_i, s_i)$, **and right is** $p_R(d_i, s_i)$.

Figure E.5: Fitted detection functions and histograms of empirical detection probabilities from the fifth ranked model in Table 5. Left is $p_{\bullet}(d_i, s_i)$, **centre is** $p_F(d_i, s_i)$, **and right is** $p_R(d_i, s_i)$.
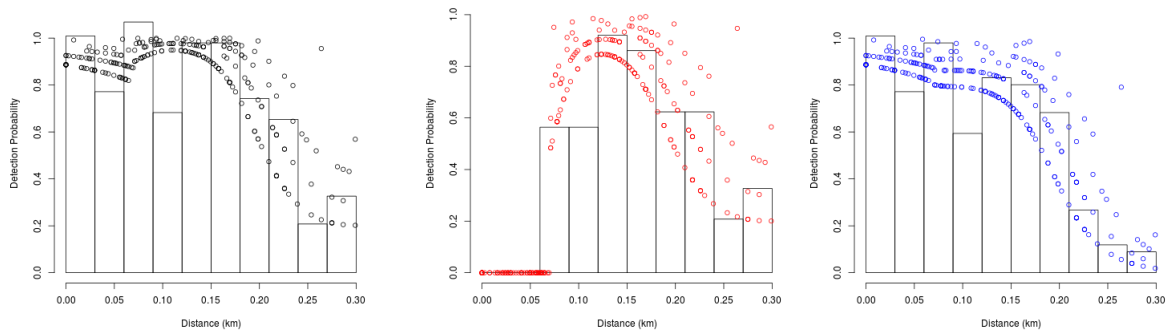
Figure E.6: Fitted detection functions and histograms of empirical detection probabilities from the sixth ranked model in Table 5. Left is $p_{\bullet}(d_i, s_i)$, **centre is** $p_F(d_i, s_i)$, **and right is** $p_R(d_i, s_i)$.
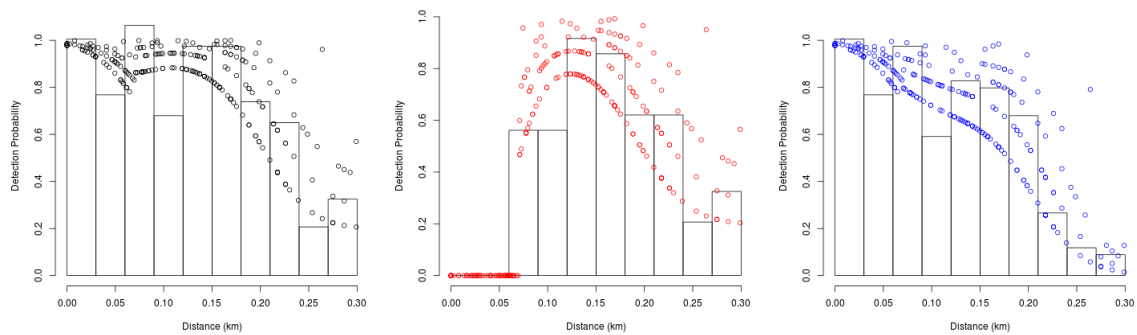
Figure E.7: Fitted detection functions and histograms of empirical detection probabilities from the seventh ranked model in Table 5. Left is $p_\bullet(d_i, s_i)$, centre is $p_F(d_i, s_i)$, and right is $p_R(d_i, s_i)$.

Figure E.8: Q-Q plot of the fitted and empirical cumulative density functions (CDF) for the top ranked model of the detection function analysis of the full summer data.

Figure E.9: Q-Q plot of the fitted and empirical cumulative density functions (CDF) for the second ranked model of the detection function analysis of the full summer data.

Figure E.10: Q-Q plot of the fitted and empirical cumulative density functions (CDF) for the third ranked model of the detection function analysis of the full summer data.
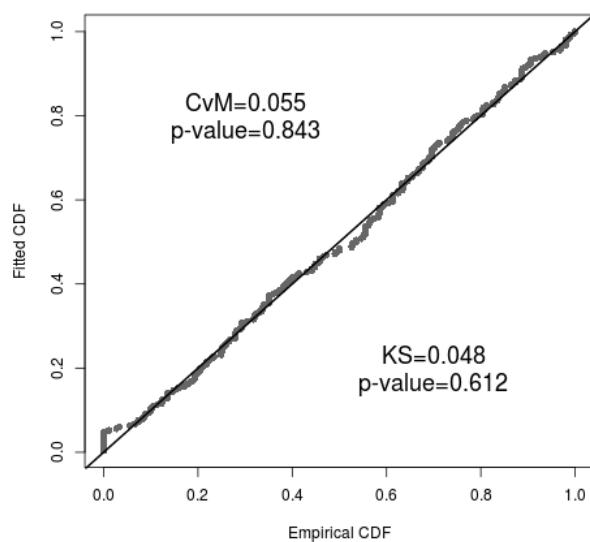
Figure E.11: Q-Q plot of the fitted and empirical cumulative density functions (CDF) for the fourth ranked model of the detection function analysis of the full summer data.
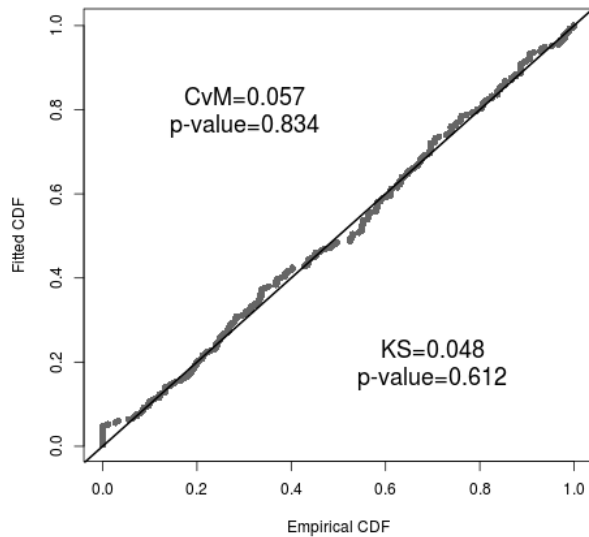
Figure E.12: Q-Q plot of the fitted and empirical cumulative density functions (CDF) for the fifth ranked model of the detection function analysis of the full summer data.

Figure E.13: Q-Q plot of the fitted and empirical cumulative density functions (CDF) for the sixth ranked model of the detection function analysis of the full summer data.

Figure E.14: Q-Q plot of the fitted and empirical cumulative density functions (CDF) for the seventh ranked model of the detection function analysis of the full summer data.
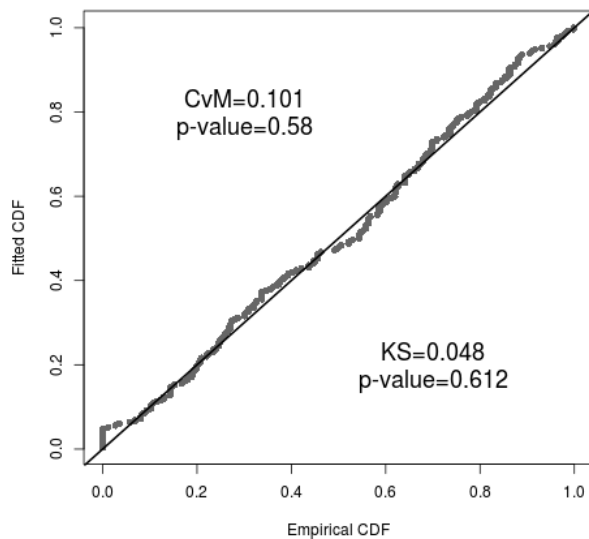
SECTION F: Diagnostic plots for detection function models fit to reduced WCSI summer sighting data; top seven models from Table 7

Figure F.1: Fitted detection functions and histograms of empirical detection probabilities from the top ranked model in Table 7. Left is $p_\bullet(d_i, s_i)$, centre is $p_F(d_i, s_i)$, and right is $p_R(d_i, s_i)$. Note that distance from the transect line has been rescaled such that an original distance of 0.071 km is now 0 km.

Figure F.2: Fitted detection functions and histograms of empirical detection probabilities from the second ranked model in Table 7. Left is $p_\bullet(d_i, s_i)$, centre is $p_F(d_i, s_i)$, and right is $p_R(d_i, s_i)$. Note that distance from the transect line has been rescaled such that an original distance of 0.071 km is now 0 km.

Figure F.3: Fitted detection functions and histograms of empirical detection probabilities from the third ranked model in Table 7. Left is $p_\bullet(d_i, s_i)$, centre is $p_F(d_i, s_i)$, and right is $p_R(d_i, s_i)$. Note that distance from the transect line has been rescaled such that an original distance of 0.071 km is now 0 km.

Figure F.4: Fitted detection functions and histograms of empirical detection probabilities from the fifth ranked model in Table 7. Left is $p_\bullet(d_i, s_i)$, cent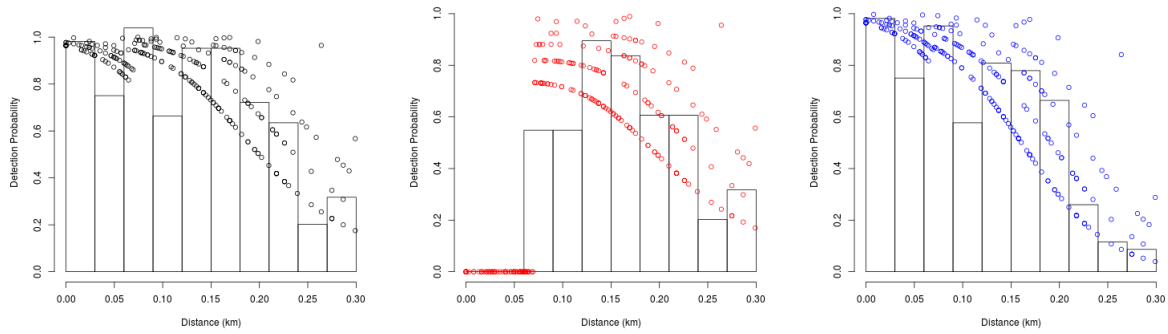re is $p_F(d_i, s_i)$, and right is $p_R(d_i, s_i)$. **Note that distance from the transect line has been rescaled such that an original distance of 0.071 km is now 0 km.**
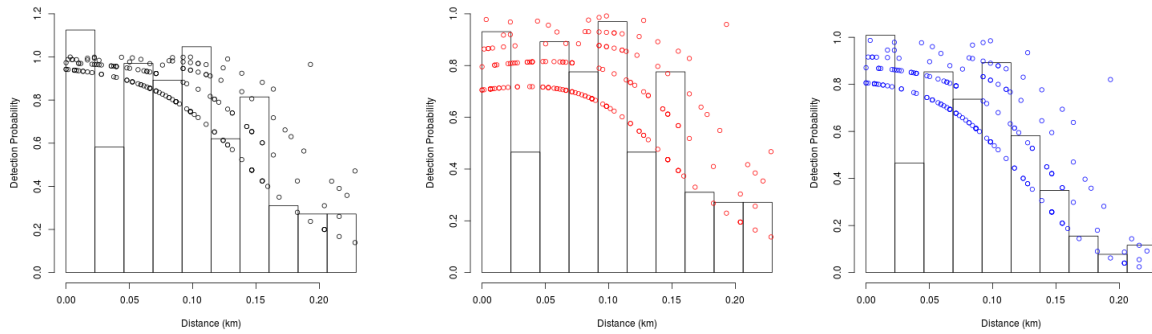
Figure F.5: Fitted detection functions and histograms of empirical detection probabilities from the sixth ranked model in Table 7. Left is $p_\bullet(d_i, s_i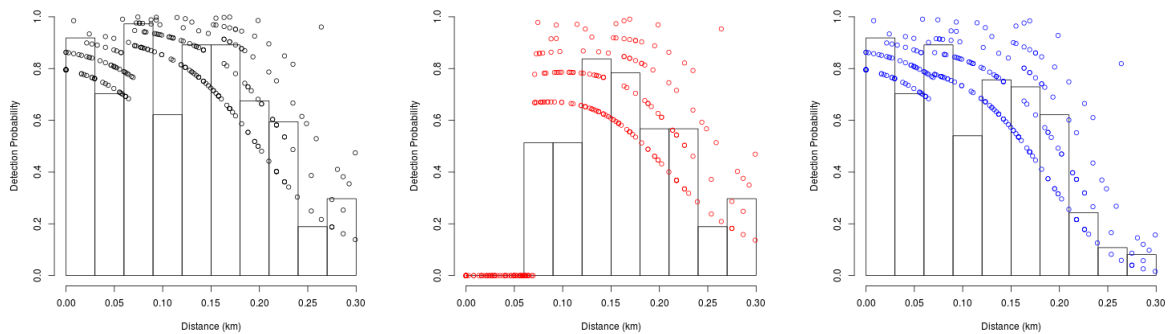)$, centre is $p_F(d_i, s_i)$, and right is $p_R(d_i, s_i)$. **Note that distance from the transect line has been rescaled such that an original distance of 0.071 km is now 0 km.**
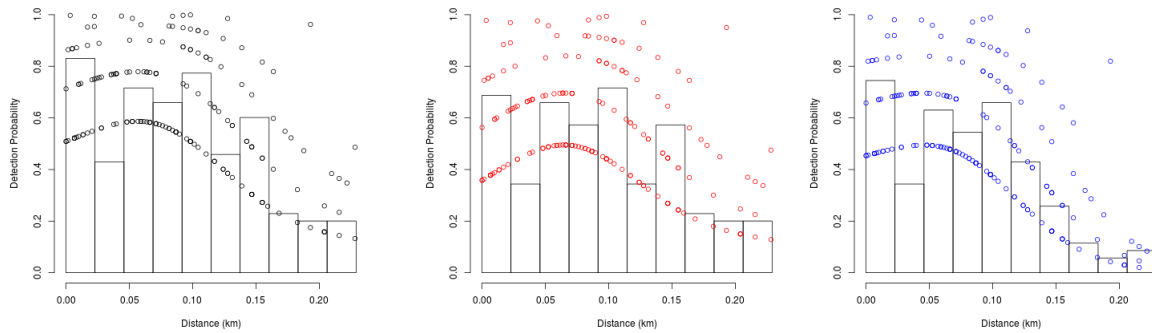
Figure F.6: Fitted detection functions and histograms of empirical detection probabilities from the seventh ranked model in Table 7. Left is $p_\bullet(d_i, s_i)$, 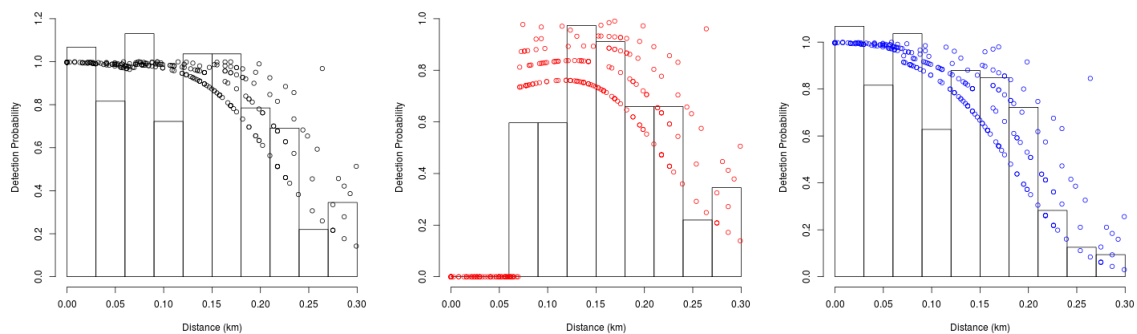centre is $p_F(d_i, s_i)$, and right is $p_R(d_i, s_i)$. **Note that distance from the transect line has been rescaled such that an original distance of 0.071 km is now 0 km.**
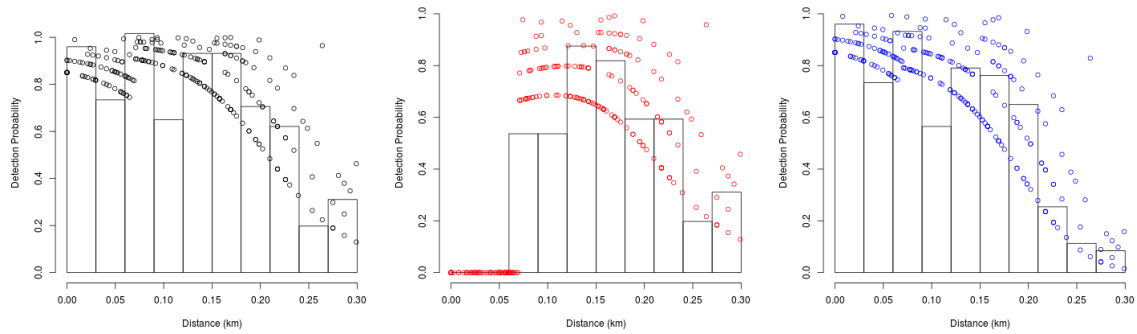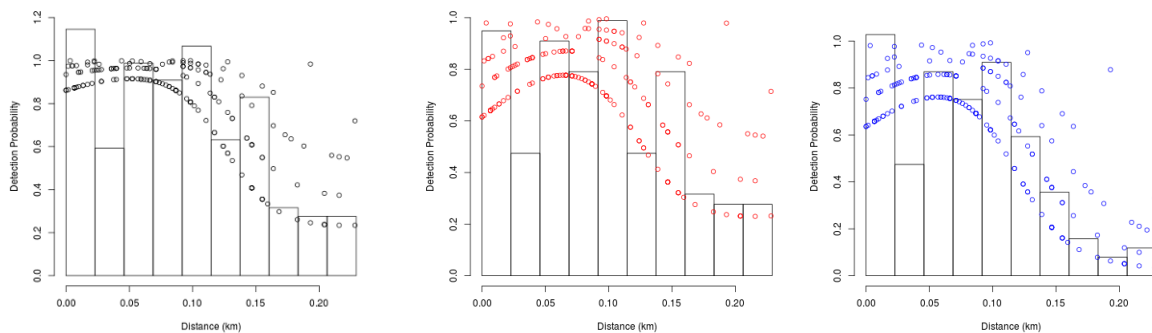
Figure F.7: Fitted detection functions and histograms of empirical detection probabilities from the eighth ranked model in Table 7. Left is $p_\bullet(d_i, s_i)$**, centre is** $p_F(d_i, s_i)$**, and right is** $p_R(d_i, s_i)$**. Note that distance from the transect line has been rescaled such that an original distance of 0.071 km is now 0 km.**
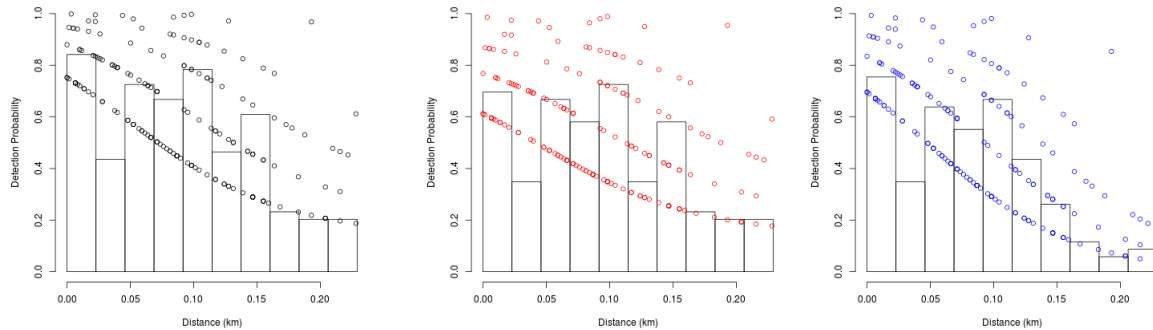
Figure F.8: Q-Q plot of the fitted and empirical cumulative density functions (CDF) for the top ranked model of the detection function analysis of the reduced summer data.
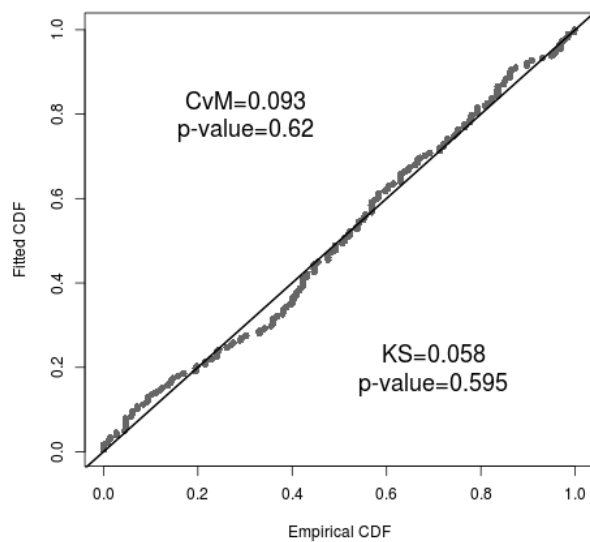
Figure F.9: Q-Q plot of the fitted and empirical cumulative density functions (CDF) for the second ranked model of the detection function analysis of the reduced summer data.
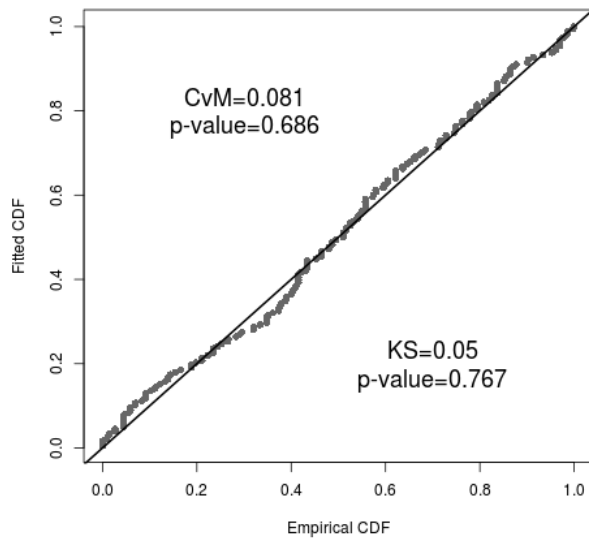
Figure F.10: Q-Q plot of the fitted and empirical cumulative density functions (CDF) for the third ranked model of the detection function analysis of the reduced summer data.
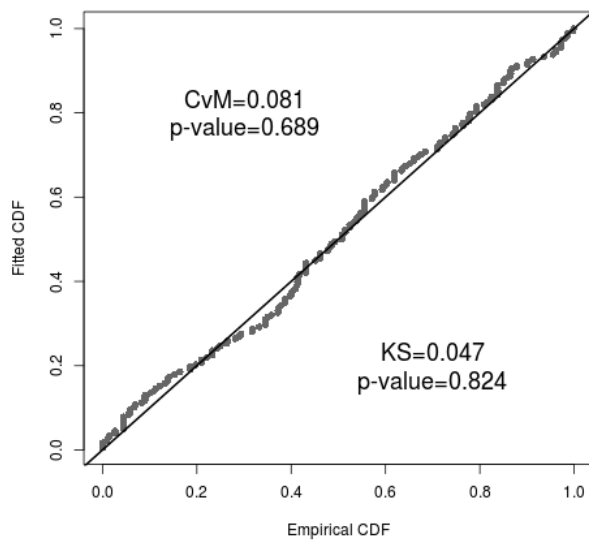
Figure F.11: Q-Q plot of the fitted and empirical cumulative density functions (CDF) for the fifth ranked model of the detection function analysis of the reduced summer data.
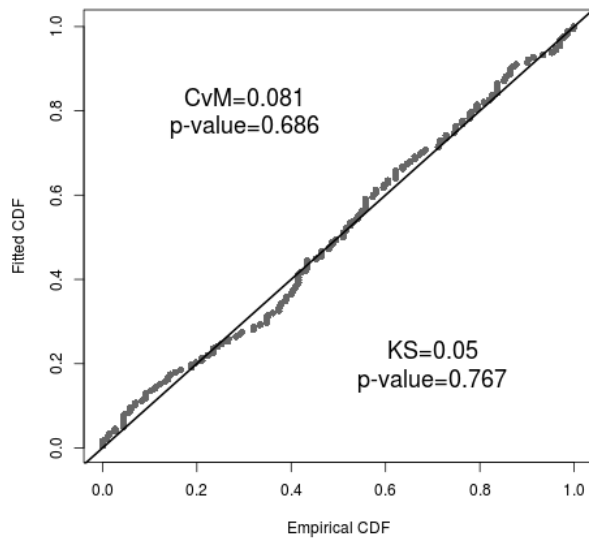
Figure F.12: Q-Q plot of the fitted and empirical cumulative density functions (CDF) for the sixth ranked model of the detection function analysis of the reduced summer data.
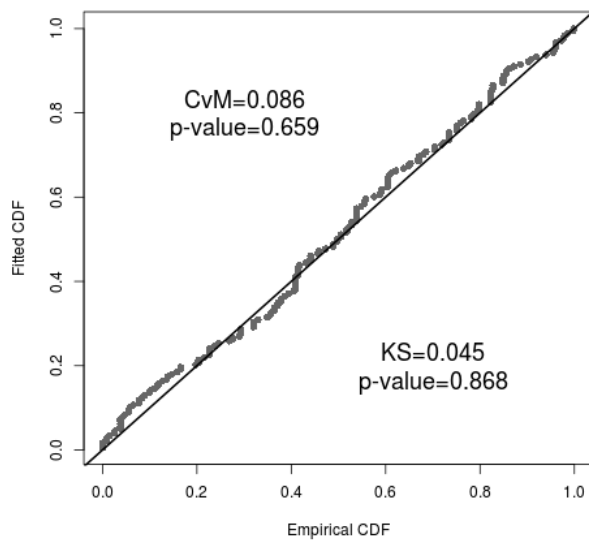
Figure F.13: Q-Q plot of the fitted and empirical cumulative density functions (CDF) for the seventh ranked model of the detection function analysis of the reduced summer data.
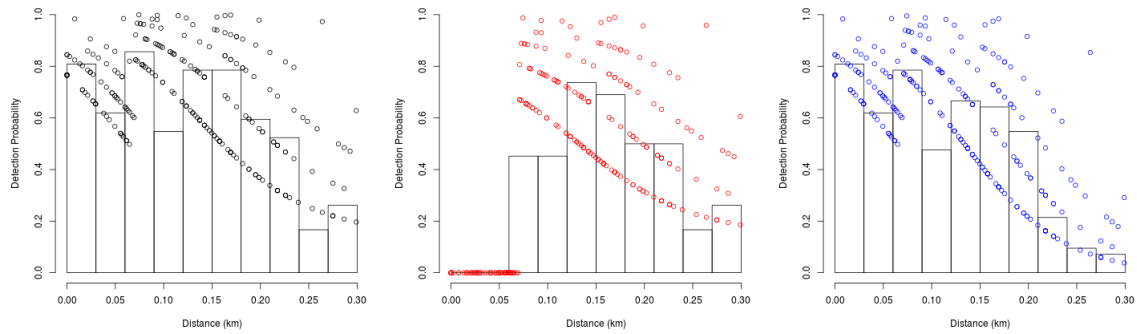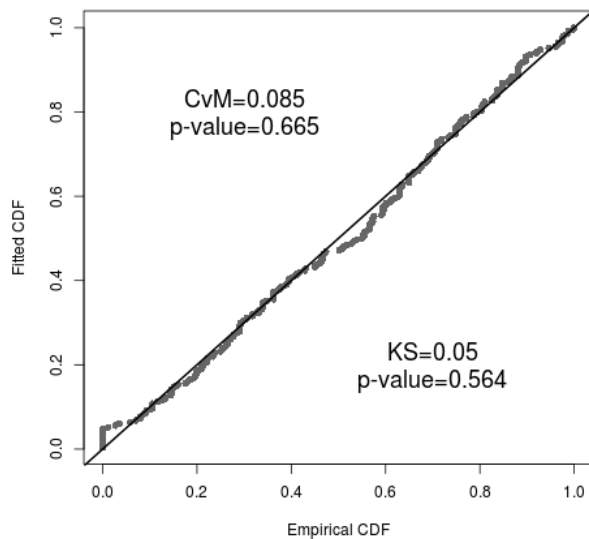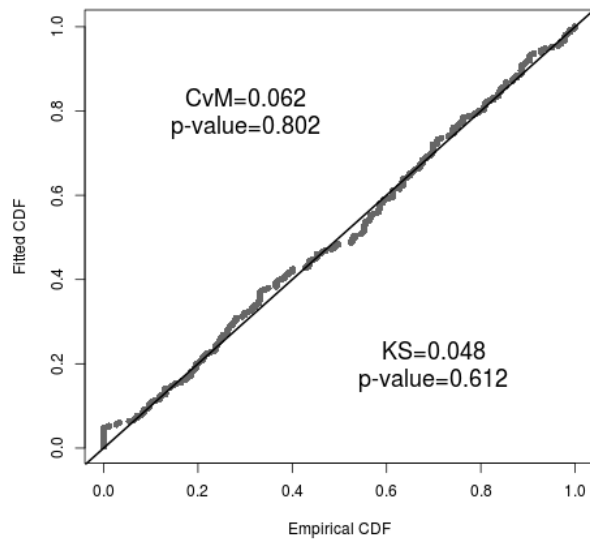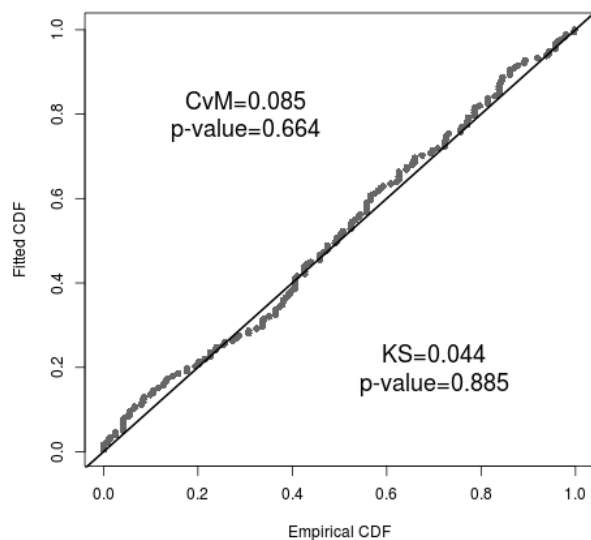

Figure F.14: Q-Q plot of the fitted and empirical cumulative density functions (CDF) for the eighth ranked model of the detection function analysis of the reduced summer data.
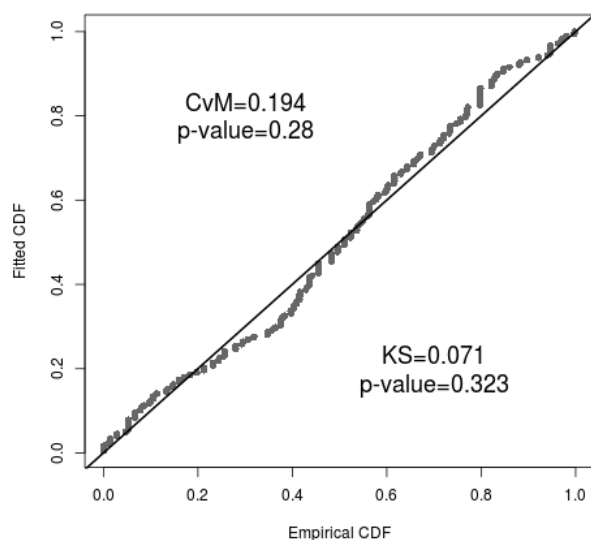
SECTION G: Diagnostic plots for detection function models fit to full WCSI winter sighting data; top eight models from Table 9

Figure G.1: Fitted detection functions and histograms of empirical detection probabilities from the top ranked model in Table 9. Left is $p_\bullet(d_i, s_i)$, **centre is** $p_F(d_i, s_i)$, **and right is** $p_R(d_i, s_i)$.
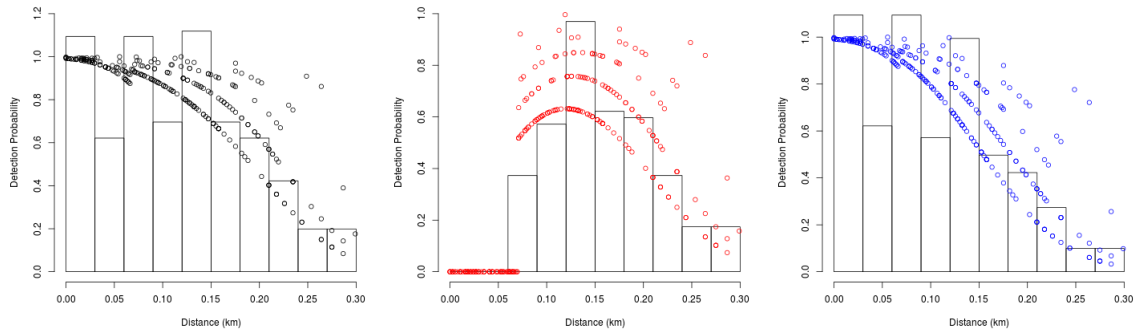
Figure G.2: Fitted detection functions and histograms of empirical detection probabilities from the second ranked model in Table 9. Left is $p_\bullet(d_i, s_i)$, **centre is** $p_F(d_i, s_i)$, **and right is** $p_R(d_i, s_i)$.
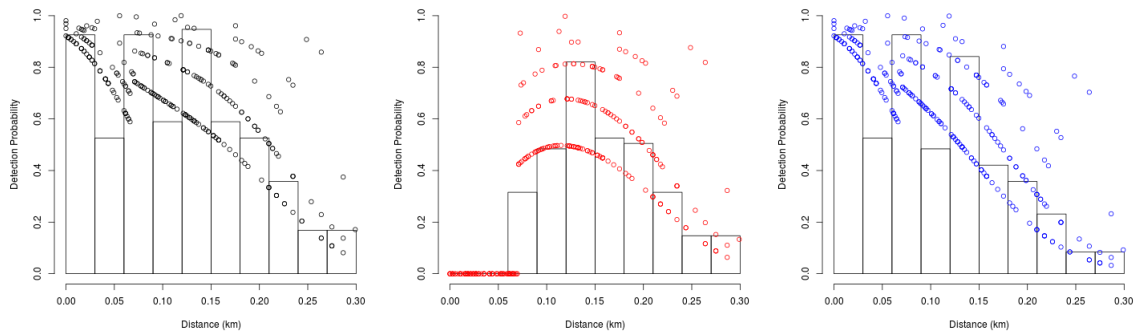
Figure G.3: Fitted detection functions and histograms of empirical detection probabilities from the third ranked model in Table 9. Left is $p_\bullet(d_i, s_i)$, **centre is** $p_F(d_i, s_i)$, **and right is** $p_R(d_i, s_i)$.
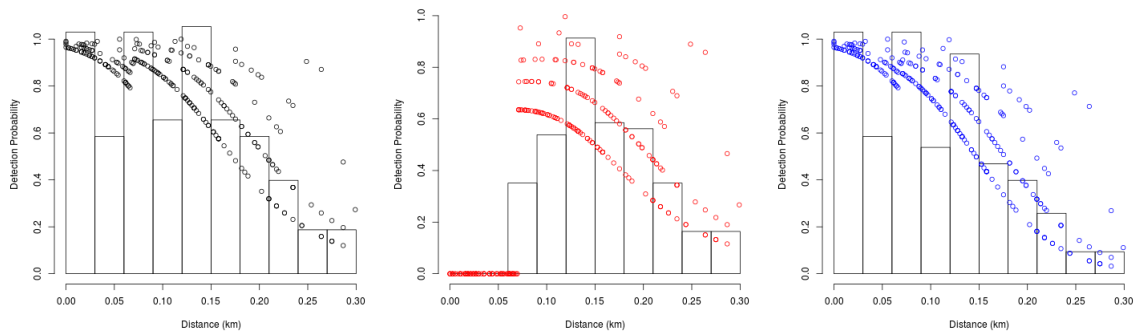
Figure G.4: Fitted detection functions and histograms of empirical detection probabilities from the fourth ranked model in Table 9. Left is $p_{\bullet}(d_i, s_i)$, centre is $p_F(d_i, s_i)$, and right is $p_R(d_i, s_i)$.
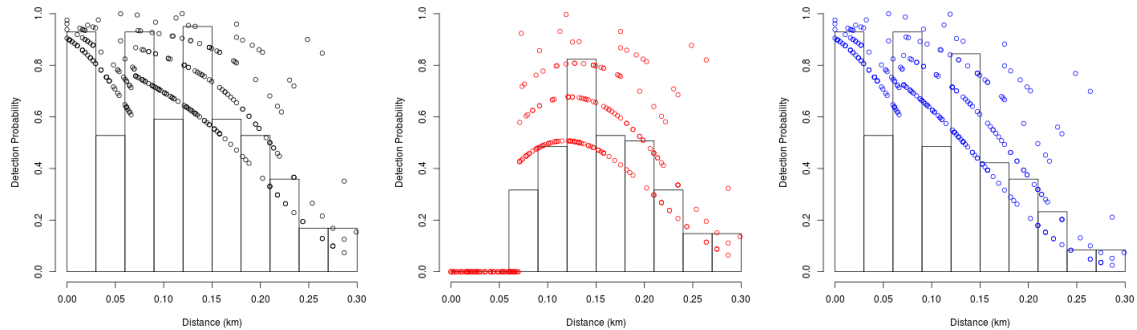
Figure G.5: Fitted detection functions and histograms of empirical detection probabilities from the fifth ranked model in Table 9. Left is $p_{\bullet}(d_i, s_i)$, centre is $p_F(d_i, s_i)$, and right is $p_R(d_i, s_i)$.
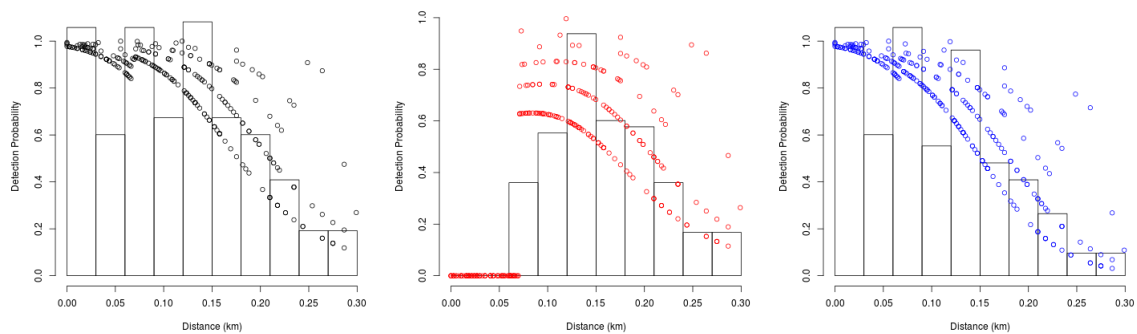
Figure G.6: Fitted detection functions and histograms of empirical detection probabilities from the sixth ranked model in Table 9. Left is $p_{\bullet}(d_i, s_i)$, centre is $p_F(d_i, s_i)$, and right is $p_R(d_i, s_i)$.
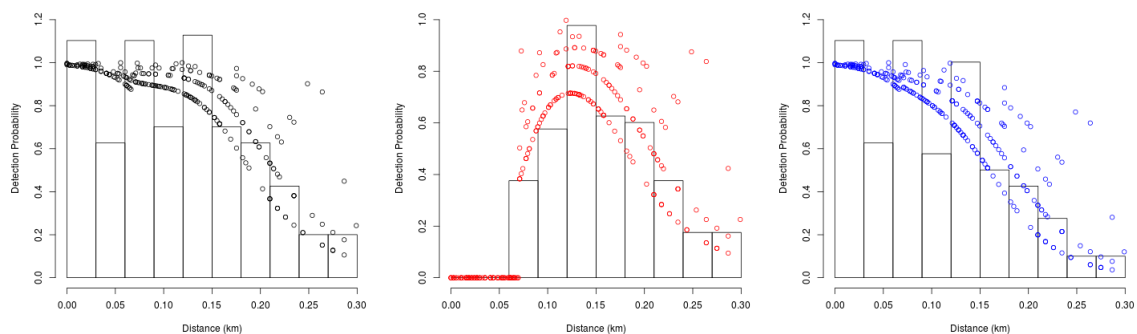
Figure G.7: Fitted detection functions and histograms of empirical detection probabilities from the seventh ranked model in Table 9. Left is $p_\bullet(d_i, s_i)$**, centre is** $p_F(d_i, s_i)$**, and right is** $p_R(d_i, s_i)$**.**
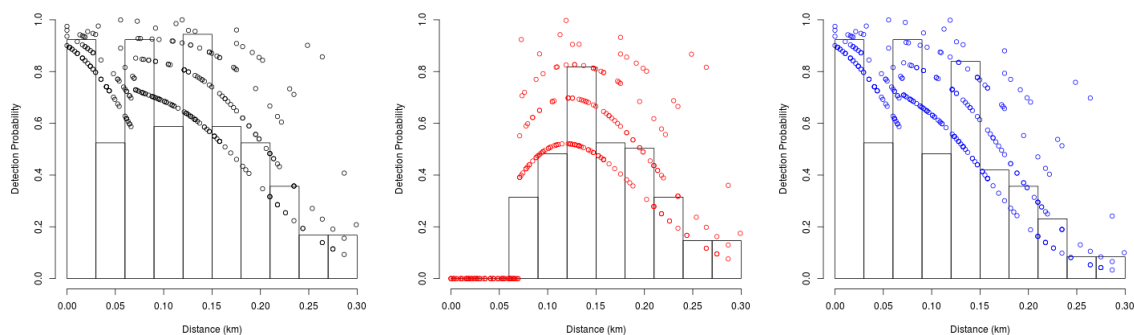
Figure G.8: Fitted detection functions and histograms of empirical detection probabilities from the eighth ranked model in Table 9. Left is $p_\bullet(d_i, s_i)$**, centre is** $p_F(d_i, s_i)$**, and right is** $p_R(d_i, s_i)$**.**
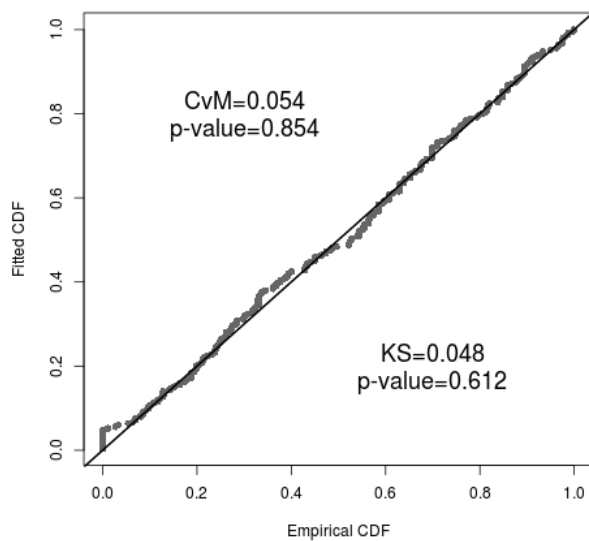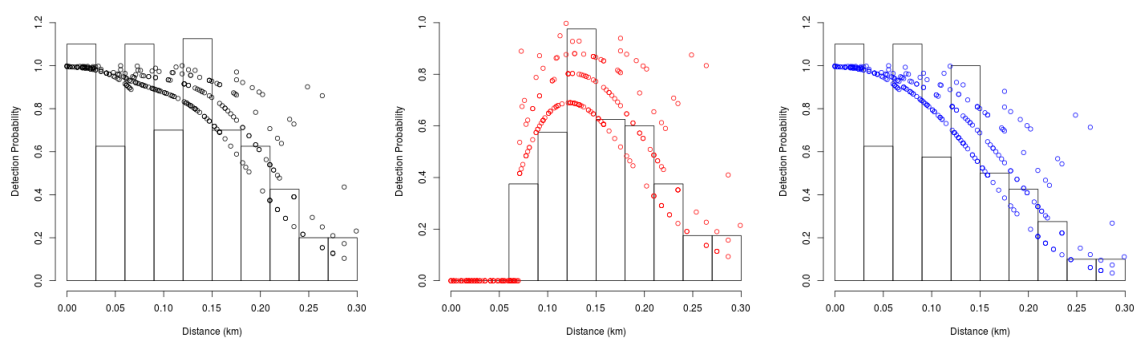
Figure G.9: Q-Q plot of the fitted and empirical cumulative density functions (CDF) for the top ranked model of the detection function analysis of the full winter data.
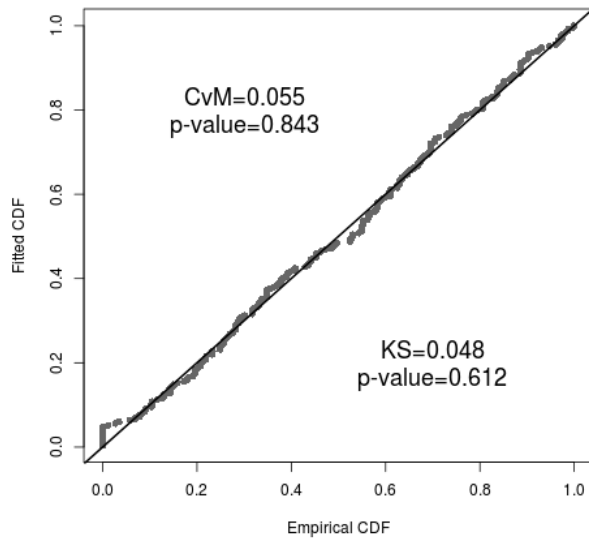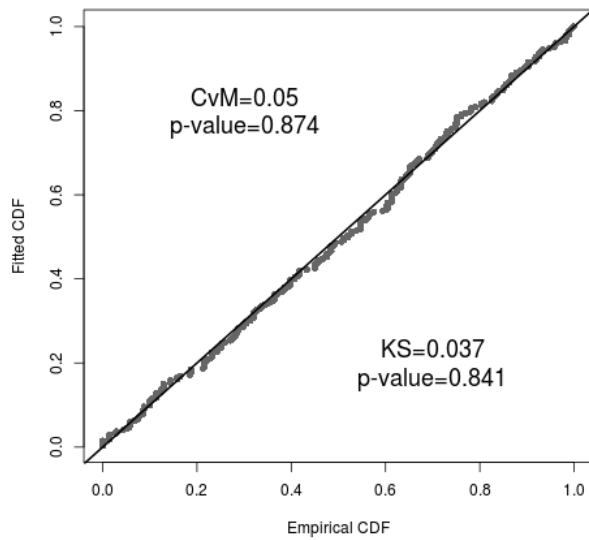

Figure G.10: Q-Q plot of the fitted and empirical cumulative density functions (CDF) for the second ranked model of the detection function analysis of the full winter data.
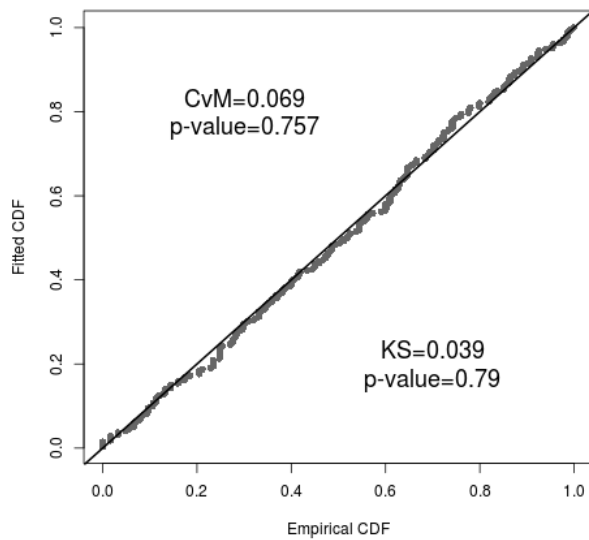
**Figure G.11: Q-Q plot of the fitted and empirical cumulative density functions (CDF) for the third ranked model of the detection function analysis of the full winter data.**

CvM=0.087
p-value=0.653

KS=0.043
p-value=0.687
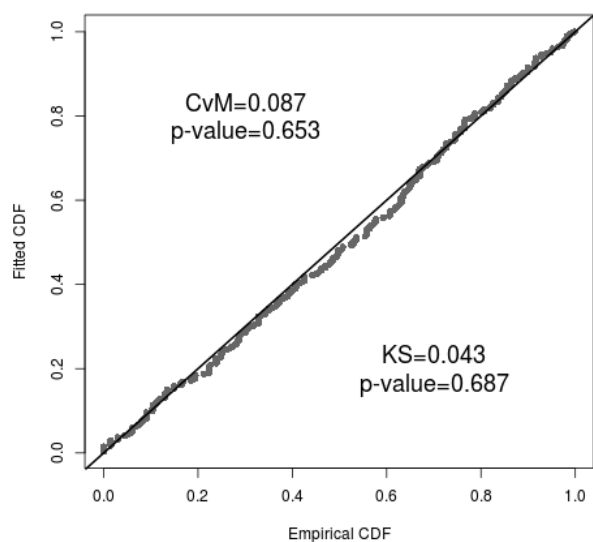
Figure G.12: Q-Q plot of the fitted and empirical cumulative density functions (CDF) for the fourth ranked model of the detection function analysis of the full winter data.

CvM=0.056
p-value=0.837

KS=0.036
p-value=0.862
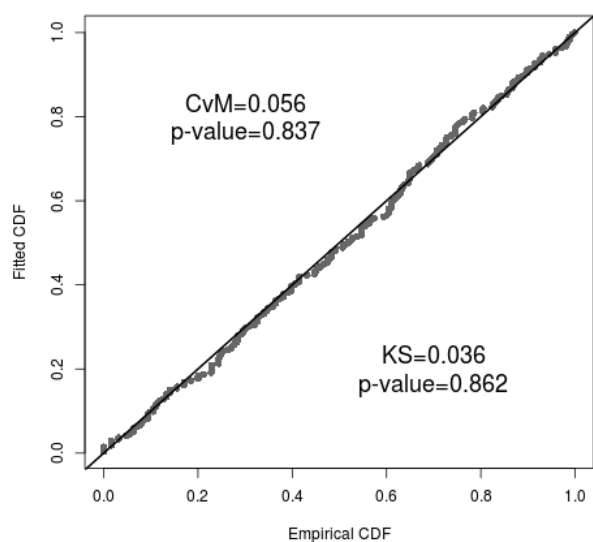
Figure G.13: Q-Q plot of the fitted and empirical cumulative density functions (CDF) for the fifth ranked model of the detection function analysis of the full winter data.
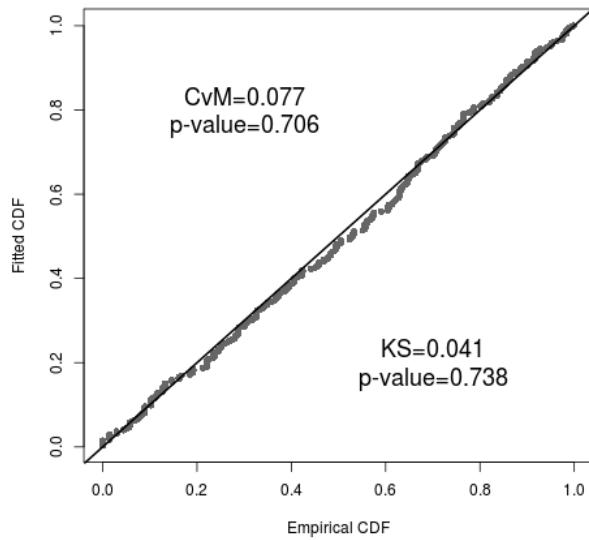
Figure G.14: Q-Q plot of the fitted and empirical cumulative density functions (CDF) for the sixth ranked model of the detection function analysis of the full winter data.
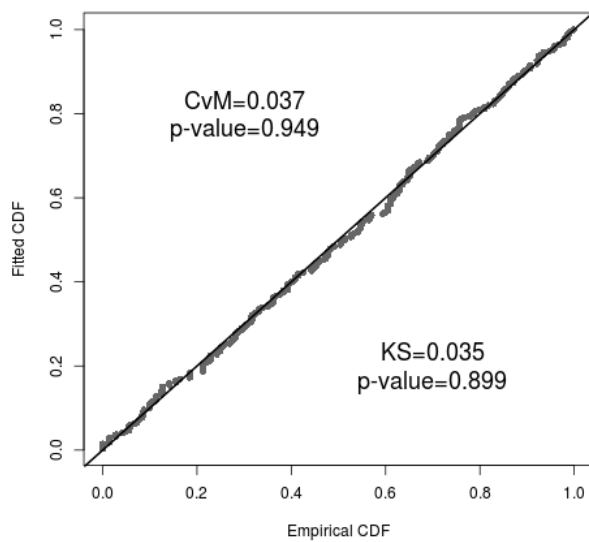
Figure G.15: Q-Q plot of the fitted and empirical cumulative density functions (CDF) for the seventh ranked model of the detection function analysis of the full winter data.
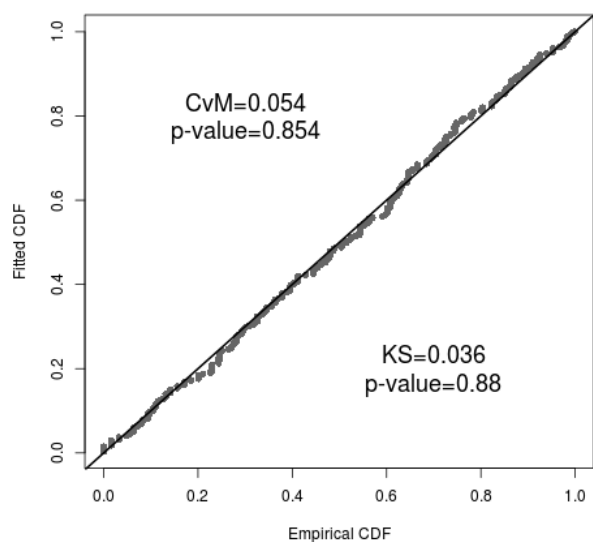
Figure G.16: Q-Q plot of the fitted and empirical cumulative density functions (CDF) for the eighth ranked model of the detection function analysis of the full winter data.
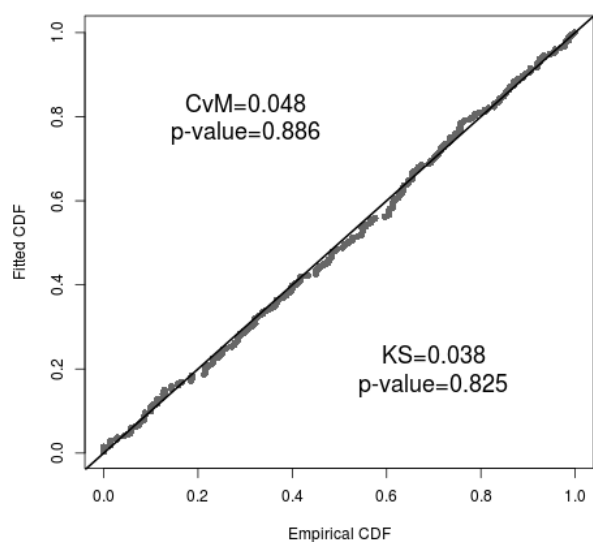
SECTION H: Diagnostic plots for detection function models fit to reduced WCSI winter sighting data; four models used for model averaging in Table 11
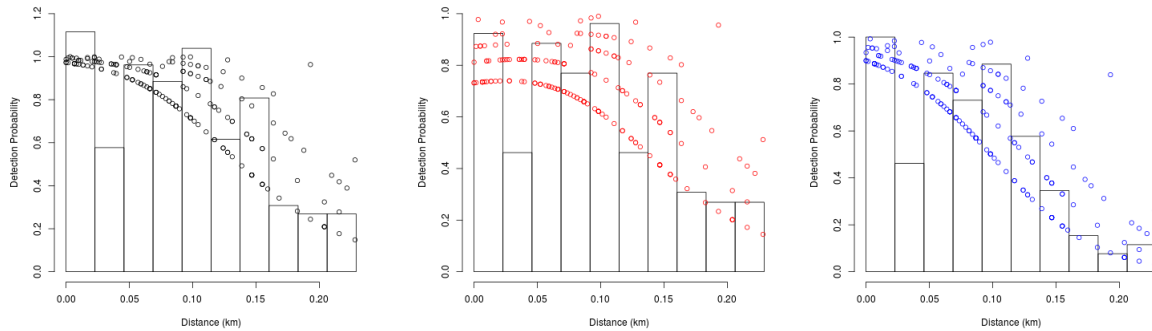
Figure H.1: Fitted detection functions and histograms of empirical detection probabilities from the second ranked model in Table 11. Left is $p_{\bullet}(d_i, s_i)$, centre is $p_F(d_i, s_i)$, and right is $p_R(d_i, s_i)$. Note that distance from the transect line has been rescaled such that an original distance of 0.071 km is now 0 km.
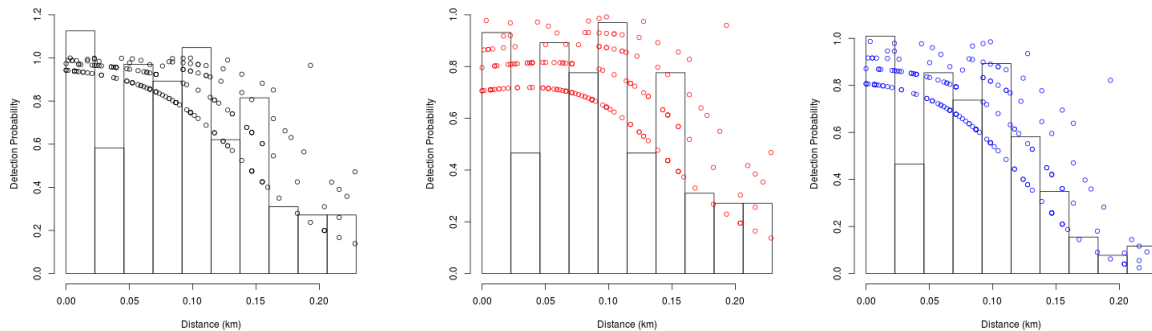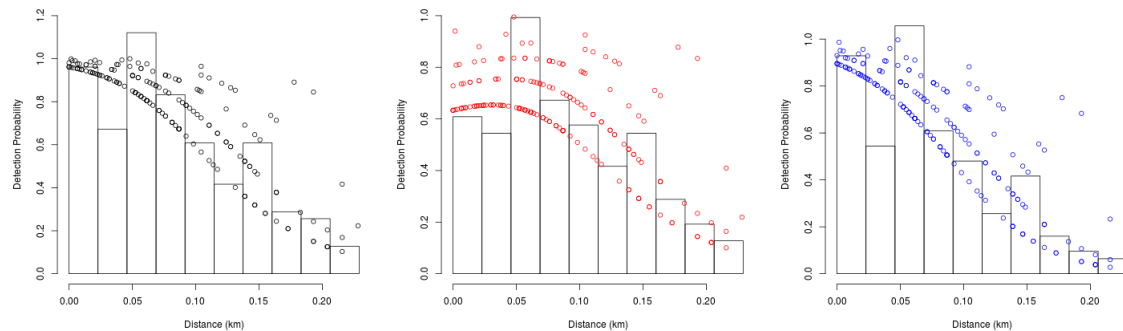

Figure H.2: Fitted detection functions and histograms of empirical detection probabilities from the fourth ranked model in Table 11. Left is $p_{\bullet}(d_i, s_i)$, centre is $p_F(d_i, s_i)$, and right is $p_R(d_i, s_i)$. Note that distance from the transect line has been rescaled such that an original distance of 0.071 km is now 0 km.
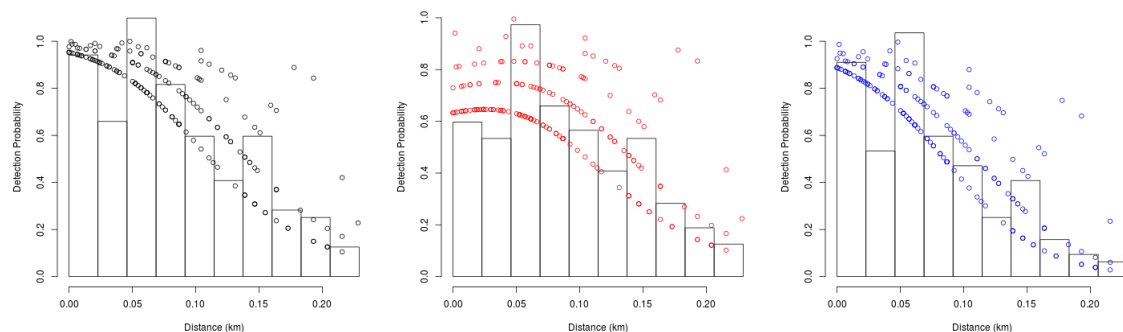
Figure H.3: Fitted detection functions and histograms of empirical detection probabilities from the sixth ranked model in Table 11. Left is $p_{\bullet}(d_i, s_i)$, centre is $p_F(d_i, s_i)$, and right is $p_R(d_i, s_i)$. Note that distance from the transect line has been rescaled such that an original distance of 0.071 km is now 0 km.
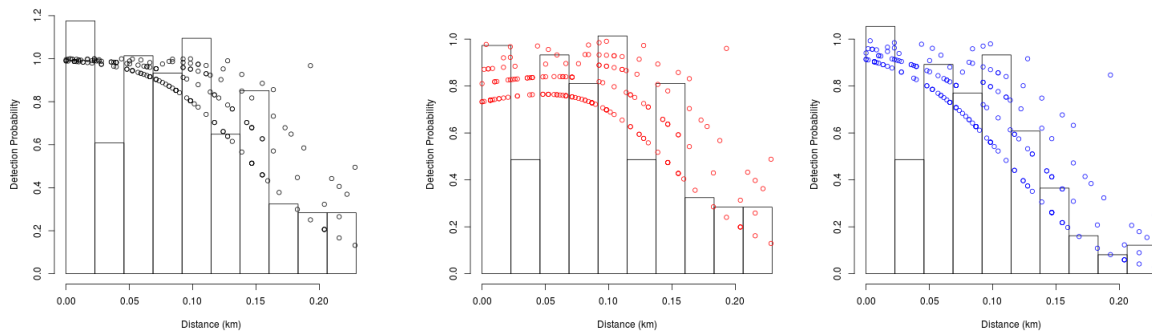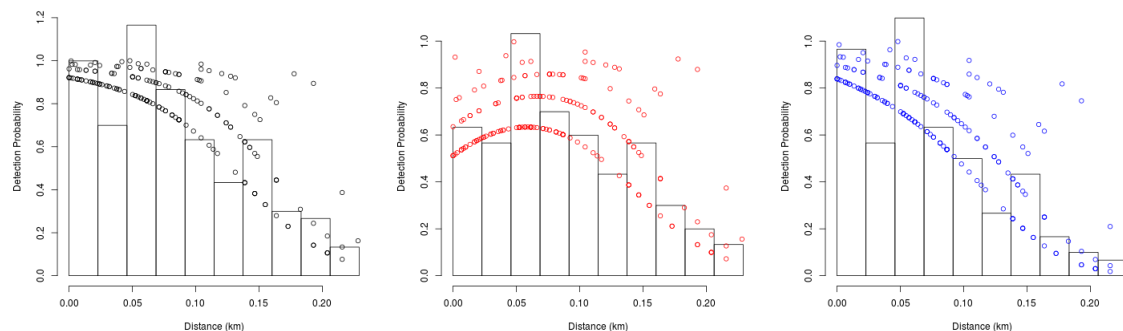
Figure H.4: Fitted detection functions and histograms of empirical detection probabilities from the ninth ranked model in Table 11. Left is $p_{\bullet}(d_i, s_i)$**, centre is** $p_F(d_i, s_i)$**, and right is** $p_R(d_i, s_i)$**. Note that distance from the transect line has been rescaled such that an original distance of 0.071 km is now 0 km.**
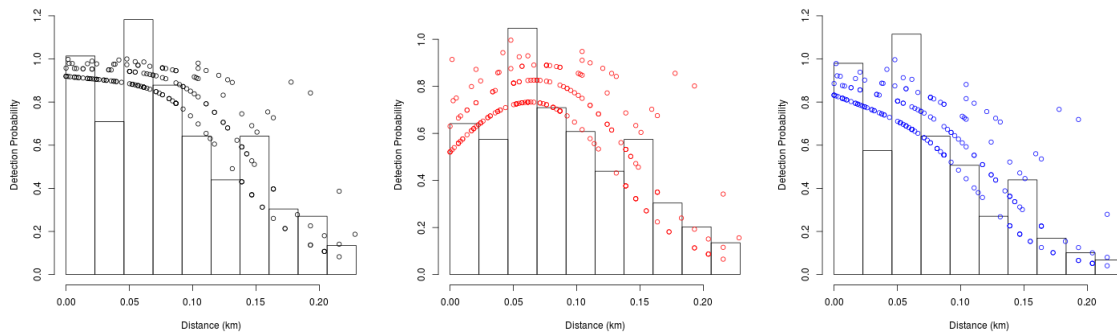

Figure H.5: Q-Q plot of the fitted and empirical cumulative density functions (CDF) for the second ranked model of the detection function analysis of the reduced winter data.
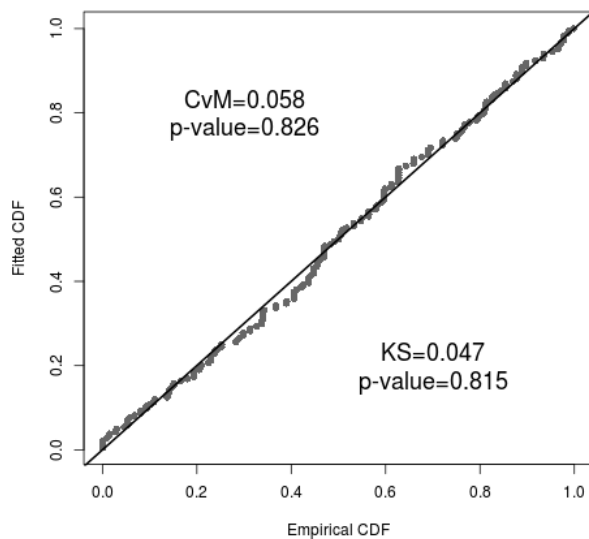
Figure H.6: Q-Q plot of the fitted and empirical cumulative density functions (CDF) for the fourth ranked model of the detection function analysis of the reduced winter data.
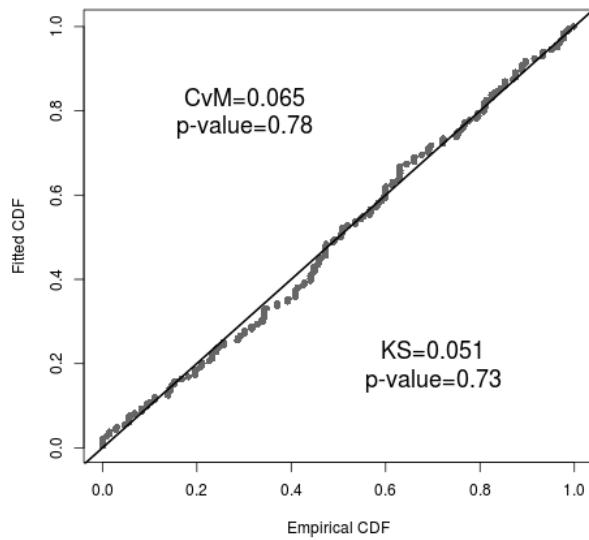
Figure H.7: Q-Q plot of the fitted and empirical cumulative density functions (CDF) for the sixth ranked model of the detection function analysis of the reduced winter data.
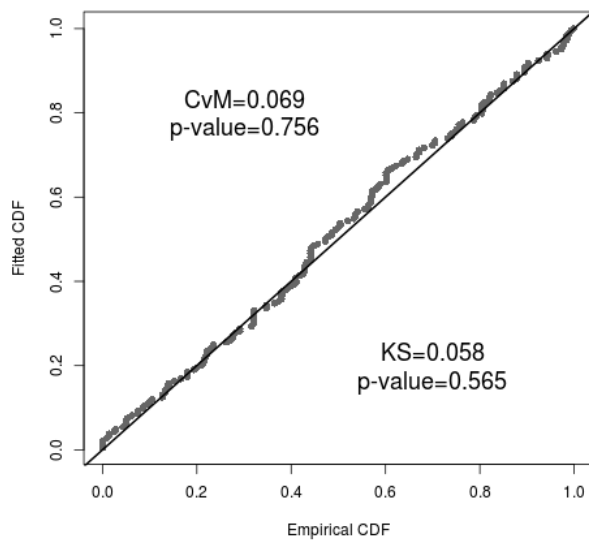
Figure H.8: Q-Q plot of the fitted and empirical cumulative density functions (CDF) for the ninth ranked model of the detection function analysis of the reduced winter data.
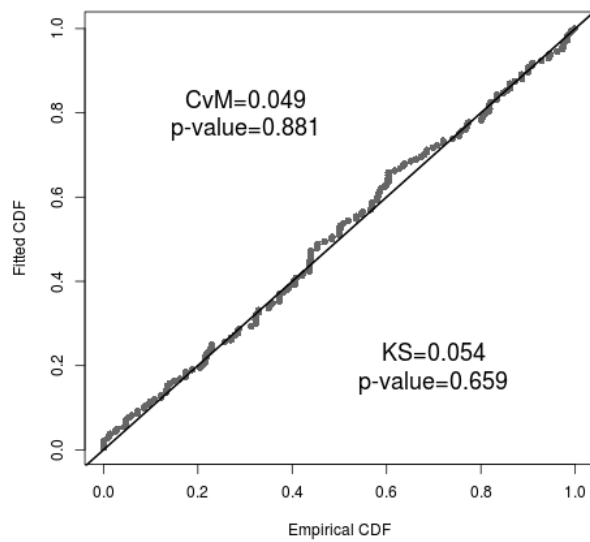
SECTION I: Model fitting summaries for analysis of circle-back availability data using the highly-ranked detection models for full, WCSI summer data set.

**Table I.1: Model selection summary for factors affecting summer availability as assessed from circle-back protocol, using the detection function from the top-ranked model in Table 5. Results presented are the relative difference in AIC values (ΔAIC), AIC model weights (*w*), twice the negative log-likelihood (-2*l*) and the number of parameters in the model (*NPar*). The '.' model assumes equal availability across all factors.**

Model	ΔAIC	*w*	-2*l*	*NPar*
.	0.00	0.48	108.40	1
offshore	0.89	0.31	107.30	2
region	2.60	0.13	107.00	3
region+offshore	3.69	0.08	106.09	4

Table I.2: Model selection summary for factors affecting summer availability as assessed from circle-back protocol, using the detection function from the second-ranked model in Table 5.

Model	ΔAIC	*w*	-2*l*	*NPar*
.	0.00	0.47	108.54	1
offshore	0.85	0.31	107.39	2
region	2.37	0.14	106.90	3
region+offshore	3.46	0.08	106.00	4

Table I.3: Model selection summary for factors affecting summer availability as assessed from circle-back protocol, using the detection function from the third-ranked model in Table 5.

Model	ΔAIC	*w*	-2*l*	*NPar*
.	0.00	0.50	108.44	1
offshore	0.94	0.31	107.39	2
region	2.87	0.12	107.32	3
region+offshore	3.97	0.07	106.42	4

Table I.4: Model selection summary for factors affecting summer availability as assessed from circle-back protocol, using the detection function from the fourth-ranked model in Table 5.

Model	ΔAIC	*w*	-2*l*	*NPar*
.	0.00	0.48	108.44	1
offshore	0.88	0.31	107.32	2
region	2.52	0.14	106.97	3
region+offshore	3.61	0.08	106.05	4

Table I.5: Model selection summary for factors affecting summer availability as assessed from circle-back protocol, using the detection function from the fifth-ranked model in Table 5. Results presented are the relative difference in AIC values (ΔAIC), AIC model weights (*w*), twice the negative log-likelihood (-2*l*) and the number of parameters in the model (*NPar*). The '.' model assumes equal availability across all factors.

Model	ΔAIC	*w*	-2*l*	*NPar*
.	0.00	0.49	108.40	1
offshore	0.91	0.31	107.31	2
region	2.73	0.13	107.13	3
region+offshore	3.82	0.07	106.22	4

Table I.6: Model selection summary for factors affecting summer availability as assessed from circle-back protocol, using the detection function from the sixth-ranked model in Table 5.

Model	ΔAIC	*w*	-2*l*	*NPar*
.	0.00	0.49	108.40	1
offshore	0.90	0.31	107.30	2
region	2.67	0.13	107.07	3
region+offshore	3.76	0.07	106.15	4

Table I.7: Model selection summary for factors affecting summer availability as assessed from circle-back protocol, using the detection function from the seventh-ranked model in Table 5.

Model	ΔAIC	*w*	-2*l*	*NPar*
.	0.00	0.42	109.39	1
offshore	0.78	0.29	108.17	2
region	1.63	0.19	107.02	3
region+offshore	2.85	0.10	106.24	4

SECTION J: Stratum-specific abundance and availability estimates using circle-back protocol from each detection function for full, WSCI summer data set.

Table J.1: Estimated Hector's dolphin abundance and circle-back availability estimate using the full sighting data and top-ranked model from Table 5.

Coastal Section	Offshore Stratum (nmi)	$\hat{N}_k$	SE	$\hat{P}_{\alpha k}$	SE
Whanganui Inlet	0–4			0.66	0.09
	4–12			0.57	0.18
	12–20			0.57	0.18
Hector	0–4	1117	268	0.66	0.09
	4–12	499	398	0.57	0.18
	12–20			0.57	0.18
Greymouth	0–4	1053	239	0.67	0.08
	4–12	50	48	0.58	0.18
	12–20			0.58	0.18
Okarito Lagoon	0–4	1052	226	0.70	0.09
	4–12	523	415	0.61	0.19
	12–20			0.61	0.19
Jackson Bay	0–4	169	101	0.67	0.08
	4–12			0.58	0.18
	12–20			0.58	0.18
Milford Sound	0–4	28	21	0.67	0.08
	4–12			0.58	0.18
	12–20			0.58	0.18
Total		**4490**	**845**		

Table J.2: Estimated Hector's dolphin abundance and circle-back availability estimate using the full sighting data and second-ranked model from Table 5.

Coastal Section	Offshore Stratum (nmi)	$\hat{N}_k$	SE	$\hat{P}_{\alpha k}$	SE
Whanganui Inlet	0–4			0.70	0.10
	4–12			0.60	0.20
	12–20			0.60	0.20
Hector	0–4	1107	272	0.70	0.10
	4–12	485	387	0.60	0.20
	12–20			0.60	0.20
Greymouth	0–4	1050	249	0.71	0.09
	4–12	51	50	0.61	0.20
	12–20			0.61	0.20
Okarito Lagoon	0–4	1042	237	0.75	0.10
	4–12	514	406	0.65	0.21
	12–20			0.65	0.21
Jackson Bay	0–4	171	102	0.71	0.09
	4–12			0.61	0.20
	12–20			0.61	0.20
Milford Sound	0–4	29	22	0.71	0.09
	4–12			0.61	0.20
	12–20			0.61	0.20
Total		**4450**	**870**		

Table J.3: Estimated Hector's dolphin abundance and circle-back availability estimate using the full sighting data and third-ranked model from Table 5.

Coastal Section	Offshore Stratum (nmi)	$\hat{N}_k$	SE	$\hat{P}_{\alpha k}$	SE
Whanganui Inlet	0–4			0.62	0.08
	4–12			0.53	0.17
	12–20			0.53	0.17
Hector	0–4	1137	271	0.62	0.08
	4–12	521	417	0.53	0.17
	12–20			0.53	0.17
Greymouth	0–4	1061	238	0.62	0.08
	4–12	48	46	0.54	0.17
	12–20			0.54	0.17
Okarito Lagoon	0–4	1068	222	0.65	0.08
	4–12	536	430	0.56	0.17
	12–20			0.56	0.17
Jackson Bay	0–4	167	100	0.62	0.08
	4–12			0.54	0.17
	12–20			0.54	0.17
Milford Sound	0–4	27	20	0.62	0.08
	4–12			0.54	0.17
	12–20			0.54	0.17
Total		**4565**	**855**		

Table J.4: Estimated Hector's dolphin abundance and circle-back availability estimate using the full sighting data and fourth-ranked model from Table 5.

Coastal Section	Offshore Stratum (nmi)	$\hat{N}_k$	SE	$\hat{P}_{\alpha k}$	SE
Whanganui Inlet	0–4			0.67	0.09
	4–12			0.58	0.19
	12–20			0.58	0.19
Hector	0–4	1113	293	0.67	0.09
	4–12	494	395	0.58	0.19
	12–20			0.58	0.19
Greymouth	0–4	1051	282	0.69	0.08
	4–12	50	50	0.59	0.19
	12–20			0.59	0.19
Okarito Lagoon	0–4	1048	267	0.72	0.10
	4–12	520	417	0.62	0.20
	12–20			0.62	0.20
Jackson Bay	0–4	170	105	0.69	0.08
	4–12			0.59	0.19
	12–20			0.59	0.19
Milford Sound	0–4	29	22	0.69	0.08
	4–12			0.59	0.19
	12–20			0.59	0.19
Total		**4476**	**1002**		

Table J.5: Estimated Hector's dolphin abundance and circle-back availability estimate using the full sighting data and fifth-ranked model from Table 5.

Coastal Section	Offshore Stratum (nmi)	$\hat{N}_k$	SE	$\hat{P}_{\alpha k}$	SE
Whanganui Inlet	0–4			0.66	0.09
	4–12			0.56	0.18
	12–20			0.56	0.18
Hector	0–4	1113	285	0.66	0.09
	4–12	501	400	0.56	0.18
	12–20			0.56	0.18
Greymouth	0–4	1045	269	0.66	0.08
	4–12	48	48	0.57	0.18
	12–20			0.57	0.18
Okarito Lagoon	0–4	1048	253	0.69	0.09
	4–12	522	420	0.60	0.19
	12–20			0.60	0.19
Jackson Bay	0–4	167	103	0.66	0.08
	4–12			0.57	0.18
	12–20			0.57	0.18
Milford Sound	0–4	27	21	0.66	0.08
	4–12			0.57	0.18
	12–20			0.57	0.18
Total		**4471**	**960**		

Table J.6: Estimated Hector's dolphin abundance and circle-back availability estimate using the full sighting data and sixth-ranked model from Table 5.

Coastal Section	Offshore Stratum (nmi)	$\hat{N}_k$	SE	$\hat{P}_{\alpha k}$	SE
Whanganui Inlet	0–4			0.65	0.09
	4–12			0.56	0.18
	12–20			0.56	0.18
Hector	0–4	1113	270	0.65	0.09
	4–12	501	401	0.56	0.18
	12–20			0.56	0.18
Greymouth	0–4	1046	243	0.66	0.08
	4–12	49	48	0.57	0.18
	12–20			0.57	0.18
Okarito Lagoon	0–4	1047	229	0.69	0.09
	4–12	522	417	0.60	0.19
	12–20			0.60	0.19
Jackson Bay	0–4	167	100	0.66	0.08
	4–12			0.57	0.18
	12–20			0.57	0.18
Milford Sound	0–4	28	21	0.66	0.08
	4–12			0.57	0.18
	12–20			0.57	0.18
Total		**4473**	**864**		

Table J.7: Estimated Hector's dolphin abundance and circle-back availability estimate using the full sighting data and seventh-ranked model from Table 5.

Coastal Section	Offshore Stratum (nmi)	$\hat{N}_k$	SE	$\hat{P}_{\alpha k}$	SE
Whanganui Inlet	0–4			0.75	0.12
	4–12			0.64	0.22
	12–20			0.64	0.22
Hector	0–4	1105	300	0.75	0.12
	4–12	466	372	0.64	0.22
	12–20			0.64	0.22
Greymouth	0–4	1057	290	0.79	0.10
	4–12	56	56	0.68	0.22
	12–20			0.68	0.22
Okarito Lagoon	0–4	1029	276	0.84	0.12
	4–12	495	389	0.74	0.24
	12–20			0.74	0.24
Jackson Bay	0–4	177	108	0.79	0.10
	4–12			0.68	0.22
	12–20			0.68	0.22
Milford Sound	0–4	32	25	0.79	0.10
	4–12			0.68	0.22
	12–20			0.68	0.22
Total		**4416**	**997**		

SECTION K: Model fitting summaries for analysis of circle-back availability data using the highly -ranked detection model for reduced, WCSI summer data set.

Table K.1: Model selection summary for factors affecting summer availability as assessed from circle-back protocol, using the reduced sighting data set and detection function from the top-ranked model in Table 7. Results presented are the relative difference in AIC values (ΔAIC), AIC model weights (*w*), twice the negative log-likelihood (*-2l*) and the number of parameters in the model (*NPar*). The '.' model assumes equal availability across all factors.

Model	ΔAIC	w	-2l	NPar
.	0.00	0.63	59.95	1
offshore	1.91	0.24	59.86	2
region	3.75	0.10	59.70	3
region+offshore	5.64	0.04	59.59	4

Table K.2: Model selection summary for factors affecting summer availability as assessed from circle-back protocol, using the reduced sighting data set and detection function from the second-ranked model in Table 7.

Model	ΔAIC	w	-2l	NPar
.	0.00	0.63	59.95	1
offshore	1.91	0.24	59.86	2
region	3.75	0.10	59.70	3
region+offshore	5.64	0.04	59.59	4

Table K.3: Model selection summary for factors affecting summer availability as assessed from circle-back protocol, using the reduced sighting data set and detection function from the third-ranked model in Table 7.

Model	ΔAIC	w	-2l	NPar
.	0.00	0.62	59.89	1
offshore	1.91	0.24	59.79	2
region	3.70	0.10	59.59	3
region+offshore	5.57	0.04	59.45	4

Table K.4: Model selection summary for factors affecting summer availability as assessed from circle-back protocol, using the reduced sighting data set and detection function from the fifth-ranked model in Table 7.

Model	ΔAIC	w	-2l	NPar
.	0.00	0.63	59.95	1
offshore	1.91	0.24	59.86	2
region	3.75	0.10	59.70	3
region+offshore	5.64	0.04	59.59	4

Table K.5: Model selection summary for factors affecting summer availability as assessed from circle-back protocol, using the reduced sighting data set and detection function from the sixth-ranked model in Table 7. Results presented are the relative difference in AIC values (ΔAIC), AIC model weights (*w*), twice the negative log-likelihood (*-2l*) and the number of parameters in the model (*NPar*). The '.' model assumes equal availability across all factors.

Model	ΔAIC	*w*	*-2l*	*NPar*
.	0.00	0.63	61.22	1
offshore	1.95	0.24	61.17	2
region	3.67	0.10	60.89	3
region+offshore	5.67	0.04	60.89	4

Table K.6: Model selection summary for factors affecting summer availability as assessed from circle-back protocol, using the reduced sighting data set and detection function from the seventh-ranked model in Table 7.

Model	ΔAIC	*w*	*-2l*	*NPar*
.	0.00	0.62	59.92	1
offshore	1.90	0.24	59.81	2
region	3.72	0.10	59.63	3
region+offshore	5.60	0.04	59.51	4

Table K.7: Model selection summary for factors affecting summer availability as assessed from circle-back protocol, using the reduced sighting data set and detection function from the eighth-ranked model in Table 7.

Model	ΔAIC	*w*	*-2l*	*NPar*
.	0.00	0.63	61.08	1
offshore	1.96	0.24	61.04	2
region	3.68	0.10	60.77	3
region+offshore	5.68	0.04	60.77	4

SECTION L: Stratum-specific abundance and availability estimates using circle-back protocol from each detection function for reduced, WCSI summer data set.

Table L.1: Estimated Hector's dolphin abundance and circle-back availability estimate using the reduced sighting data and top-ranked model from Table 7.

Coastal Section	Offshore Stratum (nmi)	$\hat{N}_k$	SE	$\hat{P}_{\alpha k}$	SE
West Haven Inlet	0–4			0.60	0.11
	4–12			0.57	0.18
	12–20			0.57	0.18
Hector	0–4	1305	375	0.60	0.11
	4–12	361	262	0.57	0.18
	12–20			0.57	0.18
Greymouth	0–4	1123	361	0.59	0.12
	4–12	73	71	0.56	0.19
	12–20			0.56	0.19
Okarito Lagoon	0–4	1219	318	0.60	0.11
	4–12	578	486	0.57	0.19
	12–20			0.57	0.19
Jackson Bay	0–4	124	112	0.59	0.12
	4–12			0.56	0.19
	12–20			0.56	0.19
Milford Sound	0–4	46	35	0.59	0.12
	4–12			0.56	0.19
	12–20			0.56	0.19
Total		**4829**	**1103**		

Table L.2: Estimated Hector's dolphin abundance and circle-back availability estimate using the reduced sighting data and second-ranked model from Table 7.

Coastal Section	Offshore Stratum (nmi)	$\hat{N}_k$	SE	$\hat{P}_{\alpha k}$	SE
West Haven Inlet	0–4			0.59	0.11
	4–12			0.57	0.18
	12–20			0.57	0.18
Hector	0–4	1307	377	0.59	0.11
	4–12	363	264	0.57	0.18
	12–20			0.57	0.18
Greymouth	0–4	1124	363	0.58	0.12
	4–12	73	71	0.55	0.19
	12–20			0.55	0.19
Okarito Lagoon	0–4	1219	321	0.60	0.11
	4–12	580	488	0.57	0.19
	12–20			0.57	0.19
Jackson Bay	0–4	124	112	0.58	0.12
	4–12			0.55	0.19
	12–20			0.55	0.19
Milford Sound	0–4	46	35	0.58	0.12
	4–12			0.55	0.19
	12–20			0.55	0.19
Total		**4836**	**1112**		

Table L.3: Estimated Hector's dolphin abundance and circle-back availability estimate using the reduced sighting data and third-ranked model from Table 7.

Coastal Section	Offshore Stratum (nmi)	$\hat{N}_k$	SE	$\hat{P}_{\alpha k}$	SE
West Haven Inlet	0–4			0.57	0.11
	4–12			0.54	0.18
	12–20			0.54	0.18
Hector	0–4	1327	390	0.57	0.11
	4–12	373	271	0.54	0.18
	12–20			0.54	0.18
Greymouth	0–4	1138	374	0.55	0.12
	4–12	71	70	0.53	0.18
	12–20			0.53	0.18
Okarito Lagoon	0–4	1229	329	0.57	0.11
	4–12	587	498	0.54	0.18
	12–20			0.54	0.18
Jackson Bay	0–4	124	113	0.55	0.12
	4–12			0.53	0.18
	12–20			0.53	0.18
Milford Sound	0–4	45	35	0.55	0.12
	4–12			0.53	0.18
	12–20			0.53	0.18
Total		**4894**	**1149**		

Table L.4: Estimated Hector's dolphin abundance and circle-back availability estimate using the reduced sighting data and fifth-ranked model from Table 7.

Coastal Section	Offshore Stratum (nmi)	$\hat{N}_k$	SE	$\hat{P}_{\alpha k}$	SE
West Haven Inlet	0–4			0.59	0.11
	4–12			0.57	0.18
	12–20			0.57	0.18
Hector	0–4	1307	448	0.59	0.11
	4–12	363	266	0.57	0.18
	12–20			0.57	0.18
Greymouth	0–4	1124	457	0.58	0.12
	4–12	73	79	0.55	0.19
	12–20			0.55	0.19
Okarito Lagoon	0–4	1219	463	0.60	0.11
	4–12	580	509	0.57	0.19
	12–20			0.57	0.19
Jackson Bay	0–4	124	119	0.58	0.12
	4–12			0.55	0.19
	12–20			0.55	0.19
Milford Sound	0–4	46	41	0.58	0.12
	4–12			0.55	0.19
	12–20			0.55	0.19
Total		**4835**	**1589**		

Table L.5: Estimated Hector's dolphin abundance and circle-back availability estimate using the reduced sighting data and sixth-ranked model from Table 7.

Coastal Section	Offshore Stratum (nmi)	$\hat{N}_k$	SE	$\hat{P}_{\alpha k}$	SE
West Haven Inlet	0–4			0.70	0.13
	4–12			0.68	0.22
	12–20			0.68	0.22
Hector	0–4	1321	513	0.70	0.13
	4–12	332	248	0.68	0.22
	12–20			0.68	0.22
Greymouth	0–4	1163	548	0.70	0.14
	4–12	90	102	0.68	0.24
	12–20			0.68	0.24
Okarito Lagoon	0–4	1304	603	0.72	0.13
	4–12	603	527	0.70	0.22
	12–20			0.70	0.22
Jackson Bay	0–4	138	136	0.70	0.14
	4–12			0.68	0.24
	12–20			0.68	0.24
Milford Sound	0–4	58	55	0.70	0.14
	4–12			0.68	0.24
	12–20			0.68	0.24
Total		**5009**	**2014**		

Table L.6: Estimated Hector's dolphin abundance and circle-back availability estimate using the reduced sighting data and seventh-ranked model from Table 7.

Coastal Section	Offshore Stratum (nmi)	$\hat{N}_k$	SE	$\hat{P}_{\alpha k}$	SE
West Haven Inlet	0–4			0.52	0.10
	4–12			0.50	0.16
	12–20			0.50	0.16
Hector	0–4	1446	435	0.52	0.10
	4–12	402	292	0.50	0.16
	12–20			0.50	0.16
Greymouth	0–4	1246	427	0.51	0.11
	4–12	82	83	0.49	0.17
	12–20			0.49	0.17
Okarito Lagoon	0–4	1355	396	0.52	0.10
	4–12	651	553	0.50	0.17
	12–20			0.50	0.17
Jackson Bay	0–4	138	126	0.51	0.11
	4–12			0.49	0.17
	12–20			0.49	0.17
Milford Sound	0–4	52	42	0.51	0.11
	4–12			0.49	0.17
	12–20			0.49	0.17
Total		**5371**	**1368**		

Table L.7: Estimated Hector's dolphin abundance and circle-back availability estimate using the reduced sighting data and eighth-ranked model from Table 7.

Coastal Section	Offshore Stratum (nmi)	$\hat{N}_k$	SE	$\hat{P}_{\alpha k}$	SE
West Haven Inlet	0–4			0.75	0.14
	4–12			0.73	0.24
	12–20			0.73	0.24
Hector	0–4	1227	413	0.75	0.14
	4–12	309	229	0.73	0.24
	12–20			0.73	0.24
Greymouth	0–4	1079	431	0.75	0.15
	4–12	82	87	0.73	0.26
	12–20			0.73	0.26
Okarito Lagoon	0–4	1208	452	0.77	0.14
	4–12	555	463	0.75	0.24
	12–20			0.75	0.24
Jackson Bay	0–4	128	120	0.75	0.15
	4–12			0.73	0.26
	12–20			0.73	0.26
Milford Sound	0–4	53	45	0.75	0.15
	4–12			0.73	0.26
	12–20			0.73	0.26
Total		**4640**	**1496**		

SECTION M: Model fitting summaries for analysis of circle-back availability data using the highly-ranked detection model for full, winter data set.

Table M.1: Model selection summary for factors affecting winter availability as assessed from circle-back protocol, using the detection function from the top-ranked model in Table 9. Parameters given are the relative difference in AIC values (ΔAIC), AIC model weights (*w*), twice the negative log-likelihood (-2*l*) and the number of parameters in the model (*NPar*). The '.' model assumes equal availability across all factors.

Model	ΔAIC	*w*	*-2l*	*NPar*
.	0.00	0.59	145.35	1
offshore	1.83	0.24	145.18	2
region	3.22	0.12	144.57	3
region+offshore	4.83	0.05	144.18	4

Table M.2: : Model selection summary for factors affecting winter availability as assessed from circle-back protocol, using the detection function from the second-ranked model in Table 9.

Model	ΔAIC	*w*	*-2l*	*NPar*
.	0.00	0.60	144.27	1
offshore	1.84	0.24	144.11	2
region	3.27	0.12	143.54	3
region+offshore	4.92	0.05	143.19	4

Table M.3: Model selection summary for factors affecting winter availability as assessed from circle-back protocol, using the detection function from the third-ranked model in Table 9.

Model	ΔAIC	*w*	*-2l*	*NPar*
.	0.00	0.60	142.44	1
offshore	1.87	0.24	142.30	2
region	3.38	0.11	141.82	3
region+offshore	5.09	0.05	141.53	4

Table M.4: Model selection summary for factors affecting winter availability as assessed from circle-back protocol, using the detection function from the fourth-ranked model in Table 9.

Model	ΔAIC	*w*	*-2l*	*NPar*
.	0.00	0.60	142.64	1
offshore	1.86	0.24	142.50	2
region	3.36	0.11	142.01	3
region+offshore	5.07	0.05	141.71	4

Table M.5: Model selection summary for factors affecting winter availability as assessed from circle-back protocol, using the detection function from the fifth-ranked model in Table 9. Parameters given are the relative difference in AIC values (ΔAIC), AIC model weights (w), twice the negative log-likelihood (-2l) and the number of parameters in the model (NPar). The '.' model assumes equal availability across all factors.

Model	ΔAIC	w	-2l	NPar
.	0.00	0.59	144.70	1
offshore	1.84	0.24	144.54	2
region	3.25	0.12	143.95	3
region+offshore	4.88	0.05	143.58	4

Table M.6: Model selection summary for factors affecting winter availability as assessed from circle-back protocol, using the detection function from the sixth-ranked model in Table 9

Model	ΔAIC	w	-2l	NPar
.	0.00	0.59	145.61	1
offshore	1.83	0.24	145.43	2
region	3.20	0.12	144.81	3
region+offshore	4.80	0.05	144.41	4

Table M.7: Model selection summary for factors affecting winter availability as assessed from circle-back protocol, using the detection function from the seventh-ranked model in Table 9.

Model	ΔAIC	w	-2l	NPar
.	0.00	0.59	145.57	1
offshore	1.83	0.24	145.40	2
region	3.20	0.12	144.77	3
region+offshore	4.81	0.05	144.38	4

Table M.8: Model selection summary for factors affecting winter availability as assessed from circle-back protocol, using the detection function from the eighth-ranked model in Table 9.

Model	ΔAIC	w	-2l	NPar
.	0.00	0.60	142.56	1
offshore	1.86	0.24	142.42	2
region	3.37	0.11	141.93	3
region+offshore	5.08	0.05	141.63	4

SECTION N: Stratum-specific abundance and availability estimates using circle-back protocol from each detection function for full, winter data set.

Table N.1: Estimated Hector's dolphin abundance and circle-back availability estimate using the full sighting data and top-ranked model from Table 9.

Coastal Section	Offshore Stratum (nmi)	$\hat{N}_k$	SE	$\hat{P}_{\alpha k}$	SE
Whanganui Inlet	0–4	182	138	0.49	0.08
	4–12			0.51	0.09
	12–20			0.51	0.09
Hector	0–4	777	200	0.49	0.08
	4–12	257	88	0.51	0.09
	12–20			0.51	0.09
Greymouth	0–4	1683	363	0.51	0.07
	4–12	475	274	0.53	0.09
	12–20			0.53	0.09
Okarito Lagoon	0–4	1177	281	0.50	0.07
	4–12	375	144	0.52	0.09
	12–20			0.52	0.09
Jackson Bay	0–4	595	255	0.51	0.07
	4–12			0.53	0.09
	12–20			0.53	0.09
Milford Sound	0–4			0.51	0.07
	4–12			0.53	0.09
	12–20			0.53	0.09
Total		**5519**	**903**		

Table N.2: Estimated Hector's dolphin abundance and circle-back availability estimate using the full sighting data and second-ranked model from Table 9.

Coastal Section	Offshore Stratum (nmi)	$\hat{N}_k$	SE	$\hat{P}_{\alpha k}$	SE
Whanganui Inlet	0–4	184	140	0.52	0.08
	4–12			0.54	0.10
	12–20			0.54	0.10
Hector	0–4	770	198	0.52	0.08
	4–12	257	88	0.54	0.10
	12–20			0.54	0.10
Greymouth	0–4	1648	354	0.54	0.08
	4–12	468	268	0.56	0.10
	12–20			0.56	0.10
Okarito Lagoon	0–4	1161	277	0.54	0.08
	4–12	374	143	0.55	0.09
	12–20			0.55	0.09
Jackson Bay	0–4	585	248	0.54	0.08
	4–12			0.56	0.10
	12–20			0.56	0.10
Milford Sound	0–4			0.54	0.08
	4–12			0.56	0.10
	12–20			0.56	0.10
Total		**5447**	**894**		

Table N.3: Estimated Hector's dolphin abundance and circle-back availability estimate using the full sighting data and third-ranked model from Table 9.

Coastal Section	Offshore Stratum (nmi)	$\hat{N}_k$	SE	$\hat{P}_{\alpha k}$	SE
Whanganui Inlet	0–4	191	152	0.58	0.09
	4–12			0.60	0.10
	12–20			0.60	0.10
Hector	0–4	762	236	0.58	0.09
	4–12	258	101	0.60	0.10
	12–20			0.60	0.10
Greymouth	0–4	1597	402	0.60	0.09
	4–12	457	267	0.62	0.10
	12–20			0.62	0.10
Okarito Lagoon	0–4	1138	322	0.59	0.08
	4–12	374	156	0.61	0.10
	12–20			0.61	0.10
Jackson Bay	0–4	572	253	0.60	0.09
	4–12			0.62	0.10
	12–20			0.62	0.10
Milford Sound	0–4			0.60	0.09
	4–12			0.62	0.10
	12–20			0.62	0.10
Total		**5348**	**1216**		

Table N.4: Estimated Hector's dolphin abundance and circle-back availability estimate using the full sighting data and fourth-ranked model from Table 9.

Coastal Section	Offshore Stratum (nmi)	$\hat{N}_k$	SE	$\hat{P}_{\alpha k}$	SE
Whanganui Inlet	0–4	190	158	0.58	0.09
	4–12			0.60	0.10
	12–20			0.60	0.10
Hector	0–4	762	272	0.58	0.09
	4–12	258	113	0.60	0.10
	12–20			0.60	0.10
Greymouth	0–4	1601	455	0.60	0.09
	4–12	459	276	0.62	0.10
	12–20			0.62	0.10
Okarito Lagoon	0–4	1141	365	0.59	0.08
	4–12	374	169	0.61	0.10
	12–20			0.61	0.10
Jackson Bay	0–4	573	268	0.60	0.09
	4–12			0.62	0.10
	12–20			0.62	0.10
Milford Sound	0–4			0.60	0.09
	4–12			0.62	0.10
	12–20			0.62	0.10
Total		**5358**	**1471**		

Table N.5: Estimated Hector's dolphin abundance and circle-back availability estimate using the full sighting data and fifth-ranked model from Table 9.

Coastal Section	Offshore Stratum (nmi)	$\hat{N}_k$	SE	$\hat{P}_{\alpha k}$	SE
Whanganui Inlet	0–4	183	141	0.51	0.08
	4–12			0.53	0.09
	12–20			0.53	0.09
Hector	0–4	773	208	0.51	0.08
	4–12	257	91	0.53	0.09
	12–20			0.53	0.09
Greymouth	0–4	1661	372	0.53	0.08
	4–12	471	272	0.55	0.09
	12–20			0.55	0.09
Okarito Lagoon	0–4	1167	290	0.52	0.08
	4–12	374	146	0.54	0.09
	12–20			0.54	0.09
Jackson Bay	0–4	588	254	0.53	0.08
	4–12			0.55	0.09
	12–20			0.55	0.09
Milford Sound	0–4			0.53	0.08
	4–12			0.55	0.09
	12–20			0.55	0.09
Total		**5475**	**979**		

Table N.6: Estimated Hector's dolphin abundance and circle-back availability estimate using the full sighting data and sixth-ranked model from Table 9.

Coastal Section	Offshore Stratum (nmi)	$\hat{N}_k$	SE	$\hat{P}_{\alpha k}$	SE
Whanganui Inlet	0–4	182	139	0.48	0.08
	4–12			0.50	0.09
	12–20			0.50	0.09
Hector	0–4	780	203	0.48	0.08
	4–12	257	89	0.50	0.09
	12–20			0.50	0.09
Greymouth	0–4	1691	368	0.51	0.07
	4–12	477	276	0.52	0.09
	12–20			0.52	0.09
Okarito Lagoon	0–4	1182	285	0.50	0.07
	4–12	376	145	0.52	0.09
	12–20			0.52	0.09
Jackson Bay	0–4	597	257	0.51	0.07
	4–12			0.52	0.09
	12–20			0.52	0.09
Milford Sound	0–4			0.51	0.07
	4–12			0.52	0.09
	12–20			0.52	0.09
Total		**5542**	**921**		

Table N.7: Estimated Hector's dolphin abundance and circle-back availability estimate using the full sighting data and seventh-ranked model from Table 9.

Coastal Section	Offshore Stratum (nmi)	$\hat{N}_k$	SE	$\hat{P}_{\alpha k}$	SE
Whanganui Inlet	0–4	182	138	0.49	0.08
	4–12			0.50	0.09
	12–20			0.50	0.09
Hector	0–4	780	198	0.49	0.08
	4–12	257	87	0.50	0.09
	12–20			0.50	0.09
Greymouth	0–4	1690	363	0.51	0.07
	4–12	477	274	0.53	0.09
	12–20			0.53	0.09
Okarito Lagoon	0–4	1182	281	0.50	0.07
	4–12	376	143	0.52	0.09
	12–20			0.52	0.09
Jackson Bay	0–4	597	255	0.51	0.07
	4–12			0.53	0.09
	12–20			0.53	0.09
Milford Sound	0–4			0.51	0.07
	4–12			0.53	0.09
	12–20			0.53	0.09
Total		**5540**	**884**		

Table N.8: Estimated Hector's dolphin abundance and circle-back availability estimate using the full sighting data and eighth-ranked model from Table 9.

Coastal Section	Offshore Stratum (nmi)	$\hat{N}_k$	SE	$\hat{P}_{\alpha k}$	SE
Whanganui Inlet	0–4	192	163	0.58	0.09
	4–12			0.60	0.10
	12–20			0.60	0.10
Hector	0–4	767	288	0.58	0.09
	4–12	260	119	0.60	0.10
	12–20			0.60	0.10
Greymouth	0–4	1607	480	0.60	0.09
	4–12	460	281	0.62	0.10
	12–20			0.62	0.10
Okarito Lagoon	0–4	1146	386	0.59	0.08
	4–12	376	176	0.61	0.10
	12–20			0.61	0.10
Jackson Bay	0–4	576	275	0.60	0.09
	4–12			0.62	0.10
	12–20			0.62	0.10
Milford Sound	0–4			0.60	0.09
	4–12			0.62	0.10
	12–20			0.62	0.10
Total		**5384**	**1586**		

SECTION O: Model fitting summaries for analysis of circle-back availability data using the highly-ranked detection model for reduced, winter data set.

Table O.1: Model selection summary for factors affecting winter availability as assessed from circle-back protocol, using the reduced sighting data set and detection function from the second-ranked model in Table 11. Results presented are the relative difference in AIC values (ΔAIC), AIC model weights (*w*), twice the negative log-likelihood (-2*l*) and the number of parameters in the model (*NPar*). The '.' model assumes equal availability across all factors.

Model	ΔAIC	*w*	-2*l*	*NPar*
.	0.00	0.55	82.28	1
offshore	1.91	0.21	82.19	2
region	2.34	0.17	80.62	3
region+offshore	4.23	0.07	80.51	4

Table O.2: Model selection summary for factors affecting winter availability as assessed from circle-back protocol, using the reduced sighting data set and detection function from the fourth-ranked model in Table 11.

Model	ΔAIC	*w*	-2*l*	*NPar*
.	0.00	0.55	81.97	1
offshore	1.91	0.21	81.88	2
region	2.39	0.17	80.36	3
region+offshore	4.28	0.07	80.25	4

Table O.3: Model selection summary for factors affecting summer availability as assessed from circle-back protocol, using the reduced sighting data set and detection function from the sixth-ranked model in Table 11.

Model	ΔAIC	*w*	-2*l*	*NPar*
.	0.00	0.55	82.25	1
offshore	1.91	0.21	82.16	2
region	2.37	0.17	80.62	3
region+offshore	4.25	0.07	80.50	4

Table O.4: Model selection summary for factors affecting summer availability as assessed from circle-back protocol, using the reduced sighting data set and detection function from the ninth-ranked model in Table 11. Results presented are the relative difference in AIC values (ΔAIC), AIC model weights (*w*), twice the negative log-likelihood (-2*l*) and the number of parameters in the model (*NPar*). The '.' model assumes equal availability across all factors.

Model	ΔAIC	*w*	-2*l*	*NPar*
.	0.00	0.54	83.75	1
offshore	1.92	0.21	83.67	2
region	2.17	0.18	81.92	3
region+offshore	4.03	0.07	81.78	4

SECTION P: Stratum-specific abundance and availability estimates using circle-back protocol from each detection function for reduced, winter data set.

Table P.1: Estimated Hector's dolphin abundance and circle-back availability estimate using the reduced sighting data and second-ranked model from Table 11.

Coastal Section	Offshore Stratum (nmi)	$\hat{N}_k$	SE	$\hat{P}_{\alpha k}$	SE
West Haven Inlet	0–4	270	215	0.51	0.15
	4–12			0.53	0.16
	12–20			0.53	0.16
Hector	0–4	607	232	0.51	0.15
	4–12	167	90	0.53	0.16
	12–20			0.53	0.16
Greymouth	0–4	1441	373	0.58	0.11
	4–12	626	370	0.59	0.14
	12–20			0.59	0.14
Okarito Lagoon	0–4	1200	338	0.58	0.11
	4–12	343	151	0.60	0.13
	12–20			0.60	0.13
Jackson Bay	0–4	545	284	0.58	0.11
	4–12			0.59	0.14
	12–20			0.59	0.14
Milford Sound	0–4			0.58	0.11
	4–12			0.59	0.14
	12–20			0.59	0.14
Total		**5199**	**1072**		

Table P.2: Estimated Hector's dolphin abundance and circle-back availability estimate using the reduced sighting data and fourth-ranked model from Table 11.

Coastal Section	Offshore Stratum (nmi)	$\hat{N}_k$	SE	$\hat{P}_{\alpha k}$	SE
West Haven Inlet	0–4	271	220	0.53	0.15
	4–12			0.54	0.17
	12–20			0.54	0.17
Hector	0–4	604	239	0.53	0.15
	4–12	167	93	0.54	0.17
	12–20			0.54	0.17
Greymouth	0–4	1435	389	0.59	0.11
	4–12	624	373	0.60	0.14
	12–20			0.60	0.14
Okarito Lagoon	0–4	1197	353	0.59	0.12
	4–12	343	156	0.61	0.13
	12–20			0.61	0.13
Jackson Bay	0–4	543	286	0.59	0.11
	4–12			0.60	0.14
	12–20			0.60	0.14
Milford Sound	0–4			0.59	0.11
	4–12			0.60	0.14
	12–20			0.60	0.14
Total		**5186**	**1180**		

Table P.3: Estimated Hector's dolphin abundance and circle-back availability estimate using the reduced sighting data and sixth-ranked model from Table 11.

Coastal Section	Offshore Stratum (nmi)	$\hat{N}_k$	SE	$\hat{P}_{\alpha k}$	SE
West Haven Inlet	0–4	271	217	0.49	0.14
	4–12			0.51	0.16
	12–20			0.51	0.16
Hector	0–4	605	232	0.49	0.14
	4–12	167	90	0.51	0.16
	12–20			0.51	0.16
Greymouth	0–4	1447	377	0.55	0.10
	4–12	625	370	0.57	0.13
	12–20			0.57	0.13
Okarito Lagoon	0–4	1198	340	0.56	0.11
	4–12	342	152	0.57	0.13
	12–20			0.57	0.13
Jackson Bay	0–4	551	289	0.55	0.10
	4–12			0.57	0.13
	12–20			0.57	0.13
Milford Sound	0–4			0.55	0.10
	4–12			0.57	0.13
	12–20			0.57	0.13
Total		**5206**	**1091**		

Table P.4: Estimated Hector's dolphin abundance and circle-back availability estimate using the reduced sighting data and ninth-ranked model from Table 11.

Coastal Section	Offshore Stratum (nmi)	$\hat{N}_k$	SE	$\hat{P}_{\alpha k}$	SE
West Haven Inlet	0–4	307	246	0.42	0.12
	4–12			0.44	0.14
	12–20			0.44	0.14
Hector	0–4	705	275	0.42	0.12
	4–12	192	104	0.44	0.14
	12–20			0.44	0.14
Greymouth	0–4	1676	437	0.48	0.09
	4–12	726	433	0.49	0.12
	12–20			0.49	0.12
Okarito Lagoon	0–4	1383	396	0.48	0.10
	4–12	390	174	0.50	0.11
	12–20			0.50	0.11
Jackson Bay	0–4	634	334	0.48	0.09
	4–12			0.49	0.12
	12–20			0.49	0.12
Milford Sound	0–4			0.48	0.09
	4–12			0.49	0.12
	12–20			0.49	0.12
Total		**6012**	**1246**		

SECTION Q: Stratum-specific WCSI summer abundance estimates using dive-cycle based availability estimates.

Table Q.1: Estimated summer abundance using the top seven models from Table 5 using the full sighting data and dive-cycle based availability estimates.

Coastal Section	Offshore Stratum (nmi)	1 $\hat{N}_k$	SE	2 $\hat{N}_k$	SE	3 $\hat{N}_k$	SE	4 $\hat{N}_k$	SE	5 $\hat{N}_k$	SE	6 $\hat{N}_k$	SE	7 $\hat{N}_k$	SE
Whanganui	0–4														
Inlet	4–12														
	12–20														
Hector	0–4	1427	295	1491	316	1353	282	1447	337	1407	319	1405	296	1608	375
	4–12	548	402	559	409	535	395	552	405	545	401	544	400	578	420
	12–20														
Greymouth	0–4	1428	326	1511	359	1330	299	1454	391	1397	360	1398	326	1677	460
	4–12	58	54	64	59	52	48	60	57	56	53	56	52	76	73
	12–20														
Okarito	0–4	1850	439	1952	482	1729	403	1882	515	1813	476	1813	437	2155	606
Lagoon	4–12	801	600	841	626	755	573	814	616	787	598	788	594	920	678
	12–20														
Jackson Bay	0–4	230	137	246	147	210	126	235	145	223	137	224	134	281	172
	4–12														
	12–20														
Milford	0–4	38	29	42	32	34	26	40	31	37	29	37	28	50	40
Sound	4–12														
	12–20														
Total		**6379**	**1057**	**6706**	**1177**	**5998**	**980**	**6484**	**1344**	**6264**	**1228**	**6266**	**1072**	**7346**	**1563**

Table Q.2: Estimated summer abundance using the top seven non-excluded models from Table 7 using the reduced sighting data and dive-cycle based availability estimates.

Coastal Section	Offshore Stratum (nmi)	1 $\hat{N}_k$	SE	2 $\hat{N}_k$	SE	3 $\hat{N}_k$	SE	5 $\hat{N}_k$	SE	6 $\hat{N}_k$	SE	7 $\hat{N}_k$	SE	8 $\hat{N}_k$	SE
Whanganui Inlet	0–4														
	4–12														
	12–20														
Hector	0–4	1506	339	1495	339	1460	337	1496	437	1776	619	1459	352	1766	510
	4–12	398	260	396	259	391	256	396	262	433	293	386	253	433	289
	12–20														
Greymouth	0–4	1325	367	1314	366	1272	360	1314	490	1653	731	1282	385	1639	598
	4–12	82	76	81	75	76	71	81	84	124	135	80	77	121	122
	12–20														
Okarito Lagoon	0–4	1837	456	1821	455	1757	447	1821	676	2344	1069	1781	500	2325	851
	4–12	832	657	827	654	800	639	827	687	1054	874	816	652	1039	820
	12–20														
Jackson Bay	0–4	146	130	145	128	138	124	145	137	196	191	142	128	195	179
	4–12														
	12–20														
Milford Sound	0–4	54	41	54	40	50	38	54	48	82	77	53	42	80	68
	4–12														
	12–20														
Total		**6179**	**1084**	**6132**	**1089**	**5943**	**1089**	**6135**	**1824**	**7661**	**2928**	**5999**	**1256**	**7598**	**2233**

SECTION R: Stratum-specific WCSI winter abundance estimates using dive-cycle based availability estimates.

Table R.1: Estimated winter abundance using the top eight models from Table 9 using the full sighting data and dive-cycle based availability estimates.

Coastal Section	Offshore Stratum (nmi)	1 $\hat{N}_k$	SE	2 $\hat{N}_k$	SE	3 $\hat{N}_k$	SE	4 $\hat{N}_k$	SE	5 $\hat{N}_k$	SE	6 $\hat{N}_k$	SE	7 $\hat{N}_k$	SE	8 $\hat{N}_k$	SE
Whanganui	0–4	173	129	187	140	215	169	213	176	180	137	171	128	171	128	216	181
Inlet	4–12																
	12–20																
Hector	0–4	739	163	780	172	859	243	857	285	761	179	733	163	735	158	861	305
	4–12	253	77	269	82	300	108	299	122	262	83	251	77	251	75	301	130
	12–20																
Greymouth	0–4	1633	377	1698	391	1823	485	1824	541	1667	398	1624	377	1626	374	1827	567
	4–12	477	273	498	284	536	314	537	323	488	281	474	273	475	272	538	328
	12–20																
Okarito	0–4	1570	321	1643	337	1781	457	1782	529	1608	349	1560	323	1563	318	1786	563
Lagoon	4–12	517	183	546	193	602	236	601	258	533	193	513	183	514	181	604	269
	12–20																
Jackson Bay	0–4	577	252	603	260	653	295	653	310	590	259	573	251	574	250	655	317
	4–12																
	12–20																
Milford	0–4																
Sound	4–12																
	12–20																
Total		**5937**	**822**	**6223**	**865**	**6770**	**1424**	**6765**	**1764**	**6089**	**951**	**5899**	**834**	**5909**	**789**	**6788**	**1914**

Table R.2: Estimated winter abundance using the top four non-excluded models from Table 11 using the reduced sighting data and dive-cycle based availability estimates.

Coastal Section	Offshore Stratum (nmi)	$\hat{N}_k$ (2)	SE (2)	$\hat{N}_k$ (4)	SE (4)	$\hat{N}_k$ (6)	SE (6)	$\hat{N}_k$ (9)	SE (9)
Whanganui Inlet	0–4	270	202	277	212	260	196	251	189
	4–12								
	12–20								
Hector	0–4	605	164	580	159	616	180	576	157
	4–12	172	77	166	75	176	83	162	73
	12–20								
Greymouth	0–4	1573	379	1515	369	1595	407	1515	367
	4–12	703	401	673	384	713	411	676	387
	12–20								
Okarito Lagoon	0–4	1835	396	1760	384	1863	435	1762	382
	4–12	539	210	518	202	550	223	512	200
	12–20								
Jackson Bay	0–4	595	305	576	297	604	312	573	297
	4–12								
	12–20								
Milford Sound	0–4								
	4–12								
	12–20								
Total		**6291**	**975**	**6049**	**963**	**6393**	**1165**	**6027**	**940**

SECTION S: SCSI reanalysis results

SCSI Data Summary

A summary of the sighting data used in the detection function analysis is given in Table S.1. The total number of unique sightings for each survey period is small and below the generally recommended minimum of 60–80 sightings for estimating abundance (Buckland et al. 2001), which is why a common detection function for both survey periods was considered. For the front observer position, 1 sighting was left truncated (had distance less than 0.04 km) and 4 sightings were right truncated (distance more than 0.300 km). For the rear observer position, 1 sighting was left truncated and 3 sightings right truncated.

Table S.1: Summary of the SCSI sighting data from the March and August 2010 survey periods. 'All' indicates the number of on effort and auxiliary sightings used to estimate the detection functions, while 'On Effort' indicates the number of on effort sightings that were used to estimate abundance. Results presented are the number of unique groups sighted, number sighted from the front (Front) and rear (Rear) observer positions, sighted from both positions (Both), the total number of individual Hector's dolphins seen, the average, standard deviation and range of the observed group size. Note that the number of groups sighted from both positions are included in the front and rear totals. Sightings outside of 0.04 - 0.30 km from the transect line have been excluded.

	March		August	
	All	**On Effort**	**All**	**On Effort**
Unique Groups	44	5	37	10
Front	31	2	23	1
Rear	29	5	27	10
Both (duplicates)	16	2	13	1
Individuals	85	8	72	15
Average Group Size	1.93	1.60	1.95	1.50
SD Group Size	1.04	0.89	1.08	0.71
Range Group Size	1–5	1–3	1–6	1–3
Total Effort (km)		**1660**		**1667**

Detection function analysis

The top 10 models (as ranked by AIC) for the full data set are given in Table S.2. Most of the AIC weight is associated with the top two models, but lower ranked models also have non-negligible weight. The third- and eighth-ranked models produced estimates with very large standard errors and the correlation between the intercept of the detection and dependence functions were close to -1; hence these models were excluded from further analysis.

All of the top-ranked models include group size as a covariate, with the majority having different relationships between detection probability and distance for each observer position (i.e., observer position-specific detection functions). The highest ranked models included a linear relationship between detection probability and distance, although this differed with the nature of the dependence function. The top-ranked model included point independence while the second-ranked model (with a very similar AIC value) includes limiting independence. These top two models provide very different ESW estimates hence will result in very different abundance estimates.

Plots of the fitted detection functions and empirical histograms of detection rates do not indicate any systematic concerns about lack of fit for any of the top-ranked models, particularly for $p_\bullet(d_i, s_i)$, which is the most relevant in terms of estimating abundance. Note that the small sample sizes will make the histograms relatively jagged. The fitted detection functions for the top ranked model are presented in Figure S.1 for illustration. Figure S.2 presents the q-q plots for the top-two models and goodness of fit tests (Table S.3) for the eight models used to estimate dolphin abundance do not indicate any evidence of lack of fit.
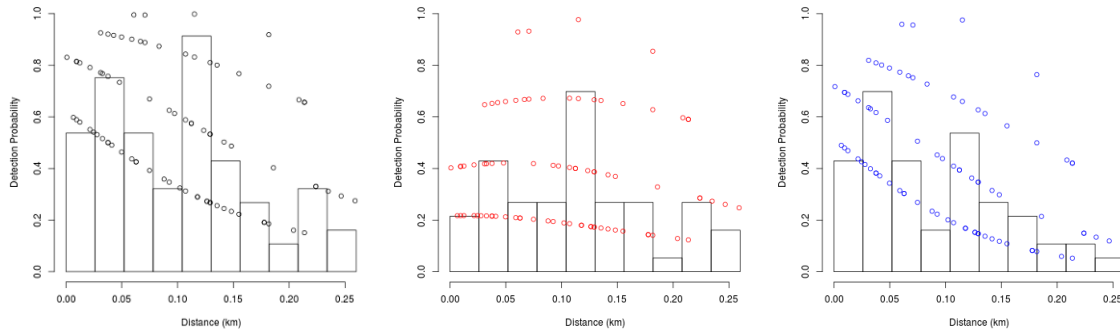
Figure S.1: Fitted detection functions and histograms of empirical detection probabilities from the top ranked model in Table S.2. Left is $p_\bullet(d_i, s_i)$**, centre is** $p_F(d_i, s_i)$**, and right is** $p_R(d_i, s_i)$**. Note that distance from the transect line has been rescaled such that an original distance of 0.04 km is now 0 km.**

A)   **B)**
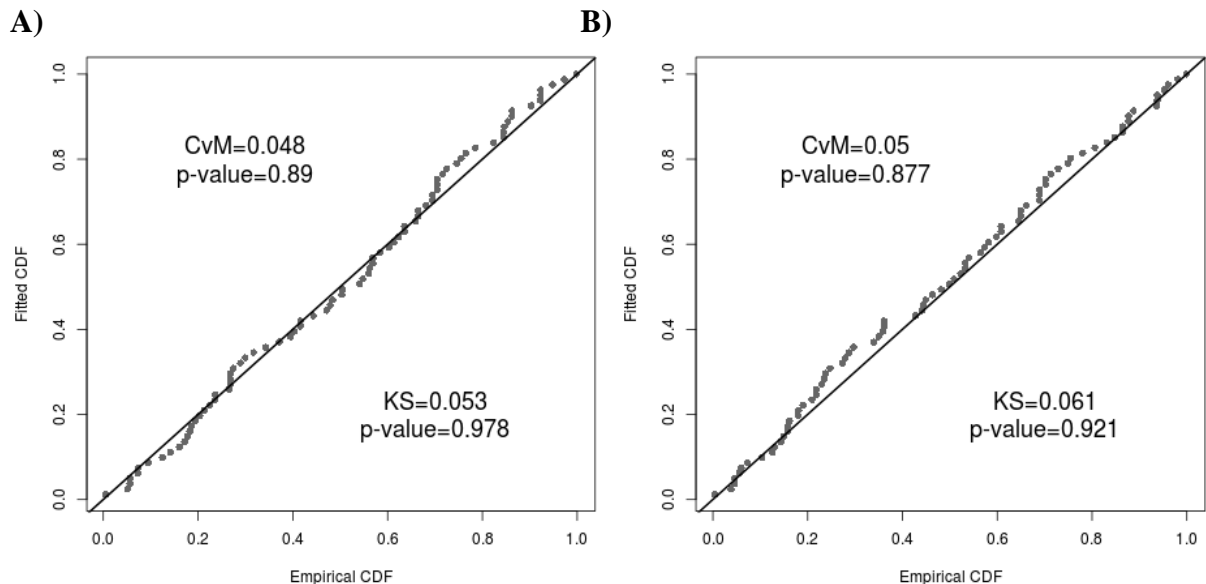
Figure S.2: Q-Q plot of the fitted and empirical cumulative density functions (CDF) for the A) top ranked model and B) second ranked model of the detection function analysis of the SCSI.

Table S.2: Top 10 AIC-ranked models for the detection function analysis for sightings between 0.04–0.30 km from the transect line in the SCSI surveys. Model components identify the structure of the detection function model; $f(d)$ is the functional relationship with distance on the logit scale (L=linear, Q=quadratic, S=Spline), Obs indicates whether the intercept term is different for each observer position (Y=Yes, N=No), $\beta_1 \neq \beta_2$ indicates whether the regression coefficients for the effect of distance on detection is different for each observer position (Y= Yes, N= No), Size indicates whether group size has an effect on detection (Y=Yes, N=No) and Dep. indicates the form of dependence in detection between observer positions (FI=Full Independence, C = Constant Dependence, P = Point Independence and L= Limiting Independence). ΔAIC is the relative difference in AIC values, wgt is the AIC model weight, wgt* is the adjusted AIC weight for the models used for inference, -2l is twice the negative log-likelihood, pars. is the number parameters in the model, $\hat{N}_{cg}$ is the estimated number of dolphin groups in the covered area, $SE(\hat{N}_{cg})$ is the standard error for $\hat{N}_{cg}$, corr. is the correlation between the intercepts of the detection and dependence components of the model and ESW is the effective strip width accounting for detection and perception bias.

| | | | | | **Model Components** | | | | | | | | |
$f(d)$	**Obs**	$\beta_1 \neq \beta_2$	**Size**	**Dep.**	**ΔAIC**	**wgt**	**wgt***	**-2l**	**pars.**	$\hat{N}_{cg}$	$SE(\hat{N}_{cg})$	**corr.**	**ESW**
L	Y	Y	Y	P	0.00	0.29	0.38	144.01	6	186	51		0.113
L	Y	Y	Y	L	0.29	0.25	0.33	142.30	7	107	16	-0.98	0.196
L	Y	Y	Y	C	2.51	0.08		146.52	6	550	893	-0.95	
L	Y	Y	Y	FI	2.92	0.07	0.09	148.93	5	134	22		0.157
Q	Y	Y	Y	P	3.12	0.06	0.08	143.13	8	181	51		0.116
Q	Y	Y	Y	L	4.22	0.03	0.05	142.23	9	107	15	-0.98	0.198
L	N	N	Y	P	4.47	0.03	0.04	152.48	4	196	56		0.107
Q	Y	Y	Y	C	5.15	0.02		145.15	8	826	2124	-0.97	
L	N	N	Y	L	5.46	0.02	0.02	151.46	5	108	19	-0.98	0.194
Q	N	N	Y	P	5.74	0.02	0.02	151.75	5	195	58		0.108

Table S.3: Goodness of fit tests for the eight detection function models from Table S.2 used to estimate dolphin abundance along SCSI. Given are the Cramer-von Mises (CvM) and Kolmogorov-Smirnov (KS) tests with associated p-values.

Model Rank	CvM	p-value	KS	p-value
1	0.048	0.89	0.053	0.98
2	0.050	0.88	0.061	0.92
4	0.226	0.22	0.114	0.24
5	0.035	0.96	0.055	0.97
6	0.050	0.88	0.061	0.92
7	0.042	0.92	0.053	0.98
9	0.049	0.88	0.062	0.92
10	0.036	0.95	0.056	0.96

SCSI Availability Bias

Helicopter Dive Profiles

Dive information was collected on 23 different dolphin groups equating to over 1000 complete dive cycles; 15 groups in March and 8 groups in August (Table S.4). Availability is estimated to have been higher in August 2010, although the August estimate is associated with a large degree of uncertainty (Figure S.3). In the ECSI survey (MacKenzie & Clement 2014), it was determined that fixed objects are within an observers view for about six seconds on average, hence $t=6$ has been used to correct for availability bias when estimating abundance (Table S.4).

Table S.4: Summary of SCSI dive-cycle data and availability estimates in each survey period. Results presented are the number of groups data were collected on (n), average time on or near the surface ($\bar{u}$), average dive time ($\bar{b}$), variance for the average surface time ($V_{\bar{u}}$), variance for the average dive time ($V_{\bar{b}}$) and covariance between average surface and dive time ($V_{\bar{u}\bar{b}}$). All times are given in seconds. Estimated probability of a group being available ($\hat{P}_{\alpha}$) for t = 6 seconds and associated standard error (*SE*).

Survey Period	n	$\bar{u}$	$\bar{b}$	$V_{\bar{u}}$	$V_{\bar{b}}$	$V_{\bar{u}\bar{b}}$	$\hat{P}_{\alpha}$	*SE*
March	15	22.0	25.5	50.5	39.0	35.9	0.57	0.07
August	8	6.1	9.7	0.8	3.8	1.2	0.67	0.19
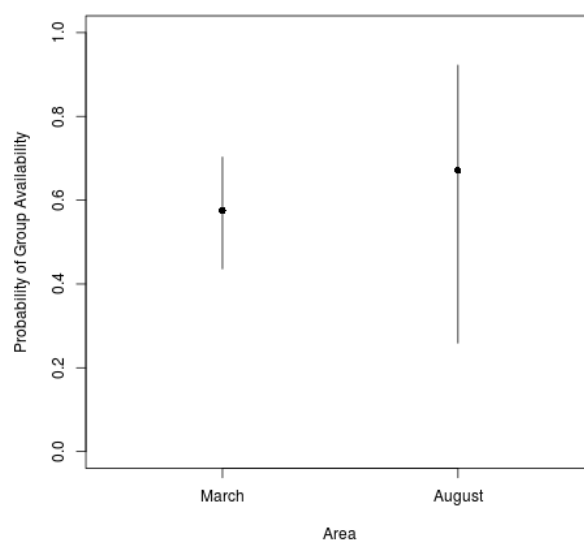
Figure S.3: Estimated availability and 95% confidence intervals obtained from the SCSI dive-cycle data.

SCSI Abundance Estimates

Estimated dolphin abundance, after correcting for availability bias using each detection function from Table S.2, are given in Table S.5. While all estimates are generally low, there is quite a lot of variation between models. The model averaged estimates (using upon adjusted AIC model weights from Table S.2) are 177 for March (CV: 37%; 95% CI: 88–358) and 299 for August (CV: 47%; 95% CI: 125–714).

Table S.5: Seasonal SCSI abundance estimates and standard errors for each detection function from sightings between 0.04–0.3 km, along with the model averaged estimate. An overall combined estimate across both seasons is also given. Availability was estimated from dive-cycle helicopter surveys only.

		March		August		Combined	
Model Rank	**wgt***	$\hat{N}$	**SE**	$\hat{N}$	**SE**	$\hat{N}$	**SE**
1	0.376	217	63	370	145	293	92
2	0.325	129	27	213	72	171	42
4	0.087	159	34	265	90	212	52
5	0.079	211	64	359	143	285	93
6	0.046	129	26	211	71	170	40
7	0.040	228	69	389	155	309	100
9	0.025	131	29	215	75	173	44
10	0.021	226	71	386	157	306	102
Model Averaged		**177**	**66**	**299**	**140**	**238**	**94**

SCSI Distribution Results

Density estimates corresponded closely to actual sighting locations. The highest dolphin density occurred within Te Waewae Bay, mainly in the northwest corner (Figure S.4). Slightly lower densities were observed off Toetoes and Porpoise Bays with these decreasing steadily toward the offshore. All sightings were made within 5 nmi. (9.3 km) of the coastline with two exceptions offshore of Porpoise Bay; one sighting at 6.5 nmi. (12 km) and the other 9.6 n.mi. (17.8 km). It is important to note that density estimates were based on only a few sightings from single season surveys. Density maps from this work should not be interpreted as the average or long-term distribution of Hector's dolphins in these areas.

Discussion

The abundance estimates for SCSI given here are substantially lower than the 628 (CV: 39%; 95% CI: 301–1310) estimated by Clement et al. (2011). This is primarily due to the different estimates of availability; 0.57 in March and 0.67 in August here, versus 0.36 in Clement et al. (2011). The estimated number of available dolphins (i.e., by multiplying each of the abundance estimates by the corresponding availability estimate) is 102, 200 and 226 for the current March, August and Clement et al. (2011) results respectively, indicating the different approaches for modelling the detection functions provide similar results for the SCSI data. Furthermore, an estimate of 226 is not unreasonable if one considers the degree of variation in the current estimates among different detection functions.

The large difference in the availability estimates is partially due to a revised data set being used, but mainly due to allowing for the length of time a dolphin group would be in an observer's field of view from the aircraft. Here a value of $t = 6$ seconds has been assumed (based on MacKenzie & Clement 2014) while Clement et al. (2011) estimated instantaneous (i.e., $t = 0$) availability following Slooten et al. (2004) and DuFresne & Mattlin (2009). Instantaneous availability calculated from the current SCSI dive cycle data is 0.46 and 0.39 for the March and August survey periods respectively. Note that allowing for the length of time that dolphins will be within the observer's field of view has a greater effect when the average dive-cycle periods are shorter.
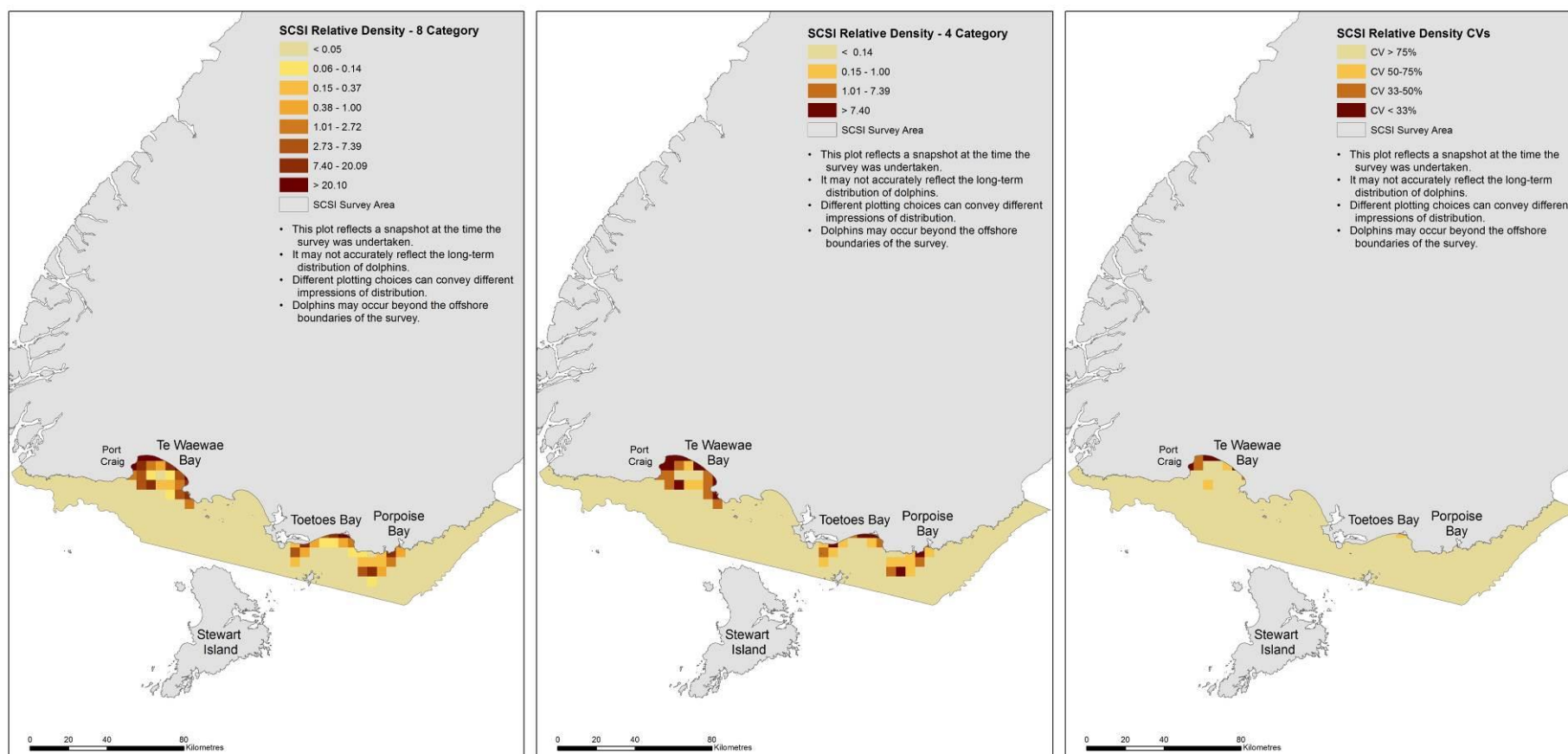
Figure S.4: Hector's dolphin distribution assessed from both summer and winter aerial line-transect surveys for SCSI. Panels represent patterns for the relative density of Hector's dolphins within 5 km × 5 km grid cells generated from the Density Surface Models with eight categories (left), with four density categories (middle) and precision of estimated relative density with darker colours indicating greater precision; i.e. smaller CVs (right). Relative densities greater than 1 indicate areas with density greater than the overall average density.

SECTION T: ECSI reanalysis results

Key results associated with the reanalysis of the ECSI aerial survey data is presented here, using the same sighting data as MacKenzie & Clement (2014a, 2014b). The notable differences to the previous ECSI analysis are the 'symmetric' parameterization of the detection function model and the methods for analysing the circle-back availability data as employed in the WCSI analysis.

ECSI Detection function analysis

Summer

The top ten AIC-ranked detection function models for the full ECSI summer sighting data are given in Table T.1. The AIC model weights gradually decline indicating a fair degree of model selection uncertainty and the top ten models have all been used to estimate abundance. There is no evidence of lack of fit for any of the top ten models (Table T.2), and the fitted detection function plots and q-q plot for the top-ranked model do not indicate any potential problems (Figure T.1, Figure T.2).

Figure T.1: Fitted detection functions and histograms of empirical detection probabilities from the top ranked model in Table T.1. Left is $p_{\bullet}(d_i, s_i)$**, centre is** $p_F(d_i, s_i)$**, and right is** $p_R(d_i, s_i)$**.**

Table T.1: Top 10 AIC-ranked models for the detection function analysis for sightings between 0–0.3 km from the transect line in the summer for ECSI. Model components identify the structure of the detection function model; $f(d)$ is the functional relationship with distance on the logit scale (L=linear, Q=quadratic, S=Spline), Obs indicates whether the intercept term is different for each observer position (Y=Yes, N=No), $\beta_1 \neq \beta_2$ indicates whether the regression coefficients for the effect of distance on detection is different for each observer position (Y= Yes, N= No), Size indicates whether group size has an effect on detection (Y=Yes, N=No) and Dep. indicates the form of dependence in detection between observer positions (FI=Full Independence, C = Constant Dependence, P = Point Independence and L= Limiting Independence). ΔAIC is the relative difference in AIC values, wgt is the AIC model weight, wgt* is the adjusted AIC weight for the models used for inference, -2l is twice the negative log-likelihood, pars. is the number parameters in the model, $\hat{N}_{cg}$ is the estimated number of dolphin groups in the covered area, $SE(\hat{N}_{cg})$ is the standard error for $\hat{N}_{cg}$, corr. is the correlation between the intercepts of the detection and dependence components of the model and ESW is the effective strip width accounting for detection and perception bias.

				<u>Model Components</u>									
$f(d)$	**Obs**	$\beta_1 \neq \beta_2$	**Size**	**Dep.**	**ΔAIC**	**wgt**	**wgt***	**-2l**	**pars.**	$\hat{N}_{cg}$	$SE(\hat{N}_{cg})$	**corr.**	**ESW**
Q	N	N	Y	L	0.00	0.27	0.29	472.95	6	436	18	-0.32	0.244
Q	Y	N	Y	L	0.62	0.20	0.21	471.57	7	449	36	-0.43	0.237
S	N	N	Y	L	1.38	0.14	0.15	472.33	7	440	24	-0.47	0.241
S	Y	N	Y	L	1.90	0.11	0.11	470.85	8	441	36	-0.16	0.241
S	N	N	Y	P	2.57	0.08	0.08	475.53	6	546	41		0.194
Q	Y	Y	Y	L	3.62	0.04	0.05	470.57	9	449	41	-0.61	0.236
S	Y	N	Y	P	3.80	0.04	0.04	474.75	7	550	24		0.193
Q	N	N	Y	P	4.05	0.04	0.04	479.01	5	582	64		0.183
Q	Y	N	Y	P	5.57	0.02	0.02	478.52	6	582	63		0.183
Q	Y	Y	N	L	5.96	0.01	0.01	480.91	5	459	42	-0.63	0.231

Table T.2: Goodness of fit tests for top ten ranked models for the detection function analysis of the full ECSI summer data set. Given are the Cramer-von Mises (CvM) and Kolmogorov-Smirnov (KS) tests with associated p-values.

Model Rank	CvM	p-value	KS	p-value
1	0.053	0.86	0.034	0.81
2	0.132	0.45	0.046	0.44
3	0.056	0.84	0.036	0.73
4	0.060	0.81	0.036	0.75
5	0.104	0.57	0.045	0.48
6	0.081	0.69	0.040	0.63
7	0.119	0.50	0.047	0.41
8	0.120	0.50	0.049	0.37
9	0.125	0.48	0.049	0.35
10	0.055	0.84	0.037	0.70

CvM=0.053
p-value=0.861

KS=0.034
p-value=0.814

Figure T.2: Q-Q plot of the fitted and empirical cumulative density functions (CDF) for the top ranked model of the detection function analysis of the full ECSI summer data.

The top ten AIC-ranked detection function models for the reduced ECSI summer sighting data are given in Table T.3. The AIC model weights are all relatively low indicating a large degree of model selection uncertainty, although the eighth-tenth ranked models all produce unrealistic estimates of abundance in the covered area. Hence, only the top seven models are used for abundance estimation. There is no evidence of lack of fit for any of the top seven models (Table T.4), and the fitted detection function plots and q-q plot for the top-ranked model do not indicate any potential problems (Figure T.3, Figure T.4).
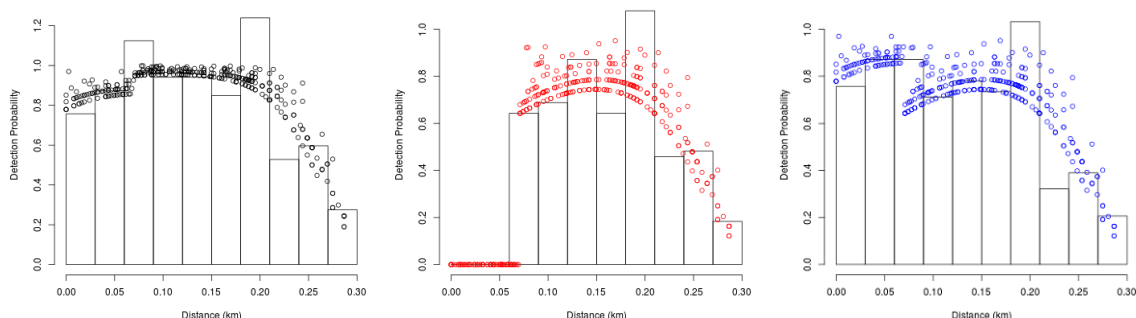
Table T.3: Top 10 AIC-ranked models for the detection function analysis for sightings reduced to between 0.071–0.3 km from the transect line in the summer for ECSI. Model components identify the structure of the detection function model; $f(d)$ is the functional relationship with distance on the logit scale (L=linear, Q=quadratic, S=Spline), Obs indicates whether the intercept term is different for each observer position (Y=Yes, N=No), $\beta_1 \neq \beta_2$ indicates whether the regression coefficients for the effect of distance on detection is different for each observer position (Y= Yes, N= No), Size indicates whether group size has an effect on detection (Y=Yes, N=No) and Dep. indicates the form of dependence in detection between observer positions (FI=Full Independence, C = Constant Dependence, P = Point Independence and L= Limiting Independence). ΔAIC is the relative difference in AIC values, wgt is the AIC model weight, wgt* is the adjusted AIC weight for the models used for inference, -2l is twice the negative log-likelihood, pars. is the number parameters in the model, $\hat{N}_{cg}$ is the estimated number of dolphin groups in the covered area, $SE(\hat{N}_{cg})$ is the standard error for $\hat{N}_{cg}$, corr. is the correlation between the intercepts of the detection and dependence components of the model and ESW is the effective strip width accounting for detection and perception bias.

<u>**Model Components**</u>

$f(d)$	Obs	$\beta_1 \neq \beta_2$	Size	Dep.	ΔAIC	wgt	wgt*	-2l	pars.	$\hat{N}_{cg}$	$SE(\hat{N}_{cg})$	corr.	ESW
Q	N	N	Y	P	0.00	0.21	0.28	473.23	5	377	27		0.165
Q	Y	N	Y	P	0.72	0.14	0.20	471.95	6	376	27		0.165
Q	N	N	Y	L	1.39	0.10	0.14	472.61	6	339	35	-0.99	0.183
S	N	N	Y	P	1.73	0.09	0.12	472.95	6	377	26		0.165
Q	Y	N	Y	L	2.16	0.07	0.10	471.38	7	341	35	-0.98	0.182
S	N	N	Y	L	2.40	0.06	0.08	471.63	7	334	25	-0.99	0.186
S	Y	N	Y	P	2.45	0.06	0.08	471.67	7	377	26		0.165
S	Y	N	Y	C	3.36	0.04		472.58	7	27 822	80 452	-1.00	
Q	N	N	Y	C	3.55	0.03		476.78	5	7 845 615 214	NA*	NA*	
S	N	N	Y	C	3.62	0.03		474.85	6	49 718	168 098	-1.00	

* maximisation algorithm resulted in a singular Hessian matrix; valid standard errors and correlations could not be calculated

Table T.4: Goodness of fit tests for top seven ranked models for the detection function analysis of the reduced ECSI summer data set. Given are the Cramer-von Mises (CvM) and Kolmogorov-Smirnov (KS) tests with associated p-values.

Model Rank	CvM	p-value	KS	p-value
1	0.122	0.49	0.050	0.52
2	0.124	0.48	0.050	0.51
3	0.147	0.40	0.054	0.41
4	0.115	0.52	0.051	0.49
5	0.154	0.38	0.055	0.40
6	0.115	0.52	0.051	0.49
7	0.120	0.50	0.049	0.54

Figure T.3: Fitted detection functions and histograms of empirical detection probabilities from the top ranked model in Table T.3. Left is $p_{\bullet}(d_i, s_i)$**, centre is** $p_F(d_i, s_i)$**, and right is** $p_R(d_i, s_i)$**.**
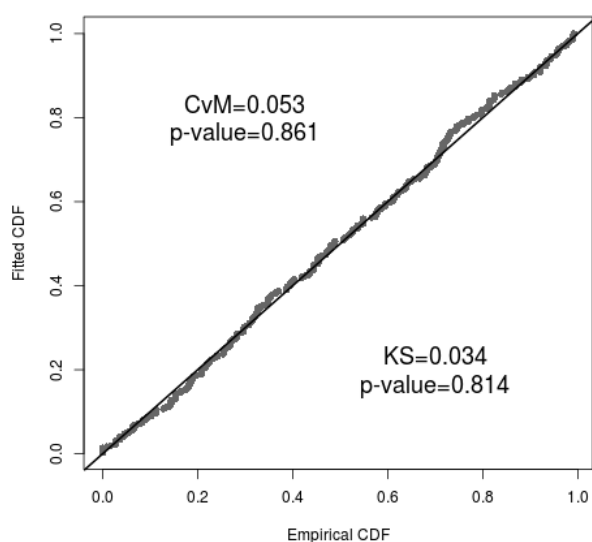

Figure T.4: Q-Q plot of the fitted and empirical cumulative density functions (CDF) for the top ranked model of the detection function analysis of the reduced ECSI summer data.

Winter

The top ten AIC-ranked detection function models for the full ECSI winter sighting data are given in Table T.5. The top-ranked model has the greatest AIC weight, although, in combination, lower ranked models have a substantial amount of support and should not be discounted. The six-highest ranked models were used for model averaging. There is no evidence of lack of fit for any of the top six models (Table T.6), and the fitted detection function plots and q-q plot for the top-ranked model do not indicate any potential problems (Figure T.5, Figure T.6).
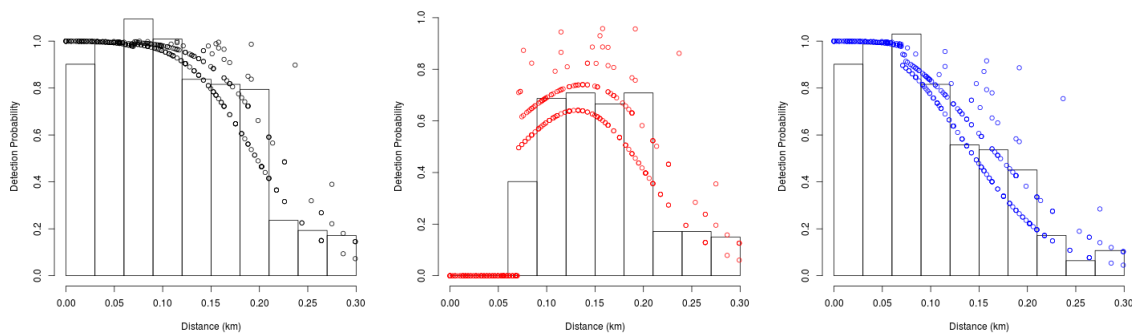
Figure T.5: Fitted detection functions and histograms of empirical detection probabilities from the top ranked model in Table T.6. Left is $p_\bullet(d_i, s_i)$, **centre is** $p_F(d_i, s_i)$, **and right is** $p_R(d_i, s_i)$.

Table T.5: Top 10 AIC-ranked models for the detection function analysis for sightings between 0–0.3 km from the transect line in the winter for ECSI. Model components identify the structure of the detection function model; $f(d)$ is the functional relationship with distance on the logit scale (L=linear, Q=quadratic, S=Spline), Obs indicates whether the intercept term is different for each observer position (Y=Yes, N=No), $\beta_1 \neq \beta_2$ indicates whether the regression coefficients for the effect of distance on detection is different for each observer position (Y= Yes, N= No), Size indicates whether group size has an effect on detection (Y=Yes, N=No) and Dep. indicates the form of dependence in detection between observer positions (FI=Full Independence, C = Constant Dependence, P = Point Independence and L= Limiting Independence). ΔAIC is the relative difference in AIC values, wgt is the AIC model weight, wgt* is the adjusted AIC weight for the models used for inference, -2l is twice the negative log-likelihood, pars. is the number parameters in the model, $\hat{N}_{cg}$ is the estimated number of dolphin groups in the covered area, $SE(\hat{N}_{cg})$ is the standard error for $\hat{N}_{cg}$, corr. is the correlation between the intercepts of the detection and dependence components of the model and ESW is the effective strip width accounting for detection and perception bias.

			Model Components										
$f(d)$	**Obs**	$\beta_1 \neq \beta_2$	**Size**	**Dep.**	**ΔAIC**	**wgt**	**wgt***	**-2l**	**pars.**	$\hat{N}_{cg}$	$SE(\hat{N}_{cg})$	**corr.**	**ESW**
Q	Y	Y	Y	L	0.00	0.64	0.65	343.10	9	466	29	-0.92	0.211
L	Y	Y	Y	L	3.41	0.12	0.12	350.51	7	499	28	-0.14	0.197
Q	Y	Y	Y	P	3.77	0.10	0.10	348.87	8	585	88		0.168
S	Y	Y	Y	L	4.00	0.09	0.09	343.09	11	500	30	0.13	0.197
S	Y	Y	Y	P	6.29	0.03	0.03	347.39	10	590	82		0.167
L	Y	Y	Y	P	6.83	0.02	0.02	355.93	6	642	75		0.153
Q	Y	Y	N	L	11.82	0.00		356.92	8	465	25	-0.95	
Q	Y	Y	Y	C	12.00	0.00		357.09	8	998	819	-0.77	
L	Y	Y	N	L	12.28	0.00		361.37	6	484	34	-0.93	
S	Y	Y	Y	C	13.13	0.00		354.23	10	616	NA	-0.16	

Table T.6: Goodness of fit tests for top six ranked models for the detection function analysis of the full ECSI winter data set. Given are the Cramer-von Mises (CvM) and Kolmogorov-Smirnov (KS) tests with associated p-values.

Model Rank	CvM	p-value	KS	p-value
1	0.061	0.81	0.041	0.65
2	0.094	0.62	0.039	0.70
3	0.136	0.44	0.047	0.46
4	0.068	0.76	0.041	0.65
5	0.170	0.34	0.056	0.26
6	0.151	0.39	0.050	0.38
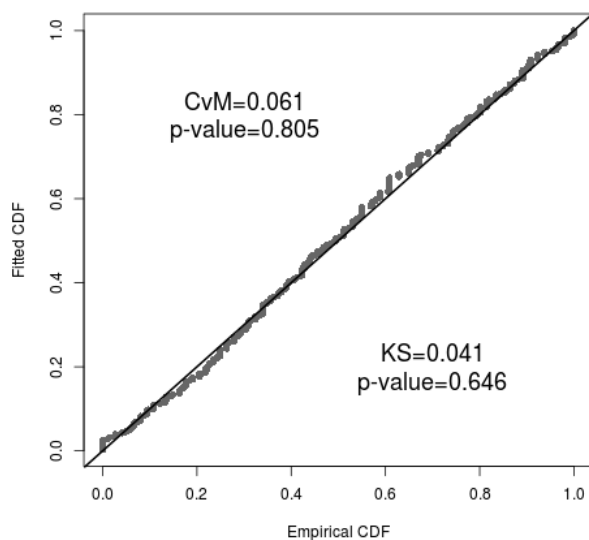
Figure T.6: Q-Q plot of the fitted and empirical cumulative density functions (CDF) for the top ranked model of the detection function analysis of the full ECSI winter data.

The top ten AIC-ranked detection function models for the reduced ECSI winter sighting data are given in Table T.7. The two highest ranked models account for most of the AIC weight, however the top three models all produce unrealistic estimates of abundance and extreme values (less than -0.99) for the correlation between the intercept of the detection and dependence components of the model. Therefore, they were excluded from the model set used to obtain model averaged estimates of abundance. The seventh ranked model was also excluded as the estimated number of dolphins in the covered region was approximately twice as large as the estimates from the fourth-sixth ranked models, its standard error was an order of magnitude greater than the higher-ranked models and it had a moderately large correlation value (-0.86). The ninth and tenth ranked models were excluded because of their substantially larger ΔAIC values.

There is no evidence of lack of fit for any of the four models used for model averaging (Table T.8), and the fitted detection function plots and q-q plot for the highest-ranked model used (fourth-ranked overall) do not indicate any potential problems (Figure T.7 and Figure T.8).
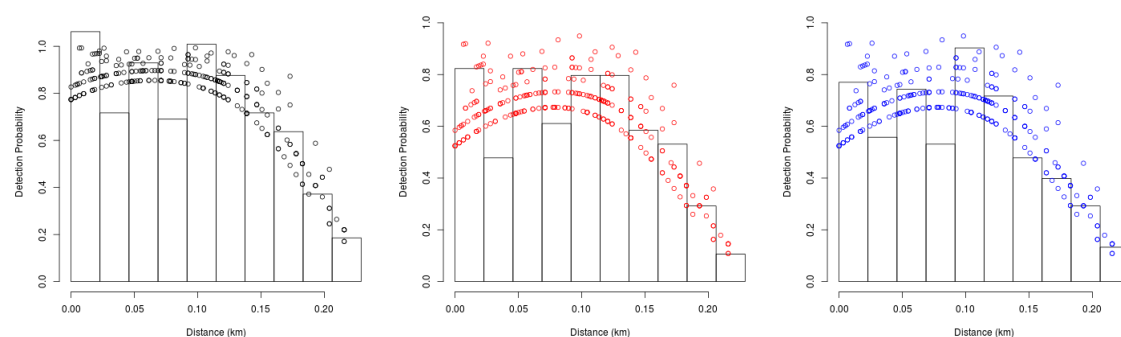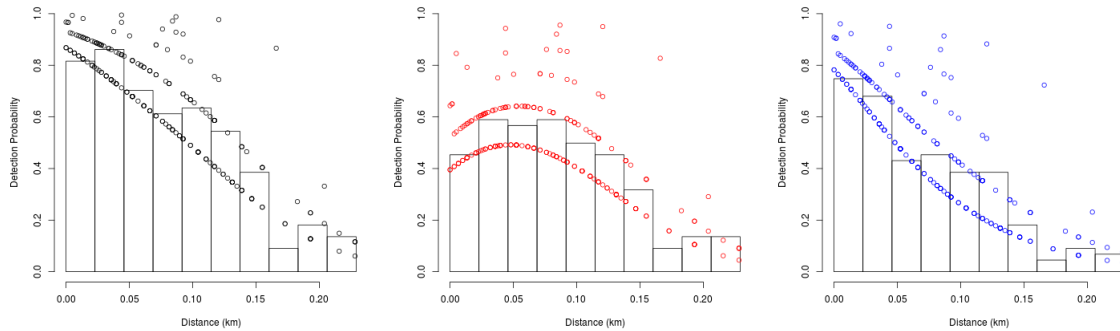

Figure T.7: Fitted detection functions and histograms of empirical detection probabilities from the highest ranked model in Table T.7 used for model averaging (i.e., fourth-ranked model). Left is $p_{\bullet}(d_i, s_i)$**, centre is** $p_F(d_i, s_i)$**, and right is** $p_R(d_i, s_i)$**.**
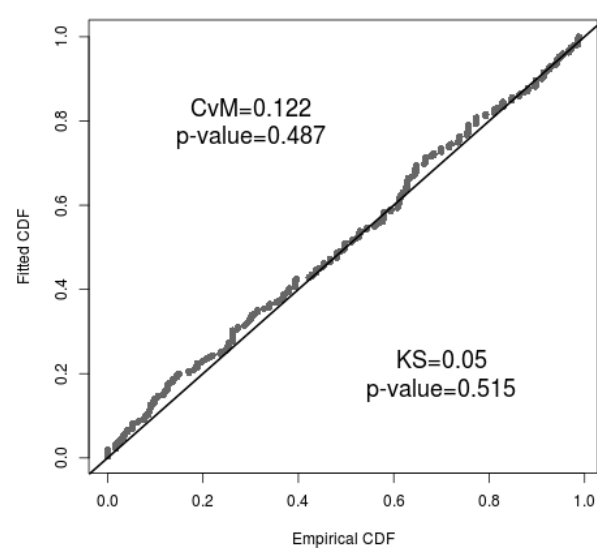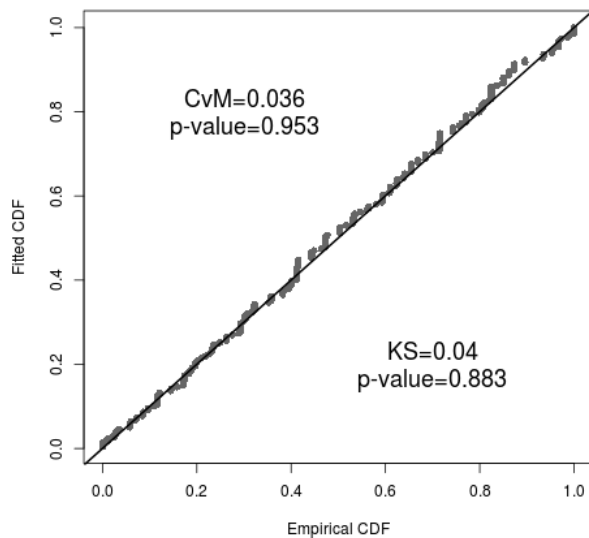

Figure T.8: Q-Q plot of the fitted and empirical cumulative density functions (CDF) for the top ranked model of the detection function analysis of the reduced ECSI winter data.

Table T.7: Top 10 AIC-ranked models for the detection function analysis for sightings reduced to between 0.071–0.3 km from the transect line in the winter for ECSI. Model components identify the structure of the detection function model; $f(d)$ is the functional relationship with distance on the logit scale (L=linear, Q=quadratic, S=Spline), Obs indicates whether the intercept term is different for each observer position (Y=Yes, N=No), $\beta_1 \neq \beta_2$ indicates whether the regression coefficients for the effect of distance on detection is different for each observer position (Y= Yes, N= No), Size indicates whether group size has an effect on detection (Y=Yes, N=No) and Dep. indicates the form of dependence in detection between observer positions (FI=Full Independence, C = Constant Dependence, P = Point Independence and L= Limiting Independence). ΔAIC is the relative difference in AIC values, wgt is the AIC model weight, wgt* is the adjusted AIC weight for the models used for inference, -2l is twice the negative log-likelihood, pars. is the number parameters in the model, $\hat{N}_{cg}$ is the estimated number of dolphin groups in the covered area, $SE(\hat{N}_{cg})$ is the standard error for $\hat{N}_{cg}$, corr. is the correlation between the intercepts of the detection and dependence components of the model and ESW is the effective strip width accounting for detection and perception bias.

<u>**Model Components**</u>

$f(d)$	Obs	$\beta_1 \neq \beta_2$	Size	Dep.	ΔAIC	wgt	wgt*	-2l	pars.	$\hat{N}_{cg}$	$SE(\hat{N}_{cg})$	corr.	ESW
Q	Y	Y	Y	L	0.00	0.49		351.39	9	759 060	6 278 826	-1.00	
Q	Y	Y	Y	C	0.78	0.34		354.16	8	37 183	92 543	-0.99	
S	Y	Y	Y	L	3.71	0.08		351.09	11	6 337	15 740	-0.99	
Q	Y	Y	Y	P	5.38	0.03	0.41	358.77	8	441	47		0.114
S	Y	Y	Y	P	5.63	0.03	0.36	355.02	10	407	39		0.123
L	Y	Y	Y	P	7.28	0.01	0.16	364.67	6	467	50		0.107
S	Y	Y	Y	C	8.07	0.01		357.45	10	809	478	-0.86	
L	Y	Y	Y	L	8.94	0.01	0.07	364.33	7	420	102	-0.96	0.119
L	Y	Y	Y	C	13.62	0.00		371.01	6	134 132	429 187	-0.99	
Q	Y	Y	N	P	15.73	0.00		371.12	7	437	42		

Table T.8: Goodness of fit tests for top seven ranked models for the detection function analysis of the reduced ECSI winter data set. Given are the Cramer-von Mises (CvM) and Kolmogorov-Smirnov (KS) tests with associated p-values.

Model Rank	CvM	p-value	KS	p-value
4	0.036	0.95	0.040	0.88
5	0.082	0.68	0.045	0.76
6	0.041	0.93	0.045	0.77
8	0.035	0.96	0.042	0.84

ECSI Availability estimates

Dive-cycle

The dive-cycle based availability estimates of MacKenzie & Clement (2014a) were used in this ECSI reanalysis. The values used for each strata are given in Table T.9.

Table T.9: Dive-cycle based estimates of Hector's dolphin availability ($\hat{P}_\alpha$) in ECSI strata and associated standard error (*SE*).

Coastal Section	Offshore Strata (nmi)	Summer $\hat{P}_\alpha$	SE	Winter $\hat{P}_\alpha$	SE
Golden Bay	0–4	0.63	0.08	0.46	0.03
North	4–12	0.63	0.08	0.46	0.03
Golden Bay A	0–4	0.63	0.08	0.46	0.03
	4–12	0.63	0.08	0.46	0.03
	12–20	0.63	0.08	0.46	0.03
Golden Bay B	0–4	0.63	0.08	0.46	0.03
	4–12	0.63	0.08	0.46	0.03
	12–20	0.63	0.08	0.46	0.03
Marlborough	0–4	0.63	0.08	0.46	0.03
Sounds	4–12	0.63	0.08	0.46	0.03
	12–20	0.63	0.08	0.46	0.03
Cloudy/Clifford	0–4	0.63	0.08	0.46	0.03
Bay	4–12	0.63	0.08	0.46	0.03
	12–20	0.63	0.08	0.46	0.03
Kaikoura	0–4	0.57	0.05	0.33	0.08
	4–12	0.57	0.05	0.33	0.08
	12–20	0.57	0.05	0.33	0.08
Clarence	0–4	0.57	0.05	0.33	0.08
	4–12	0.57	0.05	0.33	0.08
	12–20	0.57	0.05	0.33	0.08
Pegasus Bay	0–4	0.53	0.05	0.62	0.06
	4–12	0.53	0.05	0.62	0.06
	12–20	0.53	0.05	0.62	0.06
Banks Pen.	0–4	0.53	0.05	0.62	0.06
North	4–12	0.53	0.05	0.62	0.06
	12–20	0.53	0.05	0.62	0.06
Banks Pen.	0–4	0.42	0.03	0.56	0.05
South	4–12	0.42	0.03	0.56	0.05
	12–20	0.42	0.03	0.56	0.05
Timaru	0–4	0.42	0.03	0.56	0.05
	4–12	0.42	0.03	0.56	0.05
	12–20	0.42	0.03	0.56	0.05
Otago	0–4	0.40	0.05	0.56	0.05
	4–12	0.40	0.05	0.56	0.05
	12–20	0.40	0.05	0.56	0.05

Circle-back

Circle-back based availability was re-estimated for ECSI using the same data selection and analysis methods as those used for WCSI. A summary of the circle-back data used by MacKenzie & Clement (2014a) and the current analysis is presented in Table T.10 for a comparison. For each sighting data set and detection function, the circle-back availability data was analysed with four different models, with estimates from each of the four models being combined using AIC model averaging. The AIC model weights for each of the four models was very similar across the different detection functions for a given data set (Table T.11-Table T.14). These results suggest greater evidence of regional difference in the circle-back availability data in the winter compared to the summer. The circle back availability estimates that were used to estimate abundance from each detection function model and data set are given in Table T.15-Table T.21.

Table T.10: Summary of the circle back data used by MacKenzie & Clement (2014a; MC14) and the current reanalysis (MC15) to estimate availability. Results presented are the number of successful redetections of sighted groups and number of detection attempts.

		Summer		Winter	
		Full	**Reduced**	**Full**	**Reduced**
MC14	**Redetections**	93	72	68	55
	Attempts	215	176	181	142
MC15	**Redetections**	46	36	35	29
	Attempts	129	105	117	94

Table T.11: AIC model weights for each of the four models fit to the circle-back availability data for the full summer ECSI data. Separate results are provided for each detection function used for model averaging identified in Table T.1; Results presented are the detection function model rank and its AIC model weight.

Model	1 (0.29)	2 (0.21)	3 (0.15)	4 (0.11)	5 (0.08)	6 (0.05)	7 (0.04)	8 (0.04)	9 (0.02)	10 (0.01)
.	0.60	0.60	0.60	0.60	0.59	0.60	0.59	0.59	0.61	0.59
offshore	0.25	0.25	0.25	0.25	0.25	0.25	0.25	0.25	0.25	0.25
region	0.11	0.11	0.11	0.11	0.11	0.11	0.11	0.11	0.10	0.11
region+offshore	0.04	0.04	0.04	0.04	0.04	0.04	0.04	0.04	0.04	0.04

Table T.12: AIC model weights for each of the four models fit to the circle-back availability data for the reduced summer ECSI data. Separate results are provided for each detection function used for model averaging identified in Table T.3; results presented are the detection function model rank and its AIC model weight.

Model	1 (0.28)	2 (0.20)	3 (0.14)	4 (0.12)	5 (0.10)	6 (0.08)	7 (0.08)
.	0.34	0.34	0.34	0.34	0.34	0.34	0.34
offshore	0.16	0.16	0.15	0.16	0.15	0.15	0.16
region	0.37	0.37	0.37	0.37	0.37	0.37	0.37
region+offshore	0.14	0.14	0.14	0.14	0.14	0.14	0.14

Table T.13: AIC model weights for each of the four models fit to the circle-back availability data for the full winter ECSI data. Separate results are provided for each detection function used for model averaging identified in Table T.5; results presented are the detection function model rank and its AIC model weight.

Model	1 (0.65)	2 (0.12)	3 (0.10)	4 (0.09)	5 (0.03)	6 (0.02)
.	0.06	0.05	0.04	0.05	0.04	0.01
offshore	0.02	0.02	0.02	0.02	0.02	0.01
region	0.67	0.67	0.69	0.67	0.69	0.24
region+offshore	0.25	0.25	0.25	0.25	0.26	0.74

Table T.14: AIC model weights for each of the four models fit to the circle-back availability data for the reduced winter ECSI data. Separate results are provided for each detection function used for model averaging identified in Table T.7; results presented are the detection function model rank and its AIC model weight.

Model	1 (0.29)	2 (0.21)	3 (0.15)	4 (0.11)
.	0.02	0.04	0.02	0.05
offshore	0.01	0.01	0.01	0.02
region	0.32	0.42	0.27	0.67
region+offshore	0.65	0.53	0.70	0.26

Table T.15: Circle-back based estimates of Hector's dolphin availability ($\hat{P}_a$) in ECSI strata and associated standard error (*SE*) using the full summer sighting data. Separate estimates are provided for each detection function used for model averaging identified in Table T.1; results presented are the model rank and AIC model weight.

Coastal Section	Offshore Strata (nmi)	1 (0.29)		2 (0.21)		3 (0.15)		4 (0.11)		5 (0.08)	
		$\hat{P}_\alpha$	SE	$\hat{P}_\alpha$	SE	$\hat{P}_\alpha$	SE	$\hat{P}_\alpha$	SE	$\hat{P}_\alpha$	SE
Golden Bay	0–4	0.45	0.09	0.47	0.10	0.46	0.09	0.46	0.09	0.56	0.12
North	4–12	0.44	0.10	0.45	0.10	0.45	0.10	0.45	0.10	0.54	0.13
Golden Bay A	0–4	0.45	0.09	0.47	0.10	0.46	0.09	0.46	0.09	0.56	0.12
	4–12	0.44	0.10	0.45	0.10	0.45	0.10	0.45	0.10	0.54	0.13
	12–20	0.44	0.10	0.45	0.10	0.45	0.10	0.45	0.10	0.54	0.13
Golden Bay B	0–4	0.45	0.09	0.47	0.10	0.46	0.09	0.46	0.09	0.56	0.12
	4–12	0.44	0.10	0.45	0.10	0.45	0.10	0.45	0.10	0.54	0.13
	12–20	0.44	0.10	0.45	0.10	0.45	0.10	0.45	0.10	0.54	0.13
Marlborough	0–4	0.45	0.09	0.47	0.10	0.46	0.09	0.46	0.09	0.56	0.12
Sounds	4–12	0.44	0.10	0.45	0.10	0.45	0.10	0.45	0.10	0.54	0.13
	12–20	0.44	0.10	0.45	0.10	0.45	0.10	0.45	0.10	0.54	0.13
Cloudy/Clifford	0–4	0.45	0.09	0.47	0.10	0.46	0.09	0.46	0.09	0.56	0.12
Bay	4–12	0.44	0.10	0.45	0.10	0.45	0.10	0.45	0.10	0.54	0.13
	12–20	0.44	0.10	0.45	0.10	0.45	0.10	0.45	0.10	0.54	0.13
Kaikoura	0–4	0.42	0.09	0.43	0.10	0.43	0.09	0.43	0.09	0.52	0.12
	4–12	0.41	0.09	0.42	0.09	0.42	0.09	0.42	0.09	0.50	0.11
	12–20	0.41	0.09	0.42	0.09	0.42	0.09	0.42	0.09	0.50	0.11
Clarence	0–4	0.42	0.09	0.43	0.10	0.43	0.09	0.43	0.09	0.52	0.12
	4–12	0.41	0.09	0.42	0.09	0.42	0.09	0.42	0.09	0.50	0.11
	12–20	0.41	0.09	0.42	0.09	0.42	0.09	0.42	0.09	0.50	0.11
Pegasus Bay	0–4	0.44	0.06	0.45	0.06	0.45	0.06	0.45	0.06	0.54	0.08
	4–12	0.43	0.07	0.44	0.07	0.43	0.07	0.44	0.07	0.53	0.08
	12–20	0.43	0.07	0.44	0.07	0.43	0.07	0.44	0.07	0.53	0.08
Banks Pen.	0–4	0.44	0.06	0.45	0.06	0.45	0.06	0.45	0.06	0.54	0.08
North	4–12	0.43	0.07	0.44	0.07	0.43	0.07	0.44	0.07	0.53	0.08
	12–20	0.43	0.07	0.44	0.07	0.43	0.07	0.44	0.07	0.53	0.08
Banks Pen.	0–4	0.46	0.07	0.47	0.08	0.47	0.07	0.47	0.07	0.57	0.09
South	4–12	0.45	0.08	0.46	0.08	0.45	0.08	0.46	0.08	0.55	0.10
	12–20	0.45	0.08	0.46	0.08	0.45	0.08	0.46	0.08	0.55	0.10
Timaru	0–4	0.46	0.07	0.47	0.08	0.47	0.07	0.47	0.07	0.57	0.09
	4–12	0.45	0.08	0.46	0.08	0.45	0.08	0.46	0.08	0.55	0.10
	12–20	0.45	0.08	0.46	0.08	0.45	0.08	0.46	0.08	0.55	0.10
Otago	0–4	0.46	0.07	0.47	0.08	0.47	0.07	0.47	0.07	0.57	0.09
	4–12	0.45	0.08	0.46	0.08	0.45	0.08	0.46	0.08	0.55	0.10
	12–20	0.45	0.08	0.46	0.08	0.45	0.08	0.46	0.08	0.55	0.10

Table T.16: Circle-back based estimates of Hector's dolphin availability ($\hat{P}_\alpha$) in ECSI strata and associated standard error (*SE*) using the full summer sighting data. Separate estimates are provided for each detection function used for model averaging identified in Table T.1; results presented are the model rank and AIC model weight.

Coastal Section	Offshore Strata (nmi)	6 (0.05) $\hat{P}_\alpha$	6 (0.05) SE	7 (0.04) $\hat{P}_\alpha$	7 (0.04) SE	8 (0.04) $\hat{P}_\alpha$	8 (0.04) SE	9 (0.02) $\hat{P}_\alpha$	9 (0.02) SE	10 (0.01) $\hat{P}_\alpha$	10 (0.01) SE
Golden Bay North	0–4	0.47	0.10	0.56	0.12	0.60	0.13	0.60	0.13	0.48	0.10
	4–12	0.45	0.10	0.55	0.13	0.58	0.13	0.58	0.13	0.46	0.10
Golden Bay A	0–4	0.47	0.10	0.56	0.12	0.60	0.13	0.60	0.13	0.48	0.10
	4–12	0.45	0.10	0.55	0.13	0.58	0.13	0.58	0.13	0.46	0.10
	12–20	0.45	0.10	0.55	0.13	0.58	0.13	0.58	0.13	0.46	0.10
Golden Bay B	0–4	0.47	0.10	0.56	0.12	0.60	0.13	0.60	0.13	0.48	0.10
	4–12	0.45	0.10	0.55	0.13	0.58	0.13	0.58	0.13	0.46	0.10
	12–20	0.45	0.10	0.55	0.13	0.58	0.13	0.58	0.13	0.46	0.10
Marlborough Sounds	0–4	0.47	0.10	0.56	0.12	0.60	0.13	0.60	0.13	0.48	0.10
	4–12	0.45	0.10	0.55	0.13	0.58	0.13	0.58	0.13	0.46	0.10
	12–20	0.45	0.10	0.55	0.13	0.58	0.13	0.58	0.13	0.46	0.10
Cloudy/Clifford Bay	0–4	0.47	0.10	0.56	0.12	0.60	0.13	0.60	0.13	0.48	0.10
	4–12	0.45	0.10	0.55	0.13	0.58	0.13	0.58	0.13	0.46	0.10
	12–20	0.45	0.10	0.55	0.13	0.58	0.13	0.58	0.13	0.46	0.10
Kaikoura	0–4	0.43	0.10	0.52	0.12	0.55	0.13	0.55	0.13	0.44	0.10
	4–12	0.42	0.09	0.51	0.11	0.54	0.12	0.54	0.12	0.43	0.09
	12–20	0.42	0.09	0.51	0.11	0.54	0.12	0.54	0.12	0.43	0.09
Clarence	0–4	0.43	0.10	0.52	0.12	0.55	0.13	0.55	0.13	0.44	0.10
	4–12	0.42	0.09	0.51	0.11	0.54	0.12	0.54	0.12	0.43	0.09
	12–20	0.42	0.09	0.51	0.11	0.54	0.12	0.54	0.12	0.43	0.09
Pegasus Bay	0–4	0.45	0.06	0.55	0.08	0.58	0.08	0.58	0.08	0.46	0.07
	4–12	0.44	0.07	0.53	0.08	0.56	0.09	0.56	0.09	0.45	0.07
	12–20	0.44	0.07	0.53	0.08	0.56	0.09	0.56	0.09	0.45	0.07
Banks Pen. North	0–4	0.45	0.06	0.55	0.08	0.58	0.08	0.58	0.08	0.46	0.07
	4–12	0.44	0.07	0.53	0.08	0.56	0.09	0.56	0.09	0.45	0.07
	12–20	0.44	0.07	0.53	0.08	0.56	0.09	0.56	0.09	0.45	0.07
Banks Pen. South	0–4	0.47	0.08	0.57	0.09	0.61	0.10	0.61	0.10	0.48	0.08
	4–12	0.46	0.09	0.56	0.10	0.59	0.11	0.59	0.11	0.47	0.09
	12–20	0.46	0.09	0.56	0.10	0.59	0.11	0.59	0.11	0.47	0.09
Timaru	0–4	0.47	0.08	0.57	0.09	0.61	0.10	0.61	0.10	0.48	0.08
	4–12	0.46	0.09	0.56	0.10	0.59	0.11	0.59	0.11	0.47	0.09
	12–20	0.46	0.09	0.56	0.10	0.59	0.11	0.59	0.11	0.47	0.09
Otago	0–4	0.47	0.08	0.57	0.09	0.61	0.10	0.61	0.10	0.48	0.08
	4–12	0.46	0.09	0.56	0.10	0.59	0.11	0.59	0.11	0.47	0.09
	12–20	0.46	0.09	0.56	0.10	0.59	0.11	0.59	0.11	0.47	0.09

Table T.17: Circle-back based estimates of Hector's dolphin availability ($\hat{P}_\alpha$) in ECSI strata and associated standard error (*SE*) using the reduced summer sighting data. Separate estimates are provided for each detection function used for model averaging identified in Table T.3; results presented are the model rank and AIC model weight.

Coastal Section	Offshore Strata (nmi)	1 (0.28) $\hat{P}_\alpha$	SE	2 (0.20) $\hat{P}_\alpha$	SE	3 (0.14) $\hat{P}_\alpha$	SE	4 (0.12) $\hat{P}_\alpha$	SE
Golden Bay	0–4	0.42	0.17	0.42	0.17	0.38	0.16	0.41	0.17
North	4–12	0.40	0.18	0.40	0.18	0.36	0.16	0.39	0.17
Golden Bay A	0–4	0.42	0.17	0.42	0.17	0.38	0.16	0.41	0.17
	4–12	0.40	0.18	0.40	0.18	0.36	0.16	0.39	0.17
	12–20	0.40	0.18	0.40	0.18	0.36	0.16	0.39	0.17
Golden Bay B	0–4	0.42	0.17	0.42	0.17	0.38	0.16	0.41	0.17
	4–12	0.40	0.18	0.40	0.18	0.36	0.16	0.39	0.17
	12–20	0.40	0.18	0.40	0.18	0.36	0.16	0.39	0.17
Marlborough	0–4	0.42	0.17	0.42	0.17	0.38	0.16	0.41	0.17
Sounds	4–12	0.40	0.18	0.40	0.18	0.36	0.16	0.39	0.17
	12–20	0.40	0.18	0.40	0.18	0.36	0.16	0.39	0.17
Cloudy/Clifford	0–4	0.42	0.17	0.42	0.17	0.38	0.16	0.41	0.17
Bay	4–12	0.40	0.18	0.40	0.18	0.36	0.16	0.39	0.17
	12–20	0.40	0.18	0.40	0.18	0.36	0.16	0.39	0.17
Kaikoura	0–4	0.38	0.16	0.38	0.16	0.34	0.14	0.37	0.15
	4–12	0.37	0.15	0.37	0.15	0.33	0.13	0.36	0.14
	12–20	0.37	0.15	0.37	0.15	0.33	0.13	0.36	0.14
Clarence	0–4	0.38	0.16	0.38	0.16	0.34	0.14	0.37	0.15
	4–12	0.37	0.15	0.37	0.15	0.33	0.13	0.36	0.14
	12–20	0.37	0.15	0.37	0.15	0.33	0.13	0.36	0.14
Pegasus Bay	0–4	0.45	0.09	0.44	0.09	0.40	0.08	0.44	0.09
	4–12	0.43	0.09	0.43	0.09	0.39	0.09	0.42	0.09
	12–20	0.43	0.09	0.43	0.09	0.39	0.09	0.42	0.09
Banks Pen.	0–4	0.45	0.09	0.44	0.09	0.40	0.08	0.44	0.09
North	4–12	0.43	0.09	0.43	0.09	0.39	0.09	0.42	0.09
	12–20	0.43	0.09	0.43	0.09	0.39	0.09	0.42	0.09
Banks Pen.	0–4	0.60	0.15	0.60	0.15	0.54	0.14	0.58	0.15
South	4–12	0.58	0.17	0.58	0.17	0.53	0.15	0.57	0.16
	12–20	0.58	0.17	0.58	0.17	0.53	0.15	0.57	0.16
Timaru	0–4	0.60	0.15	0.60	0.15	0.54	0.14	0.58	0.15
	4–12	0.58	0.17	0.58	0.17	0.53	0.15	0.57	0.16
	12–20	0.58	0.17	0.58	0.17	0.53	0.15	0.57	0.16
Otago	0–4	0.60	0.15	0.60	0.15	0.54	0.14	0.58	0.15
	4–12	0.58	0.17	0.58	0.17	0.53	0.15	0.57	0.16
	12–20	0.58	0.17	0.58	0.17	0.53	0.15	0.57	0.16

Table T.18: Circle-back based estimates of Hector's dolphin availability ($\hat{P}_\alpha$) in ECSI strata and associated standard error (*SE*) using the reduced summer sighting data. Separate estimates are provided for each detection function used for model averaging identified in Table T.3; results presented are the model rank and AIC model weight.

Coastal Section	Offshore Strata (nmi)	5 (0.10)		6 (0.08)		7 (0.08)	
		$\hat{P}_\alpha$	SE	$\hat{P}_\alpha$	SE	$\hat{P}_\alpha$	SE
Golden Bay	0–4	0.38	0.16	0.36	0.15	0.41	0.17
North	4–12	0.36	0.16	0.35	0.15	0.39	0.17
Golden Bay A	0–4	0.38	0.16	0.36	0.15	0.41	0.17
	4–12	0.36	0.16	0.35	0.15	0.39	0.17
	12–20	0.36	0.16	0.35	0.15	0.39	0.17
Golden Bay B	0–4	0.38	0.16	0.36	0.15	0.41	0.17
	4–12	0.36	0.16	0.35	0.15	0.39	0.17
	12–20	0.36	0.16	0.35	0.15	0.39	0.17
Marlborough	0–4	0.38	0.16	0.36	0.15	0.41	0.17
Sounds	4–12	0.36	0.16	0.35	0.15	0.39	0.17
	12–20	0.36	0.16	0.35	0.15	0.39	0.17
Cloudy/Clifford	0–4	0.38	0.16	0.36	0.15	0.41	0.17
Bay	4–12	0.36	0.16	0.35	0.15	0.39	0.17
	12–20	0.36	0.16	0.35	0.15	0.39	0.17
Kaikoura	0–4	0.35	0.14	0.33	0.14	0.37	0.15
	4–12	0.33	0.13	0.32	0.13	0.36	0.14
	12–20	0.33	0.13	0.32	0.13	0.36	0.14
Clarence	0–4	0.35	0.14	0.33	0.14	0.37	0.15
	4–12	0.33	0.13	0.32	0.13	0.36	0.14
	12–20	0.33	0.13	0.32	0.13	0.36	0.14
Pegasus Bay	0–4	0.40	0.08	0.39	0.08	0.43	0.09
	4–12	0.39	0.09	0.37	0.08	0.42	0.09
	12–20	0.39	0.09	0.37	0.08	0.42	0.09
Banks Pen.	0–4	0.40	0.08	0.39	0.08	0.43	0.09
North	4–12	0.39	0.09	0.37	0.08	0.42	0.09
	12–20	0.39	0.09	0.37	0.08	0.42	0.09
Banks Pen.	0–4	0.55	0.14	0.52	0.13	0.58	0.15
South	4–12	0.53	0.15	0.51	0.15	0.57	0.16
	12–20	0.53	0.15	0.51	0.15	0.57	0.16
Timaru	0–4	0.55	0.14	0.52	0.13	0.58	0.15
	4–12	0.53	0.15	0.51	0.15	0.57	0.16
	12–20	0.53	0.15	0.51	0.15	0.57	0.16
Otago	0–4	0.55	0.14	0.52	0.13	0.58	0.15
	4–12	0.53	0.15	0.51	0.15	0.57	0.16
	12–20	0.53	0.15	0.51	0.15	0.57	0.16

Table T.19: Circle-back based estimates of Hector's dolphin availability ($\hat{P}_\alpha$) in ECSI strata and associated standard error (*SE*) using the full winter sighting data. Separate estimates are provided for each detection function used for model averaging identified in Table T.5; results presented are the model rank and AIC model weight.

Coastal Section	Offshore Strata (nmi)	1 (0.65)		2 (0.12)		3 (0.10)	
		$\hat{P}_\alpha$	SE	$\hat{P}_\alpha$	SE	$\hat{P}_\alpha$	SE
Golden Bay	0–4	0.20	0.17	0.21	0.18	0.24	0.21
North	4–12	0.20	0.18	0.21	0.19	0.24	0.23
Golden Bay A	0–4	0.20	0.17	0.21	0.18	0.24	0.21
	4–12	0.20	0.18	0.21	0.19	0.24	0.23
	12–20	0.20	0.18	0.21	0.19	0.24	0.23
Golden Bay B	0–4	0.20	0.17	0.21	0.18	0.24	0.21
	4–12	0.20	0.18	0.21	0.19	0.24	0.23
	12–20	0.20	0.18	0.21	0.19	0.24	0.23
Marlborough	0–4	0.20	0.17	0.21	0.18	0.24	0.21
Sounds	4–12	0.20	0.18	0.21	0.19	0.24	0.23
	12–20	0.20	0.18	0.21	0.19	0.24	0.23
Cloudy/Clifford	0–4	0.20	0.17	0.21	0.18	0.24	0.21
Bay	4–12	0.20	0.18	0.21	0.19	0.24	0.23
	12–20	0.20	0.18	0.21	0.19	0.24	0.23
Kaikoura	0–4	0.22	0.11	0.23	0.12	0.26	0.15
	4–12	0.22	0.09	0.23	0.10	0.25	0.11
	12–20	0.22	0.09	0.23	0.10	0.25	0.11
Clarence	0–4	0.22	0.11	0.23	0.12	0.26	0.15
	4–12	0.22	0.09	0.23	0.10	0.25	0.11
	12–20	0.22	0.09	0.23	0.10	0.25	0.11
Pegasus Bay	0–4	0.53	0.14	0.58	0.16	0.69	0.21
	4–12	0.54	0.13	0.58	0.14	0.69	0.16
	12–20	0.54	0.13	0.58	0.14	0.69	0.16
Banks Pen.	0–4	0.53	0.14	0.58	0.16	0.69	0.21
North	4–12	0.54	0.13	0.58	0.14	0.69	0.16
	12–20	0.54	0.13	0.58	0.14	0.69	0.16
Banks Pen.	0–4	0.58	0.12	0.62	0.13	0.70	0.14
South	4–12	0.58	0.13	0.62	0.14	0.70	0.16
	12–20	0.58	0.13	0.62	0.14	0.70	0.16
Timaru	0–4	0.58	0.12	0.62	0.13	0.70	0.14
	4–12	0.58	0.13	0.62	0.14	0.70	0.16
	12–20	0.58	0.13	0.62	0.14	0.70	0.16
Otago	0–4	0.58	0.12	0.62	0.13	0.70	0.14
	4–12	0.58	0.13	0.62	0.14	0.70	0.16
	12–20	0.58	0.13	0.62	0.14	0.70	0.16

Table T.20: Circle-back based estimates of Hector's dolphin availability ($\hat{P}_\alpha$) in ECSI strata and associated standard error (*SE*) using the full winter sighting data. Separate estimates are provided for each detection function used for model averaging identified in Table T.5; results presented are the model rank and AIC model weight.

Coastal Section	Offshore Strata (nmi)	4 (0.09) $\hat{P}_\alpha$	SE	5 (0.03) $\hat{P}_\alpha$	SE	6 (0.02) $\hat{P}_\alpha$	SE
Golden Bay	0–4	0.21	0.19	0.24	0.21	0.24	0.23
North	4–12	0.22	0.20	0.22	0.23	0.80	0.35
Golden Bay A	0–4	0.21	0.19	0.24	0.21	0.24	0.23
	4–12	0.22	0.20	0.22	0.23	0.80	0.35
	12–20	0.22	0.20	0.22	0.23	0.80	0.35
Golden Bay B	0–4	0.21	0.19	0.24	0.21	0.24	0.23
	4–12	0.22	0.20	0.22	0.23	0.80	0.35
	12–20	0.22	0.20	0.22	0.23	0.80	0.35
Marlborough	0–4	0.21	0.19	0.24	0.21	0.24	0.23
Sounds	4–12	0.22	0.20	0.22	0.23	0.80	0.35
	12–20	0.22	0.20	0.22	0.23	0.80	0.35
Cloudy/Clifford	0–4	0.21	0.19	0.24	0.21	0.24	0.23
Bay	4–12	0.22	0.20	0.22	0.23	0.80	0.35
	12–20	0.22	0.20	0.22	0.23	0.80	0.35
Kaikoura	0–4	0.23	0.12	0.27	0.20	0.07	0.14
	4–12	0.24	0.10	0.25	0.11	0.29	0.11
	12–20	0.24	0.10	0.25	0.11	0.29	0.11
Clarence	0–4	0.23	0.12	0.27	0.20	0.07	0.14
	4–12	0.24	0.10	0.25	0.11	0.29	0.11
	12–20	0.24	0.10	0.25	0.11	0.29	0.11
Pegasus Bay	0–4	0.59	0.16	0.73	0.25	0.34	0.31
	4–12	0.59	0.14	0.72	0.19	0.93	0.14
	12–20	0.59	0.14	0.72	0.19	0.93	0.14
Banks Pen.	0–4	0.59	0.16	0.73	0.25	0.34	0.31
North	4–12	0.59	0.14	0.72	0.19	0.93	0.14
	12–20	0.59	0.14	0.72	0.19	0.93	0.14
Banks Pen.	0–4	0.63	0.13	0.71	0.15	0.93	0.13
South	4–12	0.63	0.14	0.68	0.17	0.93	0.14
	12–20	0.63	0.14	0.68	0.17	0.93	0.14
Timaru	0–4	0.63	0.13	0.71	0.15	0.93	0.13
	4–12	0.63	0.14	0.68	0.17	0.93	0.14
	12–20	0.63	0.14	0.68	0.17	0.93	0.14
Otago	0–4	0.63	0.13	0.71	0.15	0.93	0.13
	4–12	0.63	0.14	0.68	0.17	0.93	0.14
	12–20	0.63	0.14	0.68	0.17	0.93	0.14

Table T.21: Circle-back based estimates of Hector's dolphin availability ($\hat{P}_\alpha$) in ECSI strata and associated standard error (*SE*) using the reduced winter sighting data. Separate estimates are provided for each detection function used for model averaging identified in Table T.7; results presented are the model rank and AIC model weight.

Coastal Section	Offshore Strata (nmi)	4 (0.41)		5 (0.36)		6 (0.16)		8 (0.07)	
		$\hat{P}_\alpha$	SE	$\hat{P}_\alpha$	SE	$\hat{P}_\alpha$	SE	$\hat{P}_\alpha$	SE
Golden Bay	0–4	0.35	0.31	0.33	0.29	0.37	0.33	0.31	0.27
North	4–12	0.78	0.35	0.69	0.38	0.82	0.33	0.34	0.31
Golden Bay A	0–4	0.35	0.31	0.33	0.29	0.37	0.33	0.31	0.27
	4–12	0.78	0.35	0.69	0.38	0.82	0.33	0.34	0.31
	12–20	0.78	0.35	0.69	0.38	0.82	0.33	0.34	0.31
Golden Bay B	0–4	0.35	0.31	0.33	0.29	0.37	0.33	0.31	0.27
	4–12	0.78	0.35	0.69	0.38	0.82	0.33	0.34	0.31
	12–20	0.78	0.35	0.69	0.38	0.82	0.33	0.34	0.31
Marlborough	0–4	0.35	0.31	0.33	0.29	0.37	0.33	0.31	0.27
Sounds	4–12	0.78	0.35	0.69	0.38	0.82	0.33	0.34	0.31
	12–20	0.78	0.35	0.69	0.38	0.82	0.33	0.34	0.31
Cloudy/Clifford	0–4	0.35	0.31	0.33	0.29	0.37	0.33	0.31	0.27
Bay	4–12	0.78	0.35	0.69	0.38	0.82	0.33	0.34	0.31
	12–20	0.78	0.35	0.69	0.38	0.82	0.33	0.34	0.31
Kaikoura	0–4	0.09	0.15	0.12	0.16	0.08	0.15	0.21	0.14
	4–12	0.26	0.13	0.25	0.13	0.27	0.13	0.22	0.12
	12–20	0.26	0.13	0.25	0.13	0.27	0.13	0.22	0.12
Clarence	0–4	0.09	0.15	0.12	0.16	0.08	0.15	0.21	0.14
	4–12	0.26	0.13	0.25	0.13	0.27	0.13	0.22	0.12
	12–20	0.26	0.13	0.25	0.13	0.27	0.13	0.22	0.12
Pegasus Bay	0–4	0.44	0.35	0.47	0.33	0.44	0.36	0.70	0.21
	4–12	0.94	0.15	0.88	0.18	0.96	0.13	0.72	0.17
	12–20	0.94	0.15	0.88	0.18	0.96	0.13	0.72	0.17
Banks Pen.	0–4	0.44	0.35	0.47	0.33	0.44	0.36	0.70	0.21
North	4–12	0.94	0.15	0.88	0.18	0.96	0.13	0.72	0.17
	12–20	0.94	0.15	0.88	0.18	0.96	0.13	0.72	0.17
Banks Pen.	0–4	0.91	0.15	0.87	0.18	0.94	0.13	0.67	0.16
South	4–12	0.91	0.15	0.87	0.18	0.94	0.13	0.69	0.16
	12–20	0.91	0.15	0.87	0.18	0.94	0.13	0.69	0.16
Timaru	0–4	0.91	0.15	0.87	0.18	0.94	0.13	0.67	0.16
	4–12	0.91	0.15	0.87	0.18	0.94	0.13	0.69	0.16
	12–20	0.91	0.15	0.87	0.18	0.94	0.13	0.69	0.16
Otago	0–4	0.91	0.15	0.87	0.18	0.94	0.13	0.67	0.16
	4–12	0.91	0.15	0.87	0.18	0.94	0.13	0.69	0.16
	12–20	0.91	0.15	0.87	0.18	0.94	0.13	0.69	0.16

ECSI Abundance estimates

For each data set, Hector's dolphin abundance along the ECSI was estimated using each detection function and method of estimating availability. The detection function-specific estimates were combined using model averaging based upon the detection function models AIC weights (Table T.22 and Table T.23). An overall season-specific estimate was obtained by combining the four separate estimates (full vs reduced sighting data set, and dive-cycle vs circle-back availability) with equal weighting (Table T.24 and Table T.25). Overall standard error calculations accounted for variation amongst the different sets of abundance estimates. Summer ECSI Hector's dolphin abundance is estimated to be 9,728 (CV: 17%; 95% CI: 7,001–13,517) and in winter 8,208 (CV 27%; 95% CI: 4,888–13,785).

ECSI Distribution results

The results of the summer and winter DSM are given in Figures T.9a–b. Note how the visual impression of the estimated dolphin distribution can change depending on how the results of the DSM are presented. The right-hand panels of Figures T.9b and T.10b indicate the precision of the relative abundance estimates from the DSM and tend to be greatest in those areas with higher relative density. As seen in the raw data, the DSMs support general offshore movement from summer to winter, with lower winter relative densities close to shore in Cloudy/Clifford Bay, Pegasus Bay and Banks Peninsula, and an increase in relative densities offshore of Timaru.

Discussion

The revised ECSI abundance estimates using the dive-cycle based estimates of availability are very similar to those reported by MacKenzie & Clement (2014a), suggesting that the reanalysis of the sighting data using the symmetric parameterisation has had little overall impact upon the results. The largest apparent differences in the revised abundance estimates are associated with the circle-back availability estimates, which is due to a more correct treatment of the circle-back data. MacKenzie & Clement (2014a) used the redetection attempts for those sighted dolphin groups that initiated the circle-back procedure and all detection attempts for additional dolphin groups that were sighted during the circle-backs. Therefore, the 'extra' dolphin groups must be sighted at least once (i.e., there can be no records of 'extra' groups that were never sighted during the circle backs), which will cause availability to be overestimated, and abundance underestimated. Assuming no change in detection or availability of a group after first detection, using only the observations from the redetection attempts of all groups should yield a less biased availability estimate. Rectifying this oversight in the initial analysis resulted in higher abundance estimates. Unfortunately, this has also reduced the effective sample size for estimating availability resulting in higher standard errors, particularly for the winter analysis.

Despite these differences, overall conclusions about ECSI Hector's dolphin abundance are essential unchanged by the reanalysis, especially when the degree of uncertainty associated with the estimates is considered.

Table T.22: Model averaged ECSI summer abundance estimates and standard errors for each stratum from data of sightings between 0–0.3 km (Full Data) and 0.071–0.3 km (Reduced Data). Given are the estimated abundance of ECSI Hector's dolphins (corrected for availability bias; $\hat{N}_k$) using the availability estimates from the dive-cycle data and circle-back data.

Coastal Section	Offshore Stratum (nmi)	Full Data				Reduced Data			
		Dive Cycle		Circle-back		Dive Cycle		Circle-back	
		$\hat{N}_k$	SE	$\hat{N}_k$	SE	$\hat{N}_k$	SE	$\hat{N}_k$	SE
Golden Bay North	0–4								
	4–12								
Golden Bay A	0–4								
	4–12								
	12–20								
Golden Bay B	0–4								
	4–12								
	12–20								
Marlborough Sounds	0–4								
	4–12								
	12–20								
Cloudy/Clifford Bay	0–4	401	145	525	201	413	147	650	345
	4–12	466	159	628	238	441	137	719	377
	12–20								
Kaikoura	0–4	369	198	468	268	333	190	515	361
	4–12								
	12–20								
Clarence	0–4	136	115	172	149	181	152	279	260
	4–12								
	12–20								
Pegasus Bay	0–4	417	127	478	146	436	123	545	182
	4–12	275	160	325	192	324	186	418	255
	12–20	296	282	349	332	238	235	307	310
Banks Pen. North	0–4	875	199	1003	240	889	215	1110	337
	4–12	889	333	1048	400	952	341	1230	502
	12–20	439	313	518	370	549	380	709	511
Banks Pen. South	0–4	1843	371	1597	375	1947	394	1427	451
	4–12	1050	472	936	446	1226	543	922	481
	12–20								
Timaru	0–4	715	264	619	239	749	296	549	254
	4–12	1125	510	1005	487	1076	524	809	454
	12–20								
Otago	0–4								
	4–12								
	12–20								
Total		**9297**	**1431**	**9672**	**1667**	**9753**	**1384**	**10190**	**1915**

Table T.23: Model averaged ECSI winter abundance estimates and standard errors for each stratum from data of sightings between 0–0.3 km (Full Data) and 0.071–0.3 km (Reduced Data). Given are the estimated abundance of ECSI Hector's dolphins (corrected for availability bias; $\hat{N}_k$) using the availability estimates from the dive-cycle data and circle-back data.

Coastal Section	Offshore Stratum (nmi)	Full Data				Reduced Data			
		Dive Cycle		Circle-back		Dive Cycle		Circle-back	
		$\hat{N}_k$	SE	$\hat{N}_k$	SE	$\hat{N}_k$	SE	$\hat{N}_k$	SE
Golden Bay North	0–4								
	4–12								
Golden Bay A	0–4								
	4–12	151	162	329	469	227	244	150	199
	12–20								
Golden Bay B	0–4								
	4–12								
	12–20								
Marlborough Sounds	0–4								
	4–12								
	12–20								
Cloudy/Clifford Bay	0–4	117	70	260	276	64	70	85	120
	4–12	387	155	840	851	327	125	217	176
	12–20	216	153	468	547	213	126	141	133
Kaikoura	0–4	239	120	371	489	200	134	668	1217
	4–12								
	12–20								
Clarence	0–4	409	213	632	774	320	200	1064	1901
	4–12								
	12–20								
Pegasus Bay	0–4	44	35	49	44	75	59	99	110
	4–12	519	259	556	298	677	421	461	296
	12–20	422	174	453	208	404	148	275	110
Banks Pen. North	0–4	282	87	314	156	351	119	468	395
	4–12	493	125	528	169	587	155	400	124
	12–20	491	230	527	269	546	274	372	197
Banks Pen. South	0–4	482	142	442	152	532	172	339	125
	4–12	263	74	240	81	319	106	202	76
	12–20	134	103	122	97	65	48	42	32
Timaru	0–4	271	96	249	98	231	88	147	62
	4–12	1842	418	1684	503	2162	531	1372	415
	12–20	1051	303	960	331	1343	430	852	312
Otago	0–4								
	4–12								
	12–20								
Total		**7814**	**1155**	**9023**	**2422**	**8641**	**1371**	**7355**	**2952**

Table T.24: Estimated ECSI summer abundance of Hector's dolphins in each stratum and overall obtained from averaging the four sets of results from the two different data sets and methods of estimating availability. Results presented are the average estimate and associated standard error, along with the lower and upper limits of a 95% confidence interval.

Coastal Section	Offshore Stratum (nmi)	$\overline{\hat{N}}_k$	SE	Lower	Upper
Golden Bay North	0–4				
	4–12				
Golden Bay A	0–4				
	4–12				
	12–20				
Golden Bay B	0–4				
	4–12				
	12–20				
Marlborough Sounds	0–4				
	4–12				
	12–20				
Cloudy/Clifford Bay	0–4	497	246	199	1245
	4–12	564	272	230	1381
	12–20				
Kaikoura	0–4	421	273	132	1346
	4–12				
	12–20				
Clarence	0–4	192	185	39	942
	4–12				
	12–20				
Pegasus Bay	0–4	469	155	250	880
	4–12	336	208	110	1025
	12–20	298	295	59	1504
Banks Pen. North	0–4	969	271	566	1659
	4–12	1030	420	477	2222
	12–20	554	412	151	2034
Banks Pen. South	0–4	1704	448	1026	2829
	4–12	1034	502	420	2546
	12–20				
Timaru	0–4	658	276	299	1447
	4–12	1004	509	393	2563
	12–20				
Otago	0–4				
	4–12				
	12–20				
Total		**9728**	**1644**	**7001**	**13517**

Table T.25: Estimated ECSI winter abundance of Hector's dolphins in each stratum and overall obtained from averaging the four sets of results from the two different data sets and methods of estimating availability. Results presented are the average estimate and associated standard error, along with the lower and upper limits of a 95% confidence interval.

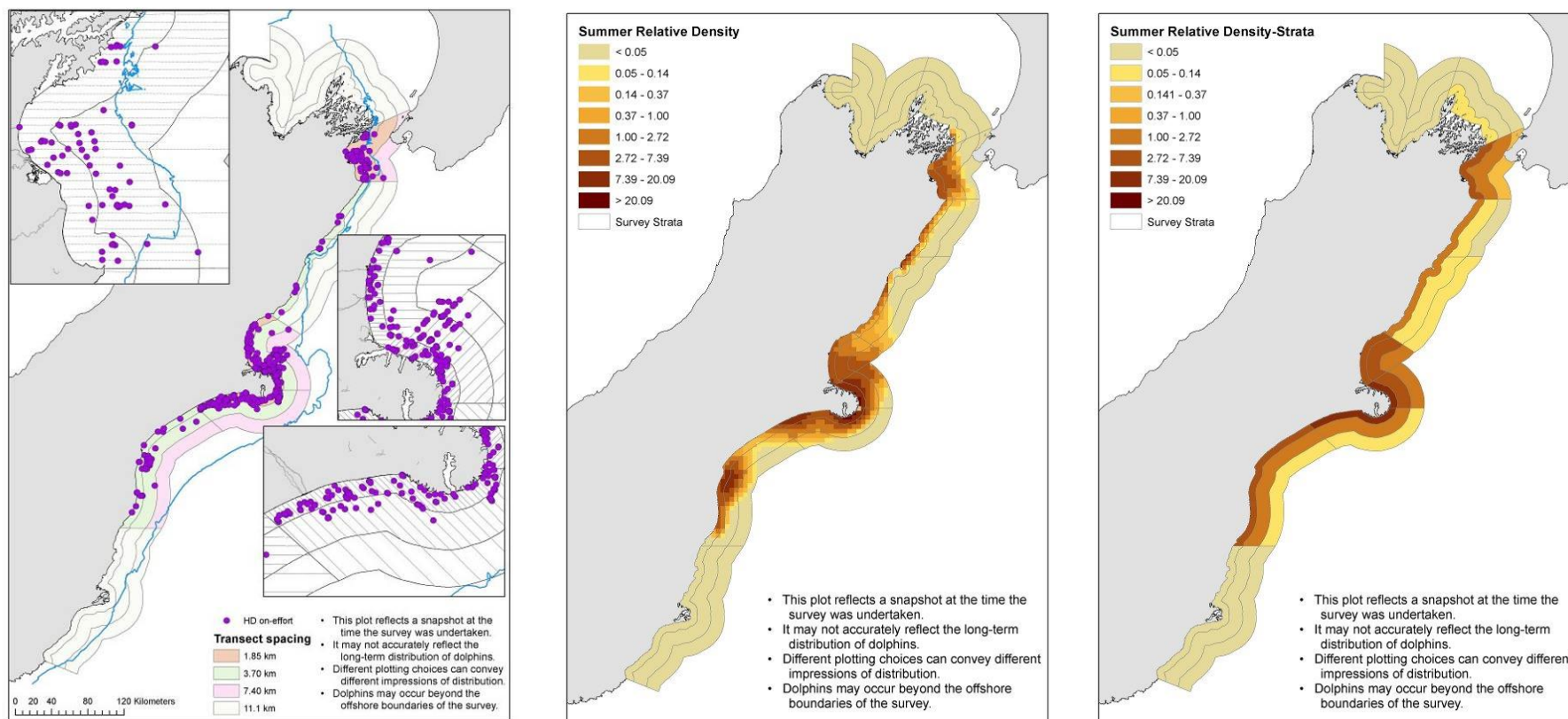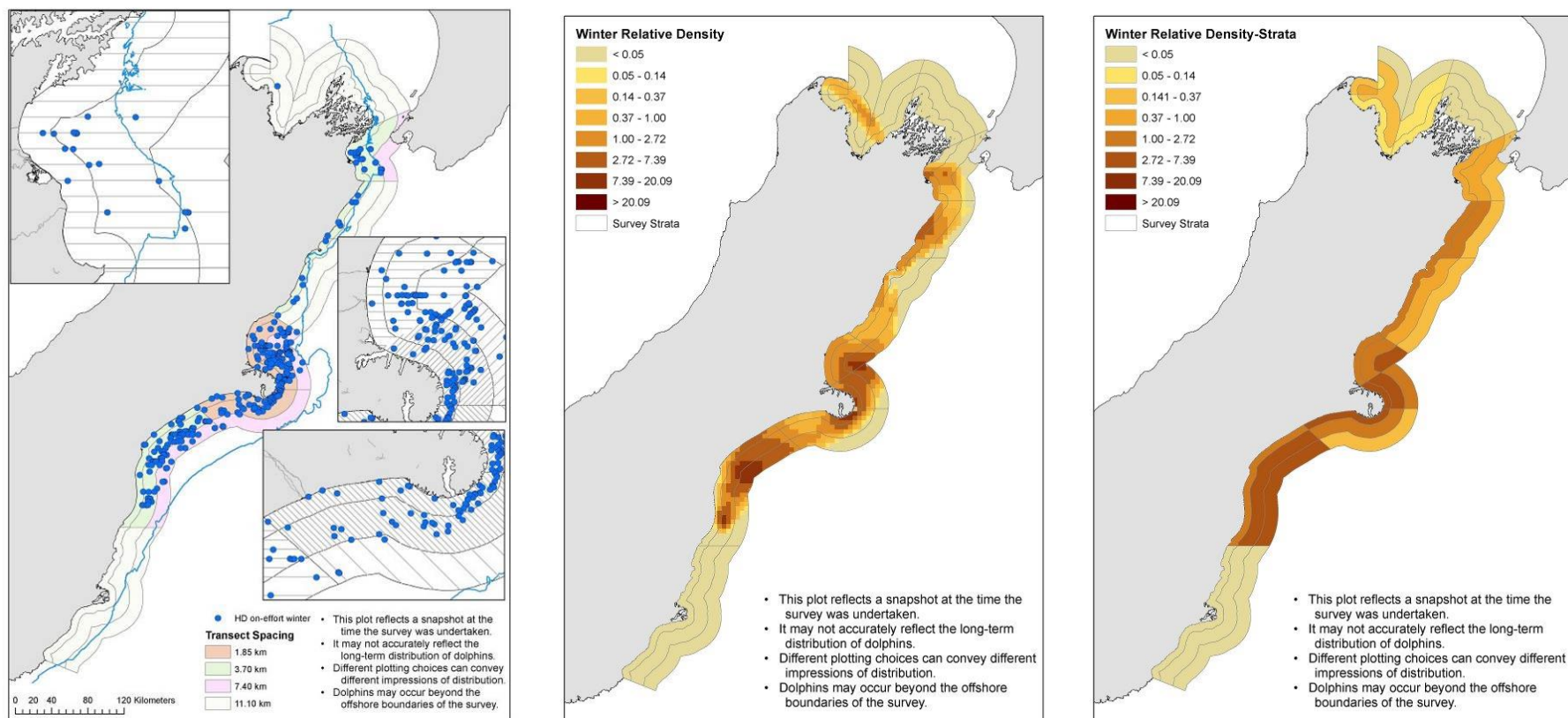| Coastal Section	Offshore Stratum (nmi)	$\overline{\hat{N}}_k$	SE	Lower	Upper
Golden Bay North	0–4				
	4–12				
Golden Bay A	0–4				
	4–12	214	303	28	1671
	12–20				
Golden Bay B	0–4				
	4–12				
	12–20				
Marlborough Sounds	0–4				
	4–12				
	12–20				
Cloudy/Clifford Bay	0–4	132	176	18	958
	4–12	443	505	74	2648
	12–20				
Kaikoura	0–4	369	687	34	4058
	4–12				
	12–20				
Clarence	0–4	606	1076	58	6281
	4–12				
	12–20				
Pegasus Bay	0–4	67	72	12	375
	4–12	553	334	186	1648
	12–20	389	177	166	912
Banks Pen. North	0–4	354	235	108	1159
	4–12	502	160	273	923
	12–20	484	254	184	1271
Banks Pen. South	0–4	449	165	223	901
	4–12	256	95	126	519
	12–20				
Timaru	0–4	224	99	98	513
	4–12	1765	549	973	3203
	12–20				
Otago	0–4				
	4–12				
	12–20				
Total		**8208**	**2210**	**4888**	**13785**

Figure T.9a: Hector's dolphin summer distribution assessed from aerial line-transect surveys. Panels represent patterns for all on-effort Hector's dolphin sightings (left), the relative density of Hector's dolphins within 5 km × 5 km grid cells generated from the Density Surface Models with eight categories (middle) and the relative density of Hector's dolphins within survey strata generated from the Density Surface Models (right). Relative densities greater than 1 indicate areas with density greater than the overall average density.
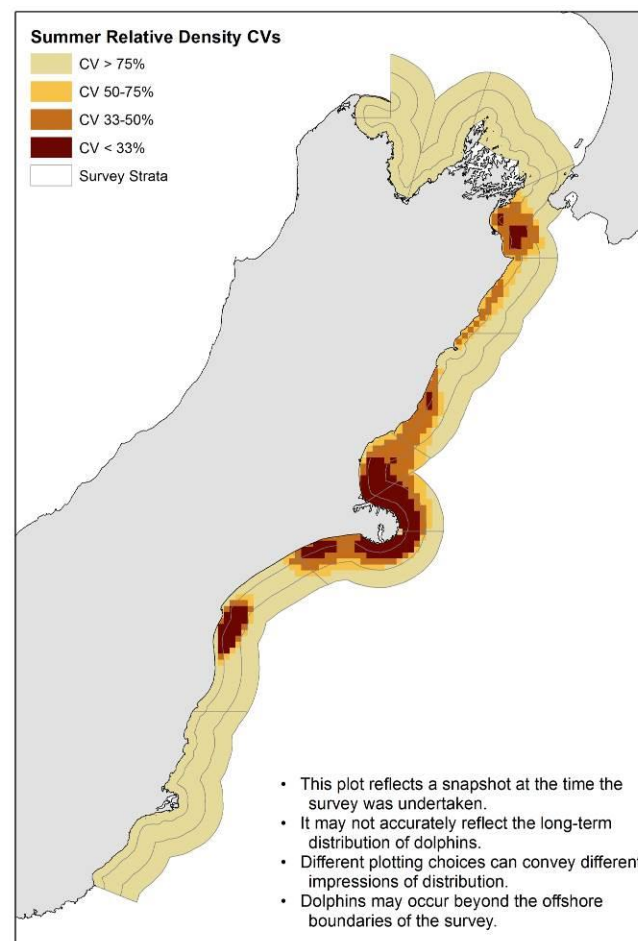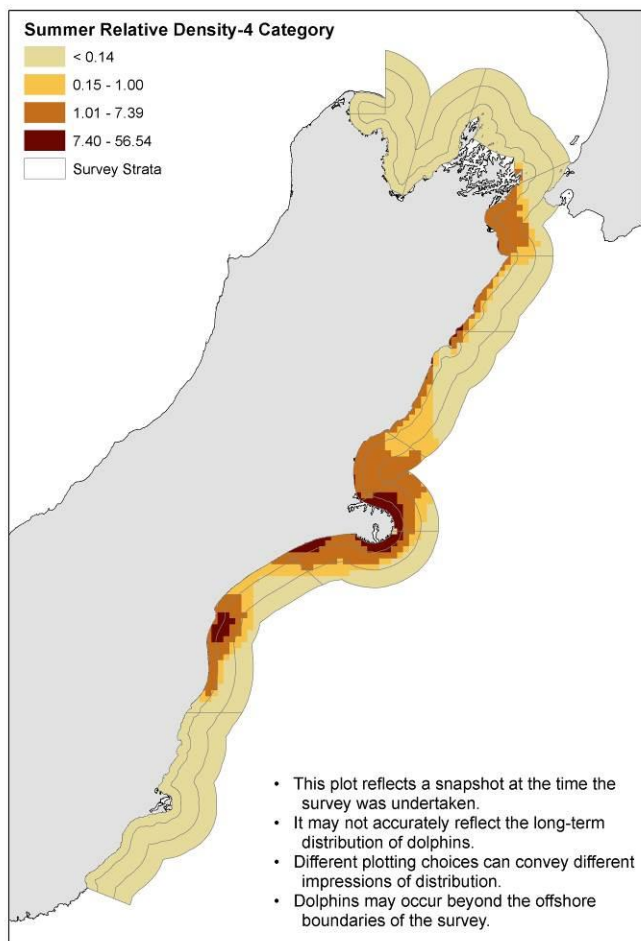
Figure T.9b: Hector's dolphins summer distribution assessed from aerial line-transect surveys. Panels represent the relative density of Hector's dolphins within 5 km × 5 km grid cells generated from the Density Surface Model with four density categories (left) and precision of estimated relative density with darker colours indicating greater precision; i.e. smaller CVs (right). Relative densities greater than 1 indicate areas with density greater than the overall average density.

Figure T.10a: Hector's dolphin winter distribution assessed from aerial line-transect surveys. Panels represent patterns for all on-effort Hector's dolphin sightings (left), the relative density of Hector's dolphins within 5 km × 5 km grid cells generated from Density Surface Models with eight density categories (middle) and the relative density of Hector's dolphins within survey strata generated from Density Surface Models (right). Relative densities greater than 1 indicate areas with density greater than the overall average density.
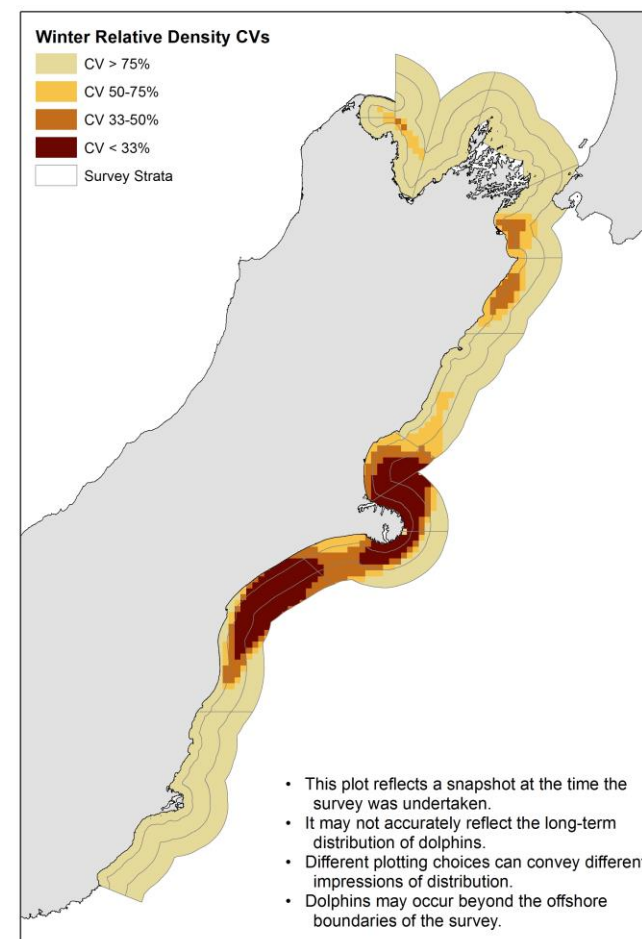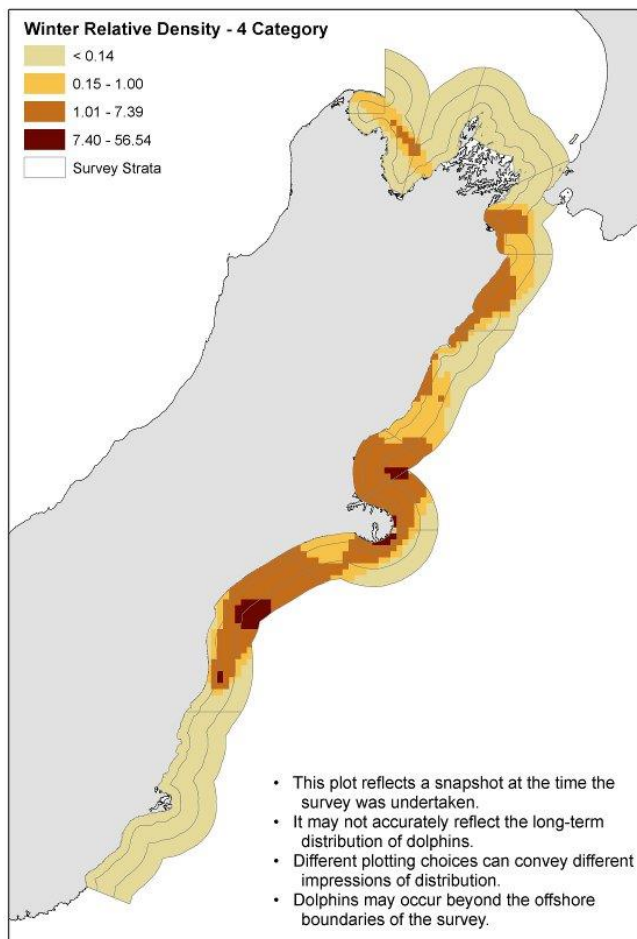
Figure T.10b: Hector's dolphin winter distribution assessed from aerial line-transect surveys. Panels represent the relative density of Hector's dolphins within 5 km × 5 km grid cells generated from the Density Surface Model with four density categories (left) and precision of estimated relative density with darker colours indicating greater precision; i.e. smaller CVs (right). Relative densities greater than 1 indicate areas with density greater than the overall average density.